UNIVERSITY OF OKLAHOMA

GRADUATE COLLEGE

ISOLATION AND STRUCTURAL ANALYSIS OF SECONDARY METABOLITES FROM THE FUNGI ASPERGILLUS TERREUS AND REMERSONIA THERMOPHILA

A THESIS

SUBMITTED TO THE GRADUATE FACULTY

in partial fulfillment of the requirements for the

Degree of

MASTER OF SCIENCE

By

MELVYNN MANGIONE

Norman, Oklahoma

2022

ISOLATION AND STRUCTURAL ANALYSIS OF SECONDARY METABOLITES FROM THE FUNGI ASPERGILLUS TERREUS AND REMERSONIA THERMOPHILA

A THESIS APPROVED FOR THE

DEPARTMENT OF CHEMISTRY AND BIOCHEMISTRY

BY THE COMMITTEE CONSISTING OF

Dr. Robert Cichewicz, Chair

Dr. Christina Bourne

Dr. Si Wu

To my mother, to whom I owe everything.

To my grandfather and mother, whose passion for chemistry and biochemistry has inspired me to pursue this degree and dedicate myself to scientific research.

Acknowledgments

Throughout this project I have received incredible support and would like to thank everyone involved in making this past year a success. The time I spent here at OU has been productive, eye opening, and has culminated with the completion of my third Master and this thesis.

I would first like to thank my supervisor, Dr. Robert Cichewicz, for giving me the opportunity to join his laboratory and above all, for his continual support regarding the projects I worked on as well as continually challenging me and my ideas, pushing me to become a better scientist. I would also like to take the time to thank Dr. Christina Bourne and Dr. Si Wu for accepting to be a part of my thesis committee and their support in establishing the best path forward for the completion of my studies. Additionally, I would like to thank the current and past members of the Natural Products Discovery Group, who have been there for me every step of the way, giving me advice when I needed it most and for being great friends. Special thanks to Dr. Jin Woo Lee and Dr. Mostafa Alilou for their valuable guidance at the key steps in this project and for mentoring me through all the uncharted territories I stepped into.

Many thanks to my academic advisor Dr. Isabelle Thomas and all the members of the Chemistry and Biochemistry department that have supported me along the way and have made this opportunity a reality.

Finally, my deep and sincere gratitude to my mother and her family for their continuous and unparalleled love, as well as giving me the experiences that have made me who I am today.

Table of Contents

List of Tables

List of Figures

List of Abbreviations

µg: microgram (10E-6g)

AcOH: acetic acid

ACS: American Chemical Society

AT: *Aspergillus terreus*

CH3CN: acetonitrile

COSY: correlated spectroscopy

DCM: dichloromethane

DEPT: distortionless enhancement of polarization transfer spectroscopy

DI: deionized

DMSO: dimethyl sulfoxide

ECD: electronic circular dichroism

ESI$^-$: negative electrospray ionization

ESI$^+$: positive electrospray ionization

EtOAc: ethyl acetate

HMBC: heteronuclear multiple bond correlation

HP20: reusable chromatography column filler (reverse phase)

HPLC: high performance liquid chromatography

HRESIMS: high resolution electrospray ionization mass spectrometry

HSQC: heteronuclear single quantum coherence

INPART: Institute for Natural Products Applications and Research Technologies

***J*:** coupling constant (in Hz**)**

LC-MS: liquid chromatography/mass spectrometry

MeOH: methanol

MIC90: Minimum Inhibitory Concentration required to inhibit the growth of 90% of organisms

MS: mass spectrometry

nm: nanometer (10E-9m)

NMR: nuclear magnetic resonance spectroscopy

NOESY: nuclear Overhauser effect spectroscopy

NPDG: Natural Products Discovery Group

ROESY: rotating frame Overhauser effect spectroscopy

RT: *Remersonia thermophila*

SAR: structure-activity relationship

STI: sexually transmitted infection

TLC: thin layer chromatography

UV: ultraviolet spectroscopy

VCD: vibrational circular dichroism

VLC: vacuum liquid chromatography

Abstract

Aspergillus terreus has shown to inhibit *M. genitalium* whereas *Remersonia thermophila* has shown to exhibit antitrichomonal activity. The compounds that were responsible for activity in their respective assays were rapidly and efficiently isolated with a bioassay-guided fractionation procedure. Following this isolation step, the active compounds could be structurally characterized. Therefore, the goal of this research project was initially to purify and identify the active compounds present in *Aspergillus terreus* and *Remersonia thermophila*.

Through the development of efficient analytical methods for the fractionation and purification of the two fungi produced natural products, several active compounds were isolated. Within the time frame of the partnership between the University of Oklahoma and SIGMA-Clermont, characterization of the active molecules was not possible due to insufficient material. However, the activity of these compounds showed promise and further research into these compounds is required. The methods that were developed to isolate the active compounds can serve as a blueprint for a more rapid and straightforward isolation of these molecules which could lead to their characterization thereafter.

To successfully complete this thesis, metabolites were studied regardless of their activity. Hence, compounds 31C and 52C were explored given their more generous quantities. The structural characterization of these compounds was followed through to completion. These two compounds were not described in the literature, and it was soon discovered that these compounds presented a novel chemical scaffold. Therefore, extensive characterization through an array of spectroscopic techniques and mass data was required to elucidate the structures of these molecules. Their absolute configurations were established through ECD and VCD

calculations. The new chemistry that was discovered will hopefully guide the discovery and synthesis of new drugs and help break through drug discovery plateaus.

Chapter I: Introduction and Background

As these two projects were originally centered around the two following sexually transmitted infections: *Mycoplasma genitalium* and *Trichomonas vaginalis*, a brief explanation of both infections will be given. This will be followed by the importance of finding novel treatments and new chemical scaffolds as it became the major focus of this thesis. This will lead into the work performed by our lab and where we find our answers. Finally, I will describe each fungus not only as a source of bioactive molecules against their respective STIs but also show that *Remersonia thermophila* is an unexplored fungus that will provide new chemistry.

I.1 Introduction

Sexually transmitted infections, or STIs are infections that are caused by bacteria, viruses or parasites and they greatly impact sexual and reproductive health worldwide. Every day, an additional one million people contract STIs in the world and an estimated 357 million people are infected by one of the following four STIs each year: trichomoniasis (156 million), chlamydia, gonorrhea, and syphilis.[1] In addition to their immediate consequences, STIs can have serious effects. Some STIs can increase the risk of acquiring HIV by at least three times whereas the transmission of a sexually transmitted infection from a mother to her child can result in a variety of problems such as low birth weight and other birth defects.

I.1.1 *Mycoplasma genitalium*

Mycoplasmas were discovered in 1980 and they remain the smallest bacteria discovered to this day.[2] Although most types of mycoplasmas are harmless, some can provoke urethritis, respiratory disorders, painful pelvic inflammations and even infertility in women.

A pathogenic species of *Mycoplasma,* known as *M. genitalium* is a sexually transmitted infection and is responsible for urethritis in men and pelvic inflammatory disease in women.

Although most patients infected with this mycoplasma do not develop symptoms, it can cause latent infections and is often found in *Chlamydia trachomatis* and HIV infections. Indeed, like other sexually transmitted infections *M. genitalium* causes inflammation in the delicate tissues of the genitals. This in turn, makes those tissues more vulnerable to infection by other STIs, including HIV. It is estimated that between 1 and 2% of adults are infected by *M. genitalium* and up to nearly 40% of those consulting for recurrent STIs.[3]

Many antibiotics, such as penicillin, do not work against mycoplasmas because *Mycoplasma* is a genus of bacteria that doesn't have cell walls. In addition to some antibiotics not working, other commonly used drugs such as azithromycin and doxycycline (**Figure 1**) have decreasing effects on *Mycoplasma* due to increasing drug resistance.[4] As drug resistance will continue to escalate in the coming years, it is important that we find new treatments for *M. genitalium*.

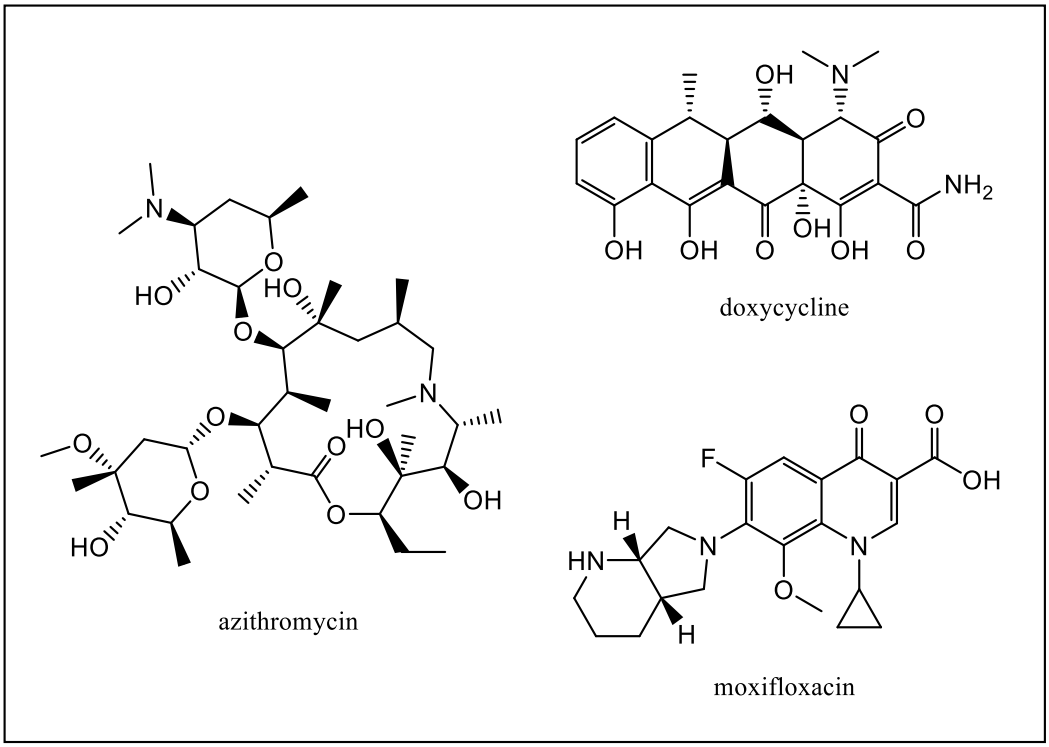

Figure 1. Active compounds against M. genitalium

I.1.2 *Trichomonas vaginalis*

With over 200 million people infected each year worldwide, *T. vaginalis* is one of the most common sexually transmitted infections. In the United States for example, it was established that 3.1% of women were infected by *T. vaginalis*.[5]

Most often benign and asymptomatic, *T. vaginalis* can lead to complications. As is the case for *M. genitalium*, *T. vaginalis* also causes inflammation in the urogenital area, increasing the risk of transmission for other STIs. Symptoms of *T. vaginalis* infection appear in nearly 50% of the cases reported for women. Symptoms include and are not limited to, vaginal discharge, itching and a burning sensation when urinating. *T. vaginalis* infection also multiplies the risks of cervical cancer and infertility.[6] It is also associated with pre-term birth, low birth weight as well as miscarriage.[7]

T. vaginalis treatments are based on the oral administration of an antiparasitic antibiotic of the nitroimidazole family, either metronidazole or tinidazole.[8] Drug resistance is of particular concern, as they are the only approved treatment pathways, and reinfection can occur. Indeed, 20% of people who have had trichomonas, get infected again in the following three months.[9] Other studies have underlined the existence of a few compounds that also possessed activity against *T. vaginalis* such as berberine, emodin and hederagenin (**Figure 2**), although their selectivity fell short of the nitroimidazoles.[10-12]

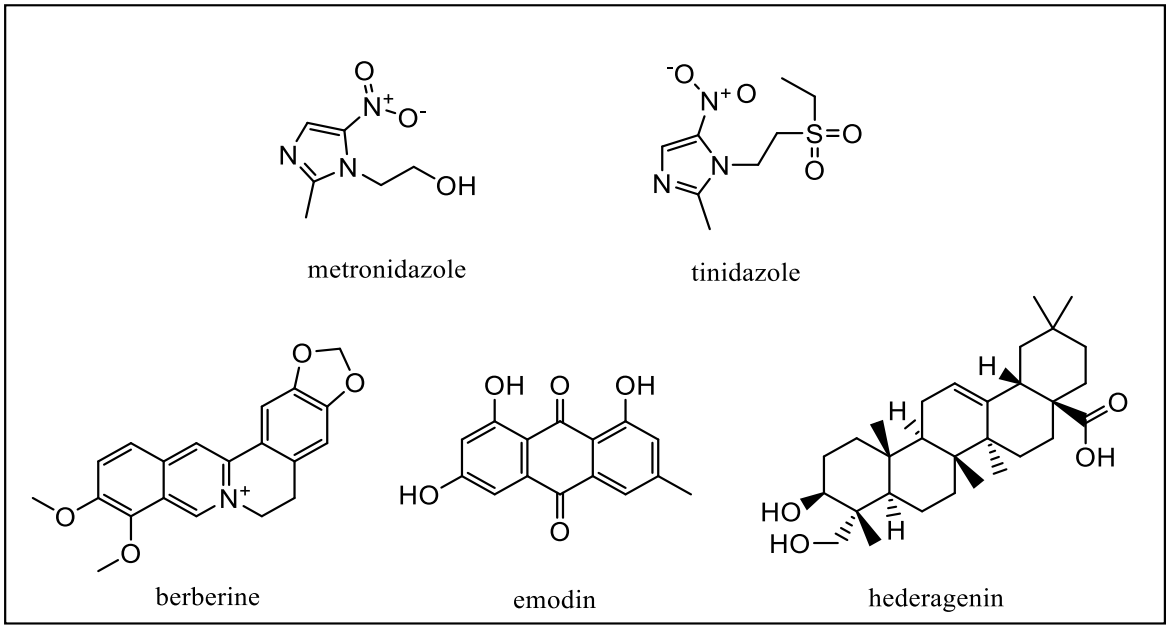

Figure 2. Active compounds against *T. vaginalis*

I.3 The potential of fungi as a source of natural products

Natural products are produced by living organisms such as bacteria, archaea, fungi, plants, and animals. As such, they have been used as the active ingredients in many traditional medicines such as in Chinese, Ayurvedic and Korean medicines.[13] For example, salicin, the precursor to aspirin, was obtained from willow bark (*Salix alba*), and is an antirheumatic.[14] Morphine, isolated from the opium poppy (*Papaver somniferum*) is a narcotic analgesic.[15] Paclitaxel, used in chemotherapy, was first isolated from the bark of the Pacific yew tree (*Taxus baccata*).[16]

Although, pharmaceutical companies have chosen to focus more recently on synthetic approaches for drug discovery due to the emergence of high-throughput screening programs and combinatorial chemistry, natural products remain a source of inspiration for the development of new pharmaceutical products.[17] Most drugs that are currently used are natural products or derivatives thereof and they represent 20% of the drugs that are approved each year.[18] Indeed, compounds isolated from natural sources have been used in treatments for

diseases for decades and have been proven time and time again to be an excellent source of therapeutics.[19] On the other hand, despite the recent efforts to generate synthetic drugs, only a fourth of the clinically approved drugs are fully synthesized.[18] As natural sources continue to yield novel pharmaceuticals, drug discovery will continue to be fueled by natural products and their derivatives. Hence, novel natural product scaffolds also have potential in pioneering new leads and represent a wealth of opportunities in the everlasting search for pharmaceuticals.

Fungi more particularly, are an enormous source of natural products. They go all the way back to Alexander Fleming's discovery of penicillin from *Penicillium notatum* in 1929 and have enabled the discovery of other classes of β-lactam antibiotics since then.[20] These include the cephamycins, monobactams and cephalosporins.[21] Other clinically relevant drugs produced by fungi are lysergic acid which is precursor to LSD, lovastatin for cholesterol control, the immunosuppressant cyclosporine and the antifungal trichodermin (**Figure 3**).[22] More generally, the secondary metabolites produced by fungi can be divided into the four following categories: indole alkaloids, polyketides, nonribosomal peptides and terpenes. The classification of these metabolites depends on their biosynthetic precursors.

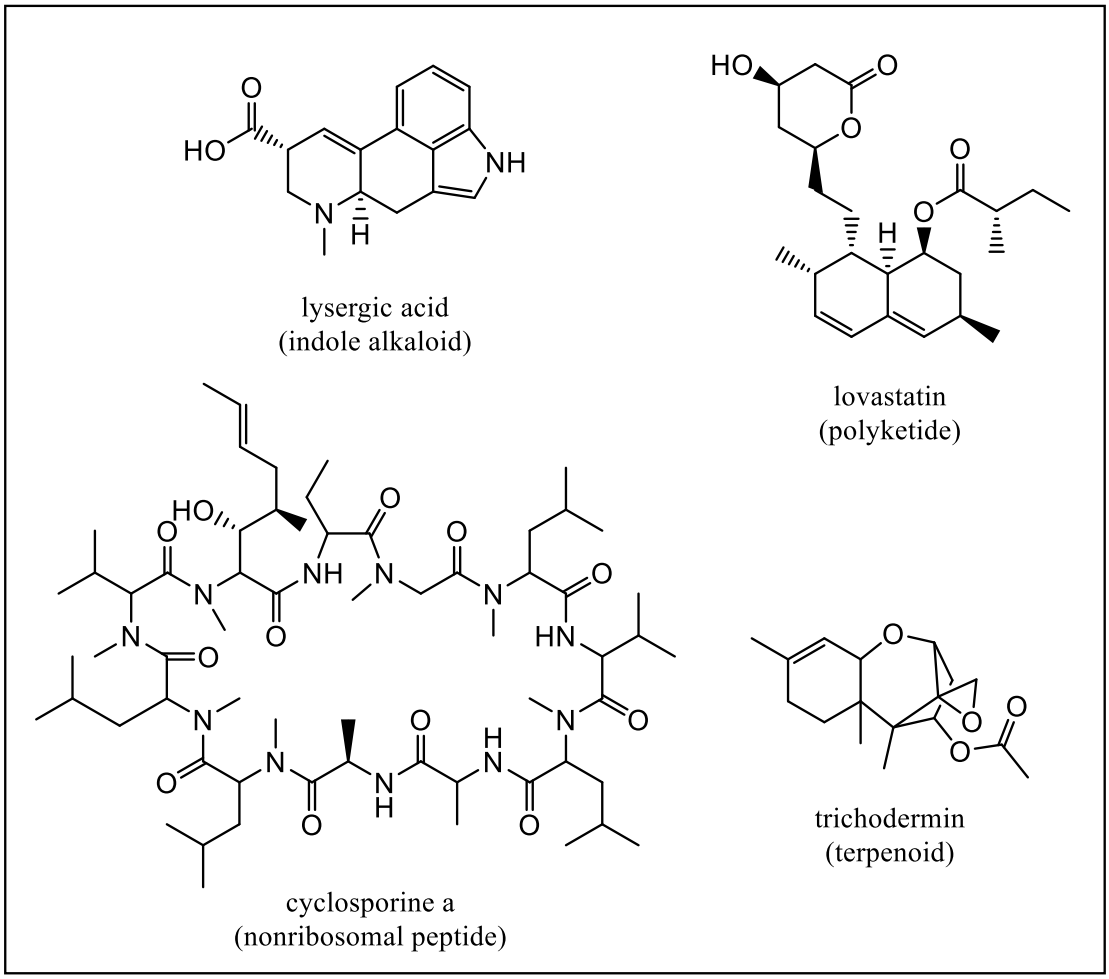

Figure 3. A natural product of every class produced by fungi

To this day, a total of 8600 bioactive fungal products have been discovered, representing nearly 40% of the known bioactive microbial compounds.[23] Moreover, it has been stated that with the new advances in DNA sequencing and synthetic biology, only 1.5% or just about 70,000 fungal species have been reported.[24] Given the biosynthetic diversity that fungi are capable of and the small fraction of described fungal species, there lies immense opportunity in this source of natural products. Many more novel bioactive compounds and novel scaffolds that could provide the inspiration needed to develop groundbreaking drug leads remain to be discovered.[25]

I.4 Fungi hits for *M. genitalium* and *T. vaginalis*

To study as many fungi and their metabolites as possible, the Natural Products Discovery Group has involved the public in their research of new fungi by establishing a citizen science soil collection program. Citizen scientists from across the country can send in samples of their soils allowing the NPDG to test many different fungi and improve their chances of finding bioactive molecules against diseases ranging from cancers and malaria to sexually transmitted diseases such as trichomonas and mycoplasma.[26]

A preliminary screening of fungi that inhibited these infections was carried out and led to the identification of the following fungi : *Aspergillus terreus* and *Remersonia thermophila*. The first one showed inhibitory activity of *M. genitalium* whereas the second fungi showed promise against *T. vaginalis*. Therefore, they were both selected for further studies and the bioassay guided fractionation of the metabolites they produced began.

The next paragraphs will go over what is known of these fungi. This will include the metabolites that are known to be produced by *A. terreus* and *R. thermophila* as these compounds will very likely be present here as well.

I.4.1 *Aspergillus terreus*

The genus *Aspergillus* is an extensively studied genus that regroups around 350 species that are divided into six subgenera. *A. terreus* lies in one of the oldest discovered subspecies, *Circumdati*, which was first documented in 1965.[27] This fungus is often found in soils, compost heaps and dust and contributes to the degradation of organic matter because of its cellulolytic activities. It is also present on cereals in storage, spices, and various plants and often contaminates feed for livestock, although it is not considered a common food spoilage mold.[28]

Aspergillus terreus is commonly used in the industry to produce a variety of compounds including organic acids such as itaconic acid and cis-aconitic acid. It was also the first source for mevinolin (lovastatin), a drug used to lower cholesterol levels.[29] *A. terreus* also produces 6-hydroxymellin an inhibitor of pollen development in *Arabidopsis thaliana*, as well as the enzyme xylanase.[30] Terpenoids (sesqui- or diterpenoids), butyrolactone and dehydrocuvularin were also discovered among the bioactive metabolites produced by *A. terreus*.[31]

I.4.2 *Remersonia thermophila*

On the other hand, the information surrounding *R. thermophila* is rather scarce given that the *Remersonia* genus has only been documented twice, an article in 2014 and more recently in 2020.[32] The following species, *Stilbella thermophila*, is a species of fungi that was transferred to the new anamorph genus, *Remersonia*. Partial ribosomal DNA sequences analysis has led to believe that this fungus might be a member of the *Sordariales*. However, it also believed to be part of the *Ascomycetes*.[33]

This species of fungi is found in compost heaps and research does not seem to indicate any use in the industry or in the biomedical field. The lack of information concerning this fungus reveals how unexplored this genus is and therefore, shows that it has great potential in providing some element of novelty whether it is in the form of new bioactive compounds or novel chemistry which could possibly provide a new source of inspiration for drug design.

I.5 A need for new scaffolds in medicinal chemistry

Initially, the goal of these two projects was to find bioactive compounds against *T. vaginalis* and *M. genitalium* that had never been characterized. Due to the poor yield of active metabolites by these fungi, the fractionation of *R. thermophila* was rerouted towards the characterization of new chemistry. Indeed, given how little was known about *R. thermophila*,

it was the perfect candidate for this new objective, and this was proved very quickly as the first purified compound did not appear in the Dictionary of Natural Products. Moreover, it possessed a scaffold that had never been described before.

As it stands, modern medicinal chemistry faces several challenges, including but not limited to, the need for novel intellectual property to secure patents as well as the requirements for low toxicity, high potency, and specificity.[34] Medicinal chemistry has become one of the most time-consuming steps in drug discovery due to the difficulty of improving the kinetic, toxicological, and metabolic profiles of a molecule.[35] In some cases, these improvements cannot be made. The solution to these problems lies in a more intensive design of scaffolds to increase the speed of preparation of analogues as well as technologic advances that would allow automated synthesis.[36]

If we were to define a biological structural space available for potential ligands, scaffolds are the complementary structures to these spaces.[37] Scaffolds serve as the structural basis for analogue creation and substitution which will interact with the desired target. They are the backbone from which a variety of compounds can be synthesized. Scaffold hopping, which is the search of active compounds containing different core structures through computer analysis, represents one of the ways that the previously mentioned challenges can be addressed.[38] Pharmacologic activity can be explained by the structural components or scaffold in any given active molecule because these govern the interactions with specific receptors.[39] In this regard, scaffolds explain the activity of some compounds due to their recognition by distinct receptors. As the human genome is sequenced, complex protein binding sites are discovered and there is an increasing demand for new chemical scaffolds. As targets diversify, creating analogues becomes insufficient and current known scaffolds become obsolete.[40] Moreover, as target and phenotype-based drug discovery remain the primary method to yield new drugs, an

approach consisting of scaffold novelty driven drug discovery could compensate this process and increase the odds of developing new drugs.[41]

Several pharmacophoric scaffolds have been recognized throughout the past decades with some of the more recognizable scaffolds presented hereafter. These include 7-oxo-4-thia-1-azabicyclo[3.2.0] heptane (1) present in penicillin, cyclopenteneperhydrophenanthrene (2) from testosterone, N-phenylpyrazole (3) in celecoxib, and 1H-pyrazolo[3,4-d]pyridine (4) which is used in drugs to treat melanomas or control pulmonary hypertension (**Figure 4**).[42-44]

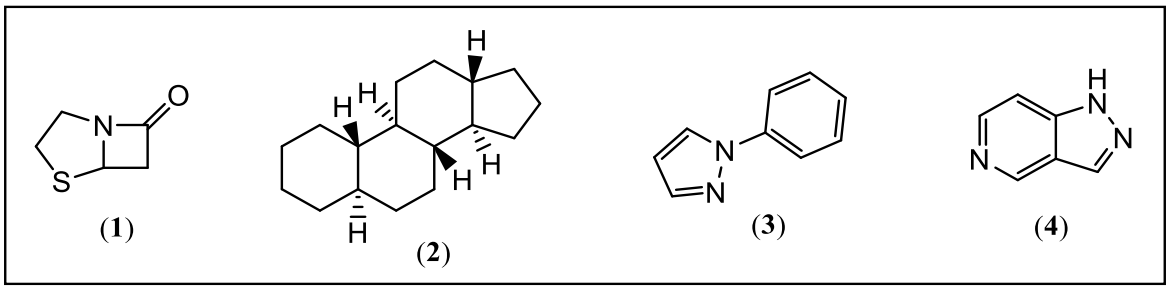

Figure 4. Common pharmacophoric scaffolds

Novel scaffolds are often desired when plateaus such as potency or selectivity are reached, and they can provide breakthrough solutions to overcoming such problems. Consequently, the isolation and characterization of compounds with novel scaffolds produced by *R. thermophila* was carried out and they will be reported in this paper.

Chapter II : Extraction of active compounds from *Aspergillus terreus*

II.1 Introduction

This second chapter focuses on *Aspergillus terreus*, a fungus which has shown activity in the mycoplasma assay in preliminary screenings. More particularly, the methods that were used to extract the compounds that possessed activity against *M. genitalium* will be detailed hereafter.

The study of this fungus and its active metabolites was facilitated through the usage of a bioassay guided fractionation process. This technique was used to quickly separate the targeted active fractions with their active metabolites from the ones that were not active. At the end of each separation, fractions were tested for biological activity before further extraction and purification. Several cycles of this procedure allowed us to target specific fractions until the active compounds were isolated.

The active compounds can then be structurally characterized using a wide variety of methods. For known molecules, analytical methods such as LC-MS in addition to the use of online libraries enable the characterization of the isolated compounds. Although a pure bioactive compound was isolated in this chapter, the material was not available in sufficient quantities for it to be fully characterized.

The fungus was regrown on a larger scale to address this problem. Given the time constraints of this project as well as the time required for assay and fractionation, structural characterization of the active compounds in the regrowth was not carried out. However, this chapter will nonetheless, review and discuss the isolated compounds from the first growth as they are compared to the literature surrounding *A. terreus*.

II.2 Results and Discussion

II.2.1 Scale-up

This fungus showed promise in its potential to inhibit *M. genitalium* in the preliminary screenings. To characterize the bioactive compounds produced by the fungus, a scale up was required to allow for sufficient metabolite production. Therefore, *A. terreus* was grown on Cheerios breakfast cereal (**Figure 5**) in three large mycobags.

Figure 5. *Aspergillus terreus* grown on Cheerios breakfast cereal

The metabolites produced by *A. terreus* went through several rounds of purification until the biologically active compounds were separated from the other metabolites. An additional scale-up became necessary when the active compounds were not extracted in sufficient quantities for characterization.

II.2.2 Establishing the standard procedure

The goal of this project was to find compounds that inhibited *M. genitalium*. Compounds that possess these inhibiting properties, must also be able to cross the cell

membrane to reach their target. Therefore, they must possess the appropriate chemical and physical propertied to do so. To find such compounds, an elaborate separation procedure must be established.

For that purpose, several different separation techniques were researched, and the result was the following method developed in Dr. Cichewicz's lab. This method is in fact a combination of several different techniques that are used one after the other. With this procedure, the isolation of bioactive compounds with said chemical and physical properties was achievable.

The standard procedure involves the combination of the following extraction and separation techniques: an organic extraction, a silica vacuum liquid chromatography and an HP20 VLC. Using a methodic combination of solvents with different polarities and at varying concentrations, fractionation of a complex crude extract into smaller fractions was achieved. The process used here enabled the separation of the metabolites produced by the fungi. Primary metabolites such as DNA, carbohydrates, lipids, and other macromolecules are set aside whereas secondary metabolites are further fractionated.

A water/EtOAc partitioning separates the water-soluble primary metabolites from the organic soluble secondary metabolites (Fraction A). Lipids that were contained in the organic phase were extracted with a hexane/DCM solution (Fraction B). The use of three different mixtures of DCM and methanol yields compounds with different polarities (from least polar to most polar). This enables the separation of the most nonpolar compounds (Fraction C) soluble in DCM, from those that are slightly more polar (Fraction D), soluble in DCM: MeOH 1:1 and those that are MeOH soluble (Fraction E). The fraction that usually possesses the active compounds is Fraction D, but they can also appear in the other fractions.

Further fractionation was pursued with a gradient of DI water and methanol (**Figure 6**). Washing of the column to be able to reuse HP20 silica, is carried out with a solution of DCM and MeOH (Fraction K). This fraction usually contains the remaining pigments that weren't eluted with the DI water/MeOH gradient.

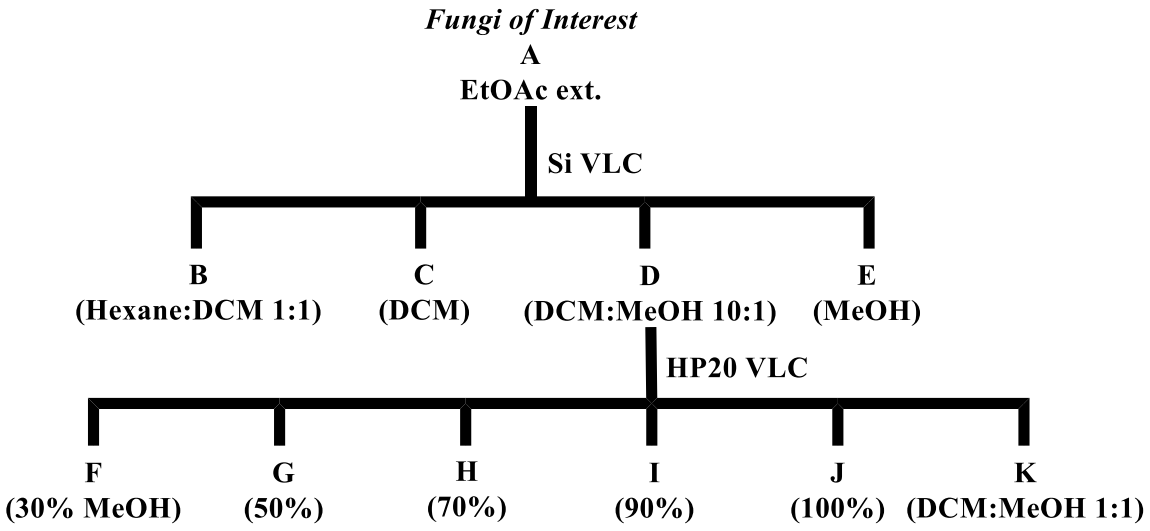

Figure 6. Fractionation template of fungi produced metabolites

The next round of fractionations was performed with an HPLC, where methods were tailored to each fraction. To find the appropriate method, the LCMS data is key. Fractions were analyzed with the LCMS in between every fractionation. The parameters of the LCMS (**Table 2**) allow for the analysis of a variety of compounds with different polarities and masses and therefore give very valuable information on the fractions.

Given those parameters, it was possible to estimate the best elution conditions for the separation of the compounds in each fraction. Indeed, LCMS analysis used a gradient of 15% MeOH to 100% MeOH in 15 minutes. The retention time gave information on the MeOH/water ratio at that specific time which allowed us to figure out what conditions to use for HPLC fractionation. Keeping in mind the polarity of the compounds, the use of a higher percentage of MeOH in the MeOH/water ratio will elute the compounds faster whereas a higher ratio of water

will elute slower and allow for better separation of the compounds composing each fraction. This can also be generalized to the usage of acetonitrile instead of MeOH when combined with water to elute fractions.

Therefore, the fractions that were active in the bioassays were further fractionated on preparative columns then on semi-preparative columns (**Figures 7, 8**) and the methods used are detailed at the end of this Chapter. On the figures below, the active fractions are noted in red and the fractions that were insoluble in MeOH are in green.

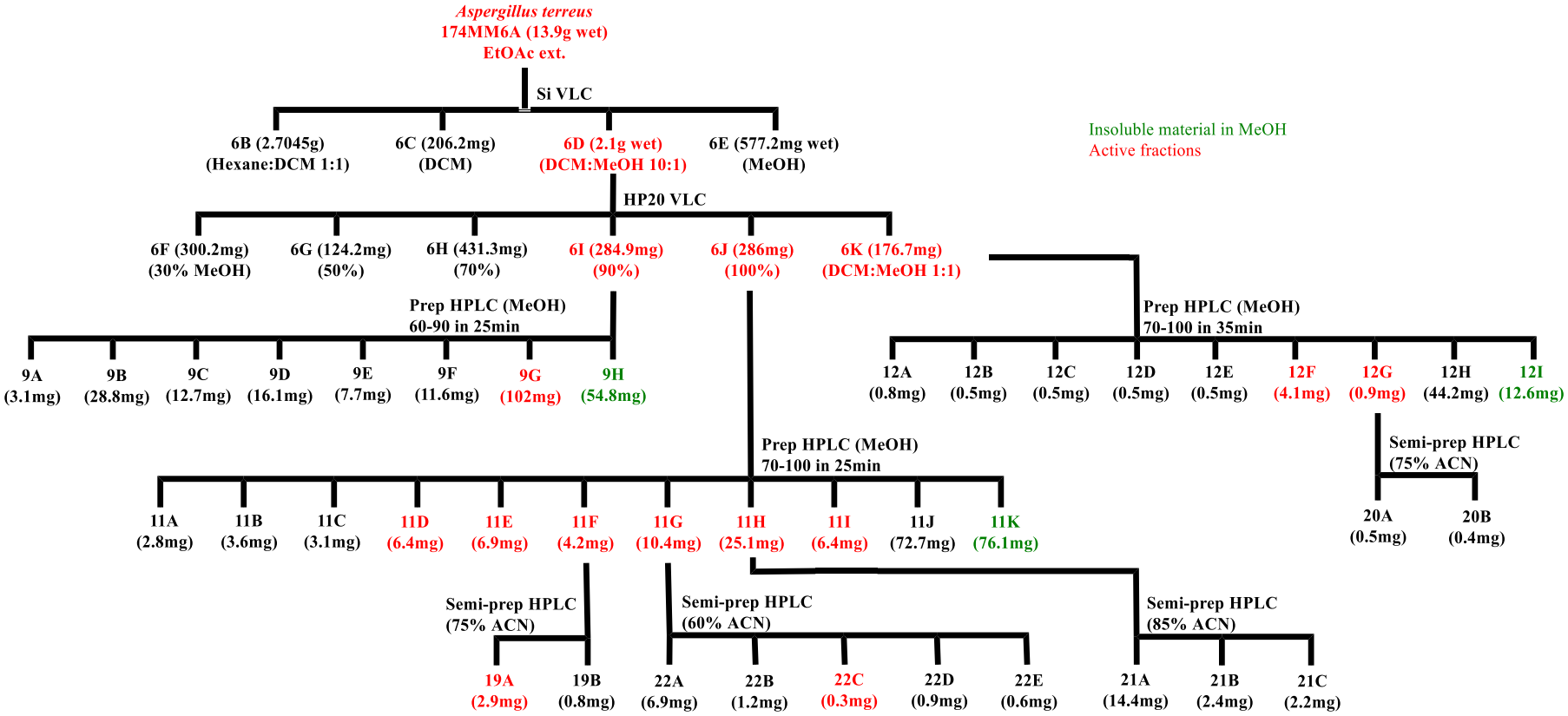

Figure 7. Fractionation template for *Aspergillus terreus*

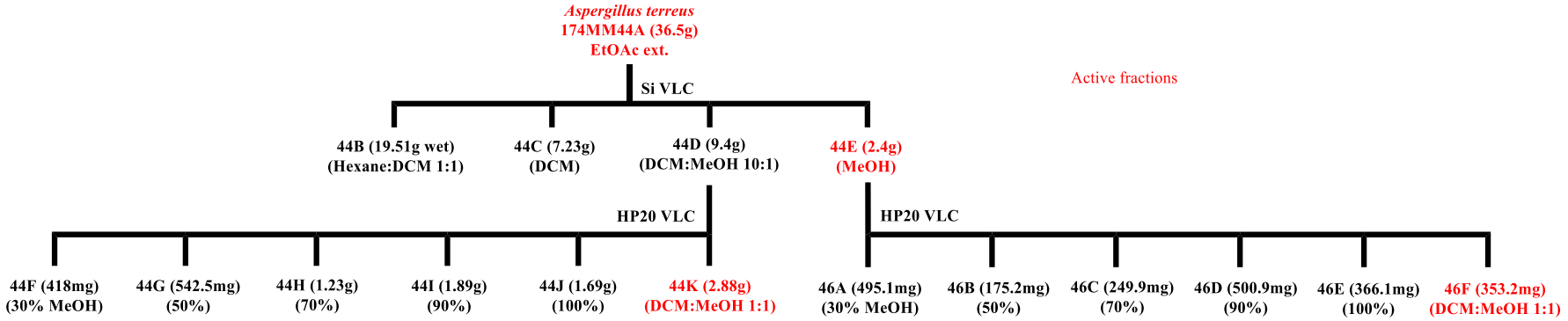

Figure 8. Fractionation template for the regrowth of *Aspergillus terreus*

II.2.3 Fractionation of *Aspergillus terreus*

After fractionation of *Aspergillus terreus* according to the standard procedure, the obtained fractions were shipped for bioassay. Bioassay was performed by Dr. Gwen Wood at the University of Washington.

Biological activity was tested in between every step of the fractionation process. This resulted in knowing which fractions were the most active and enabled the pursuit of specific fractions (most active and purest fractions) while setting aside the least active fractions.

Therefore, fractionation was only carried out on the most active fractions (fractions highlighted in yellow in **Appendix I.1-5**) until a pure compound was isolated. An example of the results of this process is fraction 22C. This active compound was obtained from the crude extract 6A according to **Figure 7**. Activity levels of the parent fractions of 22C are summarized in **Table 1**.

Sample ID	Source of the Fraction	MIC90 (µg/ml)
174MM6A	Crude material	25
174MM6D	Si VLC of 174MM6A	25
174MM6J	HP20 VLC of 174MM6D	12.5
174MM11G	Preparative HPLC of 174MM6J	3.2
174MM22C	Semi preparative HPLC of 174MM11G	2.5

Table 1. Bioassay results of the fractions that led to the isolation of 22C

MIC90 is the minimum inhibitory concentration required to inhibit the growth of 90% of organisms compared to untreated controls. As active fractions were purified; it was expected that the activity would increase which meant a lower MIC90. This was indeed the case here, as the more the bioactive fraction was purified, the less of it was required to inhibit the same

quantity of *M. genitalium* organisms. As in the example of fraction 6A above, the activity from the crude extract decreased from an initial MIC90 value of 25 µg/mL to 2.5 µg/mL for 22C.

Fractions 19A and 22C had the lowest MIC90 of all the fractions obtained. Further fractionation of 19A was required to obtain a pure bioactive compound. However, given the quantity (2.9 mg) and the number of peaks in the LCMS chromatogram, purification of 19A was not possible. Fraction 22C on the other hand was nearly pure, however, as in the case of 19A, there was not enough material for characterization (0.3 mg) (**Figure 9**). Indeed, ^{1}H NMR yielded poor results; the only observable data pertained to the solvent. ^{1}H NMR lack also meant that ^{13}C experiments and correlation NMR would not yield usable data. When dereplication does not point toward a known compound, the knowledge of a compound's approximate molecular mass and its UV pattern are not enough to start structural characterization.

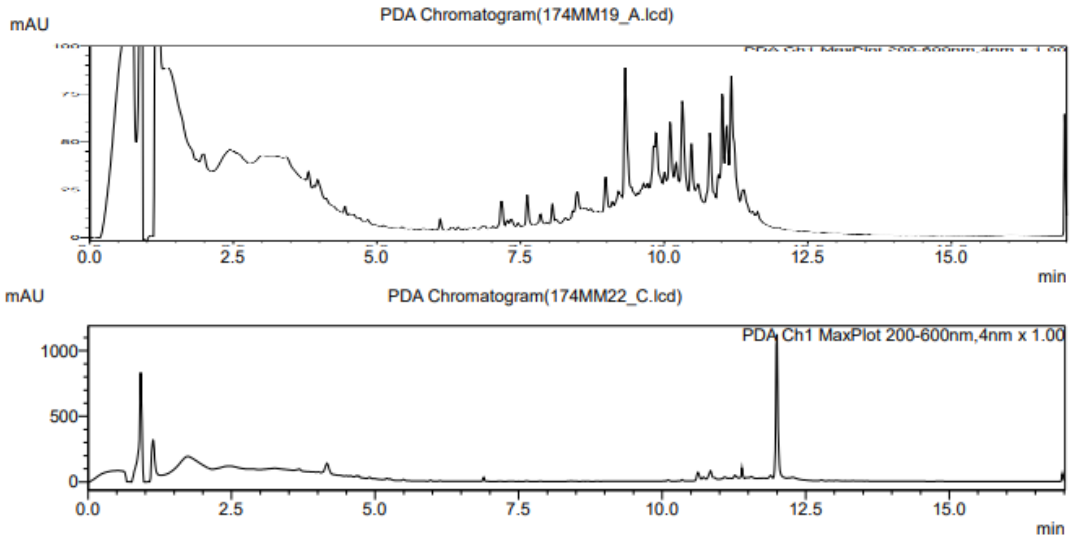

Figure 9. Chromatograms of 19A (top) and 22C (bottom)

To characterize the active compound from 19A as well as 22C, six more mycobags of Cheerios-grown *Aspergillus terreus* were grown. However, three bags were contaminated and were not used. Fractionation was initially carried out in a similar fashion (**Figure 8**). As

reported in the figure, the active fractions were different and given the turnaround for bioassay results as well as the remaining time to complete this project, further fractionation was not pursued.

II.2.4 *A. terreus – bioactive compounds*

Although further analysis of this fungus was not achieved, several active fractions and isolated compounds stand out and should be further investigated. Fractions 9G, 11D, 11E, 19A, 22C, 11I and 12F all possessed activity with a MIC90 of 6.3 µg/ml or below. Among these fractions, the most promising candidates for further analysis were 19A and 22C with MIC90 values of 2.5 µg/ml. Analysis of the LC-MS chromatograms provided the following *m/z* ratios of 298 and 432 for 19A and 22C respectively.

II.2.5 Conclusions and Future Directions

This chapter serves as a blueprint for future reference when proceeding with further fractionations of *Aspergillus terreus*. Indeed, since characterization of the active compounds produced by the fungus was not achieved, the useful information from this chapter resides in the methods that were developed for the isolation of the active compounds. These methods can be reused to isolate the active molecules from fractions 19A and 22C as well as the other active fractions.

Moreover, given the activity of 19A (of 2.5 µg/ml) and the number of impurities present in the fraction, the active compound in this fraction is the one that shows the most promise. Although fraction 22C also showed great activity and was almost pure, the quantity (0.3 mg) limited its analysis, and the active compound could not be identified.

The amount of material in the regrowth was very encouraging as the same number of mycobags yielded nearly three times the amount of crude material. Further fractionation and

study of the regrowth are required as fractions 44K and 46E have incredible activity with MIC90 values of 3.1 µg/ml and 0.2 µg/ml respectively. The activity profiles of these two fractions are on the same level (44K) or significantly better (tenfold for 46E) than the purest active fractions from the first growth, namely 19A and 22C.

II.3 Materials and Methods

II.3.1 General Experimental Procedure

Column chromatography was conducted using silica gel and HP20SS. Preparative HPLC was performed using SCL-10A VP pumps and system controller with a Phenomenex Luna 5µm C_{18}(2) column (100Å, 250 mm x 21.2 mm) with a flow rate of 10 mL/min. Semi-preparative HPLC purification were performed using Waters 1525 binary pumps with a Waters 2998 PDA detector and either a Gemini 5µm C_{18} column (110Å, 250 mm x 10 mm), a Kinetex 5 µm F5 column (100 Å, 250 x 10 mm) or a Luna 5 µm C_{18} column (100 Å, 250 mm x 10 mm) with a flow rate of 4 mL/min.

All solvents were used as purchased without further purification unless mentioned. HPLC solvents for fractionation were of ACS grade or better (≥ 99.5%). NMR spectra were recorded on a Varian VNMRS DirectDrive spectrometer equipped with an indirect observe probe at 500 MHz for ^{1}H and at 150 MHz for ^{13}C. All 2D-NMR experiments were acquired with nonuniform sampling (NUS) set to 50%. Chemical shifts for proton and carbon resonances are reported in ppm (δ) relative to the residual protons in chloroform (δ 7.26), in DMSO (δ 2.5) and in methanol (δ 3.31, δ 4.78) as references. The LC-ESIMS analyses were conducted on a Shimadzu UFLC system with a quadrupole mass spectrometer using a Phenomenex Kinetex C18 column (3.0 mm × 75 mm, 2.6 µm) and MeOH-H2O (0.1% HCOOH) gradient solvent system.

II.3.2 Fungal Material

The fungal isolate (internal designation AL09346 RBM-6) was obtained from a soil sample collected from a field in Bessemer, Alabama. The isolate was identified as belonging to the species *Aspergillus terreus*.

The fungus was grown on Cheerios breakfast cereal supplemented with a 0.3% sucrose solution and 0.005% chloramphenicol in three large mycobags (Unicorn Bags, Plano, TX, USA). The fungus was grown for 4 weeks, whereupon it had achieved complete coverage of the solid substrate.

The fungal biomass was extracted by soaking overnight in ethyl acetate. The organic extract was subjected to partitioning two times against water (1:1, vol/vol). The ethyl acetate layer was retained, and the solvent removed by evaporation in vacuo, yielding 13.9 g of light green material for the AT (174MM6A) colonized cheerios. A regrowth of AT, which originally consisted of six large mycobags, of which three were unusable, yielded 36.5g of organic soluble material (174MM44A).

II.3.3 Large-scale extract pre-fractionation

II.3.3.1 Standard Procedure

The crude material obtained beforehand was subjected to silica gel chromatography using step-wide gradient consisting of (1) 50% Hexane-50% DCM; (2) 100% DCM; (3) 90% DCM-10% MeOH; and (4) 100% MeOH to give four fractions (Fractions B-E). Solvents were evaporated in vacuo and the remaining residues were transferred into pre-weighed vials.

Fraction D was further fractionated on a HP20 VLC column using the following series of solvents completed with water: (1) 30% MeOH; (2) 50% MeOH; (3) 70% MeOH; (4) 90% MeOH; (5) 100% MeOH; (6) 50% MeOH-50% DCM to give six fractions (Fractions F-K). The above procedure was also applied to fraction E when it was the active fraction.

II.3.3.2 Pre-fractionation of *Aspergillus terreus*

174MM6A yielded fractions 174MM6B (2.7045 g), 174MM6C (206.2 mg), 174MM6D (2.1 g), and 174MM6E (577.2 g) from silica gel chromatography. HP20 VLC of 174MM4D provided the following fractions: 174MM6F (300.2 mg), 174MM6G (124.2 mg), 174MM6H (431.3 mg), 174MM6I (284.9 mg), 174MM6J (286 mg) and 174MM6K (176.7 mg).

Only fractions 6I, 6J and 6K showed *Mycoplasma* inhibitory activity (MIC90 of 12.5 µg/mL) (**Appendix I.1**).

For the regrowth, 174MM44A yielded fractions 174MM44B (19.51 g), 174MM44C (7.23 g), 174MM44D (9.4 g), and 174MM44E (2.4 g) through silica gel chromatography. HP20 VLC of 174MM44D provided the following fractions: 174MM44F (418 mg), 174MM44G (542.5 mg), 174MM44H (1.23 g), 174MM44I (1.89 g), 174MM44J (1.69 g) and 174MM44K (2.88 g). 174MM44E yielded fractions 174MM46A (495.1 mg), 174MM46B (175.2 mg), 174MM46C (249.9 mg), 174MM46D (500.9 mg), 174MM46E (366.1 mg) and 174MM46F (353.2 mg).

Fractions 46F, 44E and 44K showed mycoplasma inhibitory activity with 46F and 44K having the best activities in their respective fractions (MIC90 of 0.2 µg/mL for 46F and 3.1 µg/mL for 44K) (**Appendix I.2, 5**).

II.3.4 LC-MS analysis

For every fraction, two sets of Eppendorf tubed were prepared. The first set was weighed empty and was sent for bioassay whereas the second one was used for LC-MS analysis.

Fractions were analyzed by LC-MS. The organic residues were solubilized in MeOH (5 mg/mL). The material was completely solubilized using a Branson 5510 sonicator. Further

dilution in MeOH (0.5 mg/mL) was carried out in the second set of Eppendorf tubes. The samples are vortexed and centrifuged (14,800 rpm, 10 min) at room temperature. Aliquots consisting of 100 µL of samples prepared at 0.5 mg/mL were transferred to HPLC vials for LC-MS analysis. LC-MS instrument parameters can be found as follows below (**Table 2**).

MS	
Acquisition Time (min)	15 min
Acquisition Mode	Scan
m/z Range	200-2000
Voltage (kV)	1.55
Interface	
DL Temperature (°C)	250
Heat Block Temperature (°C)	200
Nebulizing Gas Flow (mL/min)	1.5
Drying Gas Flow (mL/min)	10
Pump	
Solvent A	Methanol (MeOH)
Solvent B	Water + 0.1% Formic Acid
Total Flow (mL/min)	0.4
Mode	Binary Gradient

Table 2. LC-MS Instrument Parameters

LC gradient was set according to **Table 3**.

Time (min)	**%MeOH**
0	10
15	100

Table 3. LC-MS Gradient

II.3.5 Bioassay sample preparation

LCMS sample preparation was carried out at the same time as samples were prepared for bioassay. A portion of the previously prepared solutions were added to pre-weighed sets of Eppendorf tubes so that the mass after solvent evaporation is in the following ranges for the assay: 0.3 – 2 mg for the *Mycoplasma* assay.

The solvent was evaporated with the Genevac EZ-2 Elite centrifugal evaporator. Eppendorf tubes were weighed to verify that the mass was sufficient to proceed to bioassay. Samples for the *Mycoplasma* assay were shipped dry.

For very small fractions, solutions of 1 mg/mL were prepared directly in the vials. In weighed Eppendorf tubes, the appropriate quantity of material for LC-MS analysis and bioassay was collected. The samples were vortexed and centrifuged like previously. For LCMS analysis, 100 µL of each sample was collected. Bioassays required 0.1 mg (minimum mass measurable on the scale).

II.3.6 Fractionation

Fractions that showed inhibitory activity were subjected to further purification on a C_{18} HPLC column (5µm, 250 × 21.2 mm) at a flow rate of 10 mL/min with the linear gradients that are described for each fraction in the following paragraphs. Every run was completed with a 100% MeOH wash, followed by a 5-minute column reconditioning to set MeOH/H_2O concentrations at the starting values for the next run. Each fraction was prepared for preparative HPLC by adding a volume of MeOH such that the concentration was 100 mg/mL.

Fractions 6I, 6J and 6K were respectively fractionated into 8 fractions 174MM9A-H, 11 fractions 174MM11A-K, and 9 fractions 174MM12A-I. The methods used for separation are described below (**Table 4**).

Fraction	Time (min)	%MeOH start	%MeOH end	Duration of 100% MeOH rinse (min)
6I	25	60	90	4
6J	25	70	100	10
6K	35	70	100	5

Table 4. Preparative HPLC gradients for purification of 174MM6I-K

Fraction 6I yielded subfractions 9A (3.1 mg), 9B (28.8 mg), 9C (12.7 mg), 9D (16.1 mg), 9E (7.7 mg), 9F (11.6 mg), 9G (102 mg) and 9H (54.8 mg). Fraction 6J gave subfractions 11A (2.8 mg), 11B (3.6 mg), 11C (3.1 mg), 11D (6.4 mg), 11E (6.9 mg), 11F (4.2 mg), 11G (10.4 mg), 11H (30.1 mg), 11I (6.4 mg), 11J (72.7 mg) and 11K (76.1 mg). Fraction 6K provided subfractions 12A (0.8 mg), 12B (0.5 mg), 12C (0.5 mg), 12D (0.5 mg), 12E (0.5 mg), 12F (4.1 mg), 12G (0.9 mg), 12H (44.2 mg) and 12I (12.6 mg).

The last subfractions (9H, 11K and 12I) are additional fractions created from the insoluble material collected at the bottom of the Eppendorf tubes after centrifuging before HPLC injection.

The fractions that showed the best activity were (**Appendix I.3**):

- 11D, 11E, 11F, 11G and 11H with a MIC90 of 3.2ug/mL.
- 9G, 11H, 11I, 12F and 12G with a MIC90 of 6.3ug/mL.

II.3.7 Further fractionation and isolation

The fractions with the best activity were further purified with HPLC semi-preparative columns. Usually, at the end of this step, pure compounds were collected, and structural characterization could begin.

Only fractions that had the best activity (MIC90 <6.3 µg/ml), had ample available material, and presented the fewest peaks in LCMS analysis were further fractionated. Therefore, given these three parameters, only fractions 11F, 11G, 11H and 12G were fractionated on semi-preparative HPLC columns according to **Table 5**.

Fraction	Time (min)	%CH3CN	Column
11F	13	75	Gemini 5 µm C18, 250 x 10mm
11G	12	60	Kinetex 5 µm F5, 250 x 10mm
11H	18	85	Gemini 5 µm C18, 250 x 10mm
12G	13	75	Gemini 5 µm C18, 250 x 10mm

Table 5. Semi-preparative HPLC isocratic methods used for AT

Fraction 11F was fractionated into 19A (2.9 mg) and 19B (0.8 mg). Fraction 11G gave fractions 22A (6.9 mg), 22B (1.2 mg), 22C (0.3 mg), 22D (0.9 mg) and 22E (0.6 mg). Fraction 11H yielded fractions 21A (14.4 mg), 21B (2.4 mg) and 21C (2.2 mg). Fraction 12G provided fractions 20A (0.5 mg) and 20B (0.4 mg). The most active fractions were 19A and 22C (**Appendix I.4**).

Chapter III : Secondary metabolites from the fungus *Remersonia thermophila*

III.1 Introduction

This third chapter focuses on the extraction of compounds from *Remersonia thermophila*, a fungus which has shown antitrichomonal activity in preliminary screenings.

The study of this fungus and its active metabolites was facilitated through the usage of a bioassay-guided fractionation process. This technique was used to quickly separate the targeted active fractions with their active compounds from the ones that weren't active. At each fractionation step, fractions were tested for biological activity before further extraction and purification. Several cycles of this procedure enabled the targeting of specific fractions until the active compounds were isolated.

The active compounds were then chemically characterized using a wide variety of methods. In the case of known molecules, analytical methods such as LCMS in addition to the use of online libraries enabled the structural characterization of the compounds. For novel scaffolds or new derivatives, the structures were primarily established through extensive 1D and 2D NMR experiments, as well as the methods detailed previously. The absolute configuration of a compound can be deduced through NOESY NMR, as well as ECD and VCD calculations.

The second part of this chapter details the structural characterization of two compounds 31C and 52C that possess a novel chemical scaffold. This chapter will detail how the compounds were discovered and compare them to known molecules in the literature. Finally, the structural characterization through several analytical techniques and the elucidation of the

absolute configuration of these two molecules which possess seven stereocenters will be detailed.

III.2 Results and Discussion

III.2.1 Scale-up

This fungus showed inhibitory activity of *T. vaginalis* in the preliminary screenings. To characterize the bioactive compounds produced by the fungus, a scale up was required to allow for sufficient metabolite production. Therefore, *R. thermophila* was grown on Cheerios breakfast cereal (**Figure 10**) in three large mycobags.

Figure 10. *Remersonia thermophila* grown on Cheerios breakfast cereal

The metabolites produced by *R. thermophila* went through several rounds of purification until the compounds of interest were separated from the other metabolites. An additional scale-up became necessary when the quantities of active compounds were not sufficient for characterization.

III.2.2 Establishing the standard procedure

As mentioned previously, the goal of this project was to find compounds that inhibited *T. vaginalis*. Compounds that possess these inhibiting properties, must also be able to cross the cell membrane to reach their target. Therefore, they must possess the appropriate chemical and physical propertied to do so. To find such compounds, an elaborate separation procedure must be established.

The following extraction and separation techniques were used: an organic extraction, a silica vacuum liquid chromatography and an HP20 VLC. Using a combination of solvents with different polarities and at varying concentrations, fractionation of a complex crude extract into smaller fractions was achieved. The process used here enabled the separation of the metabolites produced by the fungi. Primary metabolites such as DNA, carbohydrates, lipids, and other macromolecules are set aside whereas secondary metabolites are further fractionated.

A water/EtOAc partitioning separates the water-soluble primary metabolites from the organic soluble secondary metabolites (Fraction A). Lipids that were contained in the organic phase were extracted with a hexane/DCM solution (Fraction B). The use of three different mixtures of DCM and methanol yields compounds with different polarities (from least polar to most polar). This enables the separation of the most nonpolar compounds (Fraction C) soluble in DCM, from those that are slightly more polar (Fraction D), soluble in DCM: MeOH 1:1 and those that are MeOH soluble (Fraction E). Further fractionation was pursued with a gradient of DI water and methanol and the column was washed with a solution of DCM and MeOH. (Fraction K).

The next round of fractionations was performed with an HPLC, where methods were tailored to each fraction. Fractions were analyzed with the LCMS in between every

fractionation. With those parameters, it was possible to estimate the best elution conditions for the separation of the compounds in each fraction.

Therefore, the fractions that were active as well as the other fractions of interest were further fractionated on preparative columns then on semi-preparative columns (**Figures 11, 12**) where the used methods are detailed at the end of this Chapter. On the figures below, the active fractions are noted in red, the characterized compounds are in purple and the fractions that were insoluble in MeOH are in green. In some cases where the material could possibly clog the HPLC column, alternative separation methods were used, namely open column chromatography as in the first two steps of the procedure, and methods were developed to facilitate this process. The numbers next to the branches indicate the order in which fractions were obtained when multiple fractionations of the same extract were carried out with different separation methods.

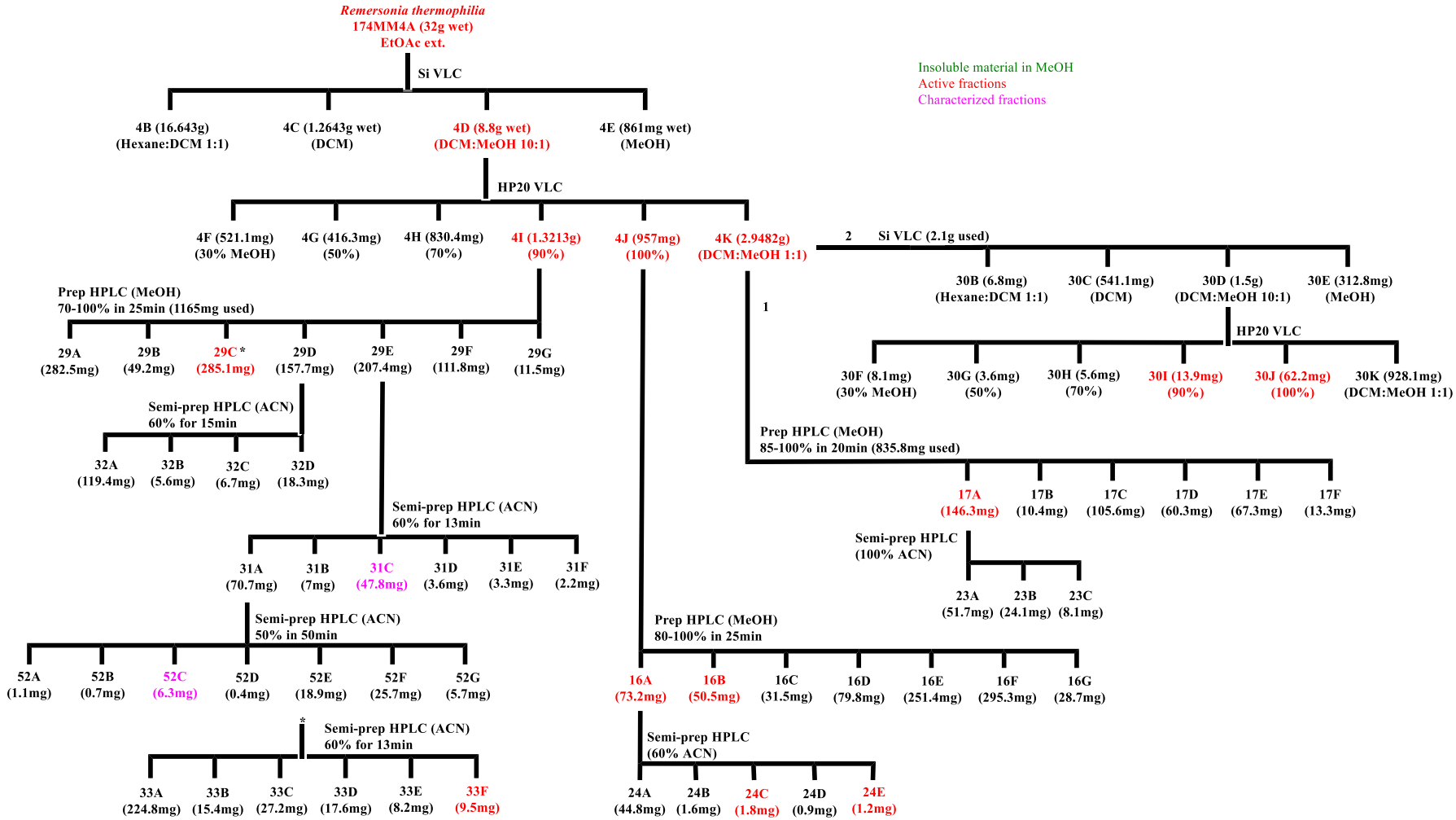

Figure 11. Fractionation template for *Remersonia thermophila*

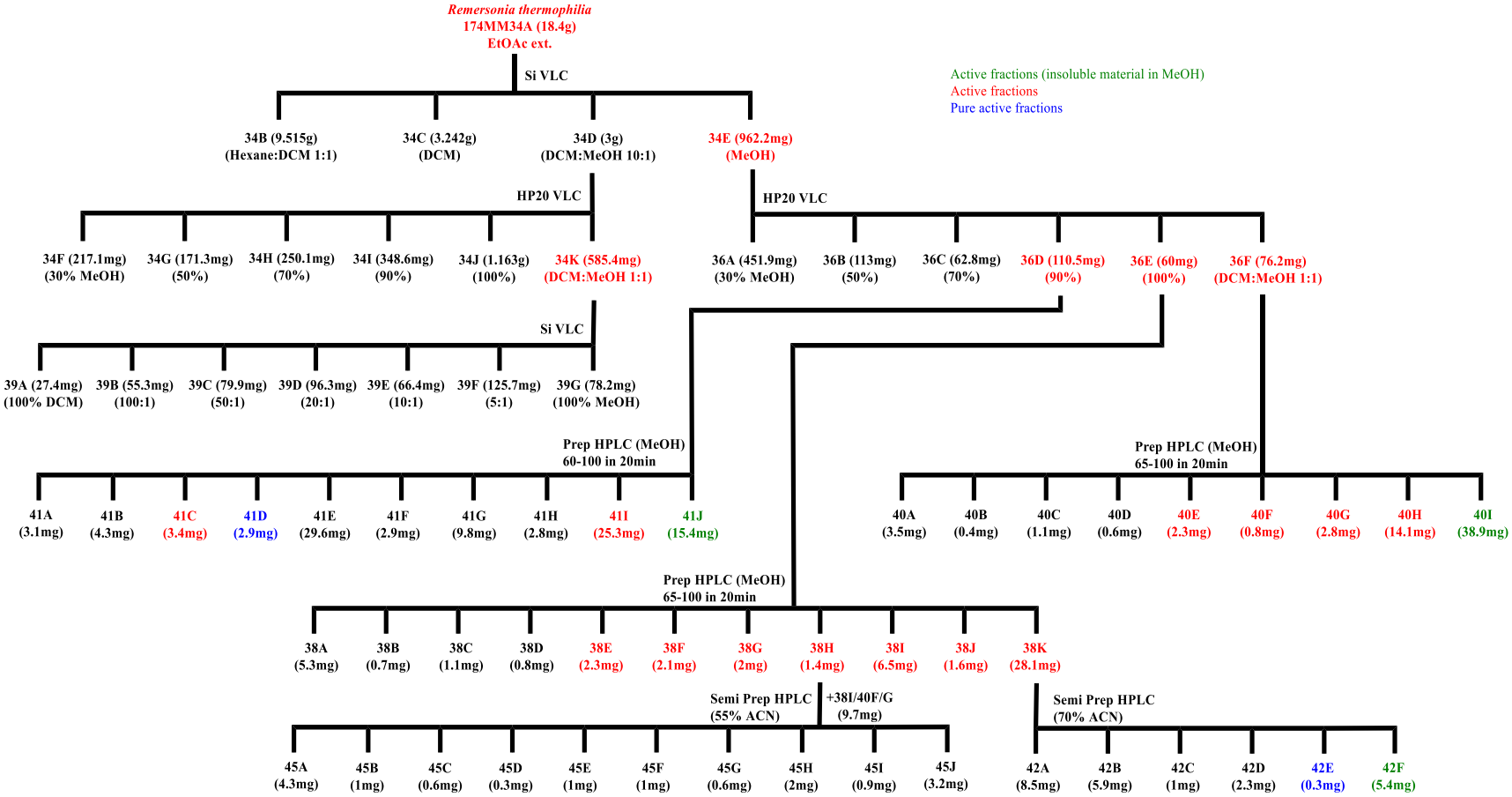

Figure 12. Fractionation template for *Remersonia thermophila*'s regrowth

III.2.3 Fractionation of *Remersonia thermophila*

III.2.3.1 Fractions requiring additional separation

Several fractions from *R. thermophila* required additional preparation for HPLC because of their polarity (apolar components). Indeed, it was quickly noted that the material from these fractions would clog the HPLC columns and extensive column washing would be needed for their elution. Therefore, these fractions were separated with flash chromatography.

To find the best elution conditions, a few solvents were examined. A DCM/MeOH was tested first in the following proportions: 100% MeOH, 3:1 DCM:MeOH and 9:1 DCM:MeOH. Water and acetonitrile mixes were tried next with 60% CH3CN and 100% CH3CN. Finally, a a toluene/ethyl acetate mix spiked with 1% AcOH. The results were reported in **Appendix III.23-25**. No clear separation was achieved, and the standard silica and HP20 procedure was applied on the remaining material from fraction 4K yielding fractions 30B-K (**Figure 11**) where 30I and 30J exhibited *T. vaginalis* inhibitory activity. Considering the amounts obtained for each fraction as well as the number of compounds present in each fraction, further fractionation was not carried out.

Fraction 34K from the regrowth also required further fractionation with flash chromatography. Given the previous insights into which solvents yielded the best separation, a DCM/MeOH gradient was selected. The following proportions were tested with TLCs: DCM 100%, DCM:MeOH 100:1, DCM:MeOH 50:1, DCM:MeOH 20:1, DCM:MeOH 10:1, DCM:MeOH 5:1, and DCM:MeOH 1:1. The best separation occurred between the 100:1 and 10:1 DCM:MeOH (**Appendix III.26**). Therefore, 34K was fractionated according to the previous figure (**Figure 12**).

III.2.3.2 Active fractions and isolated compounds

The *T. vaginalis* assay was carried out in house with a high-throughput and high-content screening system.[6] The results were expressed as the number of live trichomonads. Hence, the lower the number of live trichomonads was for a given fraction, the better the activity of that fraction. Results of the *T. vaginalis* assay (**Appendix II.6-22**) led to active fractions 24C, 24E, 29C, 30I, 30J and 33F in the first growth. In the regrowth, the active fractions were 38E-J, 40E-I, 41C-D, 41I-J, and 42E-F.

At the exception of fraction 38H, 38J, 40F, and 41D, none of the active fractions were pure enough for ^{1}H NMR. Among these fractions, a ^{1}H NMR spectrum was obtained only for fraction 41D, although it was of poor quality (**Appendix VI.43**). This compound was not present in the NPDG library of compounds and the Dictionary of Natural Products indicating that the compound was not known. Further characterization was not achieved due to unusable spectra in 2D NMR and no apparent peaks in ^{13}C NMR after an overnight experiment.

As the focus of this project shifted to characterizing new chemistry, pure compounds 31C and 52C were isolated from fraction 29E. The amount of material collected was more than enough for structural characterization. Hence, extensive NMR analysis (^{1}H, ^{13}C, COSY, HSQC, HMBC, NOESY) was carried out for each compound (**Appendix IV.29-35, V.36-42**).

III.2.4 Structural Characterization

Once the fractionation process was completed, pure compounds were collected. Thus, the remainder of this Chapter will focus on the structural characterization of these compounds with novel scaffolds, namely 31C and 52C. They will also be compared to the literature, more specifically to scaffolds that have already been described.

Fractionation of 29E yielded fractions 31A-F, with further fractionation of 31A yielding 52C. 31C and 52C's retention times (**Figure 13**) were 9.71 and 9.59 respectively.

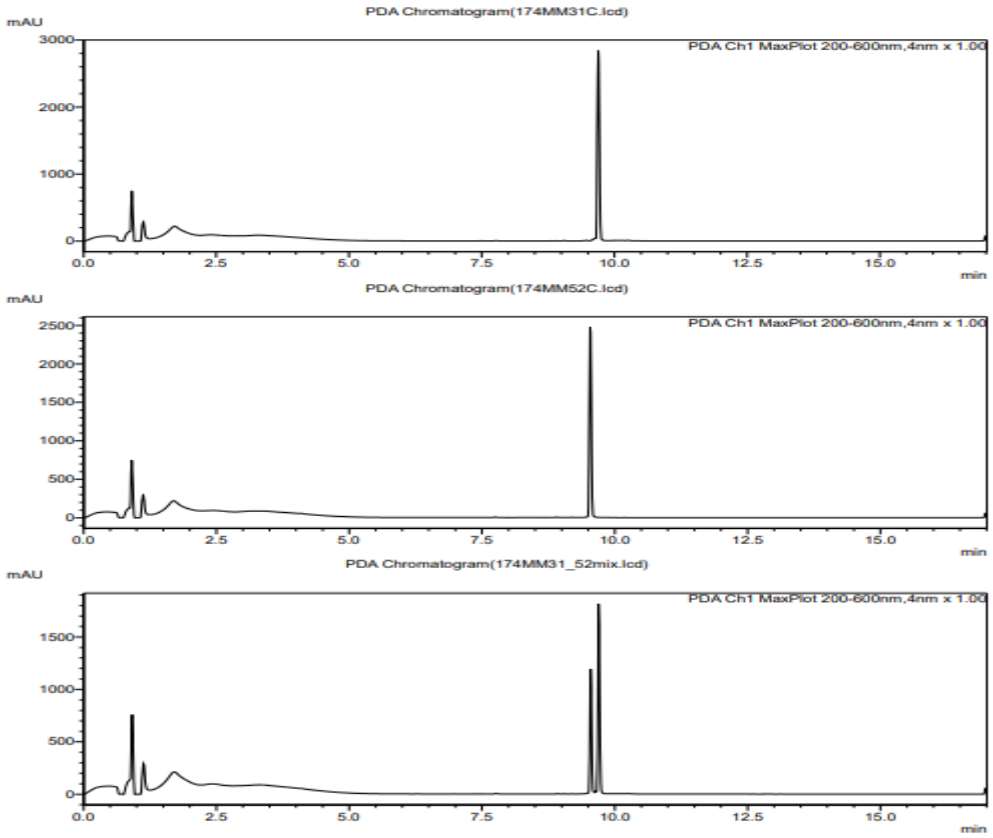

Figure 13. LC-MS chromatograms of 31C, 52C and an equimolar mix of both (from top to bottom)

III.2.4.1 Characterization of 31C

The molecular formula for 31C was established to be $C_{23}H_{31}NO_4$ based on a combination of LCMS data with ^{1}H and ^{13}C NMR data in MeOH and DMSO (**Appendix IV.27-31**). Two prominent peaks were observed [m/z 386 $[M + H]^+$] and [m/z 384 $[M - H]^-$] in LCMS ESI^+ and ESI^- modes suggesting m/z 385 (**Appendix IV.27**). The odd nominal mass indicated an odd number of nitrogens in the compound.

^{1}H NMR was first collected in MeOH. In addition to the molecular weight obtained with the LCMS, it still wasn't possible to get the exact molecular formula. Indeed, in correlation

NMR, the length of the carbon chains hinted at oxygen and nitrogen interspacing. At this point the only exact information was the number of carbons and the mass. Therefore, the solvent for ^{1}H NMR was changed from MeOH to DMSO due to its aprotic properties. Two additional signals appeared in ^{1}H NMR and the exact number of hydrogens in the compound was found. Subtracting the mass of the carbons and hydrogens as well as the mass of the nitrogen, the number of oxygens was found, and the molecular formula was established.

The molecular formula was confirmed through HRESIMS (**Appendix IV.28**). The compound's molecular formula was considered exact if its experimental mass (from HRESIMS) was equal to the theoretical mass with a maximum mass error of 5ppm. $C_{23}H_{31}NO_4$ has a calculated [m/z 386.2326 $[M + H]^+$]. The mass error associated with the $[M + H]^+$ peak equaled 0.0019. Therefore, $m/z \in [386.2307;386.2345]$. HRESIMS data showed a prominent peak [m/z 386.2333 $[M + H]^+$]. This *m/z* value was included in the previous range; therefore, the established molecular formula was correct. The same principle could be applied to the $[M + Na]^+$ peak, which would lead to the same conclusion.

The next step was to structurally characterize the compound. Using the molecular formula, the degree of unsaturation was calculated. The molecule had nine units of unsaturation. The ^{13}C NMR spectrum enabled the identification of five units of unsaturation. Two units of unsaturation were caused by alkenes, two others were identified as carbonyls (δ_C 207.73 and 208.06) and the last known unsaturation was an amide (δ_C 169.94). The four remaining units of unsaturation were assumed to be rings, one involving the amide. Indeed, the amide shift obtained experimentally was upfield compared to the expected shift of an amide and was within the expected shift of a cyclic amide.

Along with the previously assigned data, combined ^{1}H, ^{13}C, and HSQC NMR data (**Appendix IV.32**) indicated the presence of one oxymethine (δ_C 60.05), three sp^2 methines (δ_C

122.83, 128.61 and 128.93), a nonprotonated sp^2 carbon (δ_C 135.27), five methylenes (δ_C 15.69, 26.82, 27.53, 28, and 29.95), three aliphatic methyls (δ_C 12.82, 18.69 and 22.64), and two quaternary carbons (δ_C 45 and 74.06). COSY correlations revealed three isolated spin systems: H_1-H_2-H_3-H_4-H_5-H_6, H_8-H_7-H_{11}-H_{12}-H_{13} and H_{20}-H_{21}-H_{22}-H_{23}. Consolidation of the data obtained from ^1H, ^{13}C, ^1H–^{13}C HSQC in addition to the data from ^1H–^{13}C HMBC and ^1H–^1H COSY NMR (**Appendix IV.33,34**) enabled the elucidation of the compound's bond-line structure (**Figure 14**) which will be detailed in the following paragraphs.

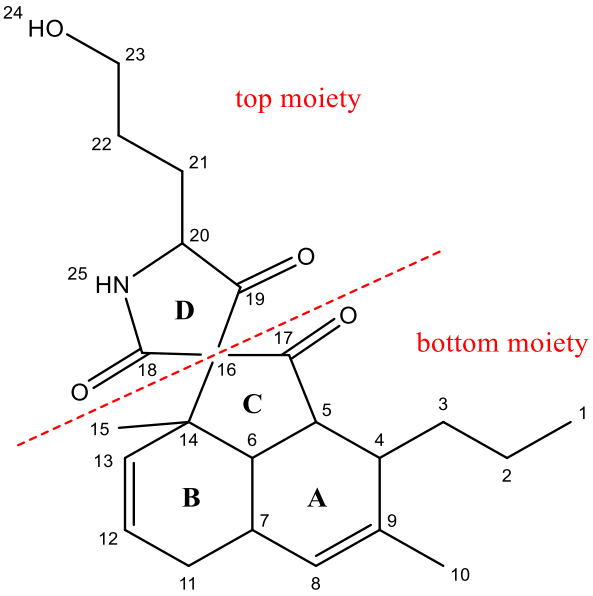

Figure 14. Bond-line structure of 31C with labeled carbons and rings

HMBC correlations between C-8 with C-6 and C-4, as well as the correlation between C-5 and C-7, along with the alkene bond between C-8 and C-9 established ring **A** (correlation of H-8/C-10) (see **Figure 14**). Additional C-6/C-14 HMBC correlation with the COSY resolved H_8-H_7-H_{11}-H_{12}-H_{13} established ring **B**. The methyl (H-15) correlated with C-14 and C-13 indicating its position on C-14.

Two of the four previously mentioned rings were left for assignment. Parts of the two previously established rings A and B as well as the correlations between H-15/C-14 and C-16

along with H-5/C-17 and C-16, allow for the identification of the third ring **C** which is a cyclopentanone (C-17 ketone). One unit of unsaturation, a carbonyl, an amide (intramolecular), and C-20 remained, and the quaternary carbon C-16 had two unassigned bonds. HMBC correlations between H-20/C-18 and C-19 enabled the elucidation of the last five membered ring **D** in the compound.

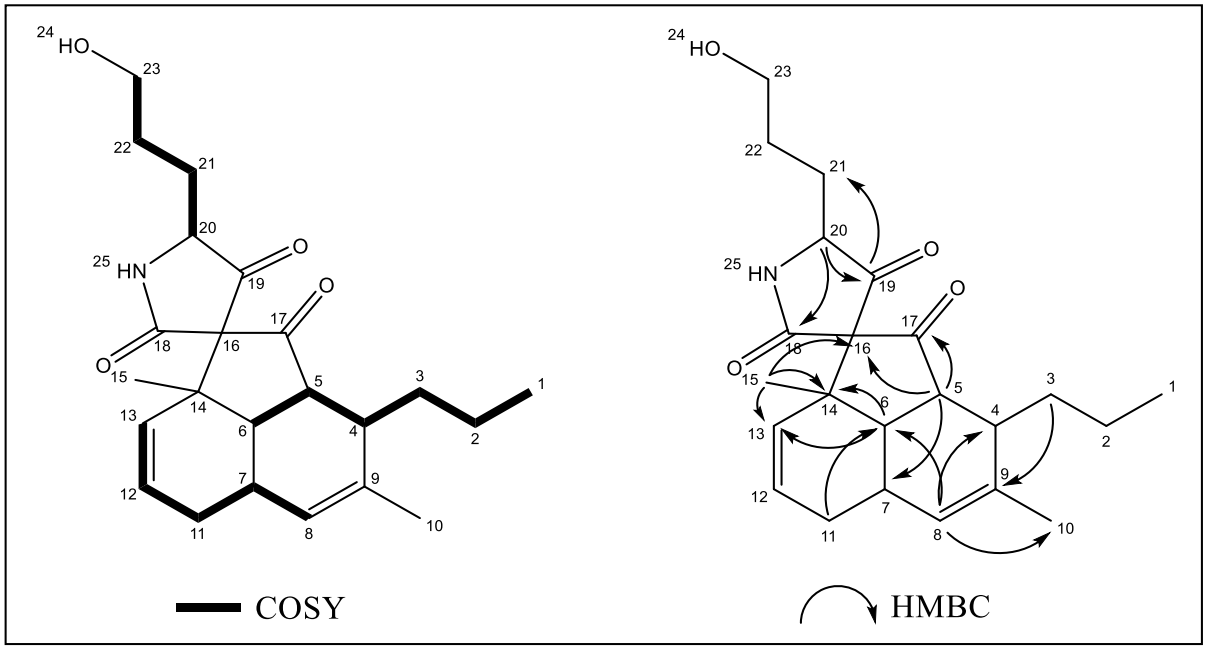

Figure 15. Key COSY and HMBC correlations for 31C

NMR spectroscopic data **(**^{1}H 600 MHz, ^{13}C 150 MHz**)** for compound 31C in MeOH-d_4 was regrouped in the following table (**Table 6**).

Position	δ_C, type	δ_H (*J* in Hz)	COSY	HMBC	NOESY
1	12.82, CH3	0.92, t	2	2, 3	
2	15.69, CH2	Hα: 1.05, m	1,3		
		Hβ: 1.27, m	1,3	4	5 b
3	29.95, CH2	Hα: 1.61, m	2,4		
		Hβ: 1.95, m	2,4		
4	40.56, CH	2.44, d (10.5)	3α, 3β, 5	5	
5	47.47, CH	2.62, dd (14.1, 10.5)	4,6	7, 17	2
6	43.85, CH	2.33, dd (14.1, 3.7)	5	11, 14	7, 15 b
7	27.53, CH	2.53, ddt (10.6, 5.3, 3.7)	11α, 8	9, 11	6, 8, 15
8	128.61, CH	5.78, d (6.2)	7	4, 6, 10	10, 11
9	135.27, C			10	
10	18.69, CH3	1.69, s		4	8
11	26.82, CH2	Hα: 1.76, m	7	13	8, 12
		Hβ: 2.36, m	12		
12	122.83, CH	5.66, ddd (10.4, 5.3, 2.3)	11β, 13	11, 13	11
13	128.93, CH	5.83, d (10.4)			15
14	45, C				
15	22.64, CH3	1.21, s		6, 13, 14, 16	6, 7, 13
16	74.06, C				
17	208.06, C				
18	169.94, C				
19	207.73, C			21, 22	
20	61.88, CH	3.95, dd (8.1, 5.3)	21α, 21β	18, 19	21α, 21β
21	28, CH2	Hα: 1.66, m	20, 22	20, 23	20
		Hβ: 1.84, m	20, 22		
22	27.52, CH2	1.66-1.68, m	21α, 21β, 23		
23	60.05, CH2	3.61, t (6)	22		21α, 21β
23-OH			23		
NH		a			

[a] Not observed

[b] 3D confirmed

Table 6. NMR Spectroscopic Data (^{1}H 500 MHz, ^{13}C 150 MHz) for 31C in MeOH-d_4

Once the bond-line structure was established, the absolute configuration of the compound was established. Molecule 31C contained seven asymmetric carbons indicating seven stereocenters to solve. A first step in resolving the configuration of this compound was

to establish the relative configuration of these seven carbons through space correlation methods such as NOESY and ROESY NMR which can also be coupled with 3D modeling. The remaining stereocenters which were not assigned through these methods, were assigned through electronic circular dichroism (ECD) and vibrational circular dichroism (VCD) data.

With the coupling constants obtained in ^{1}H NMR, three carbons relative configurations were immediately resolved. Indeed, a coupling constant of $J_{5\text{-}6}$= 14.1 Hz was observed for H-5/H-6 indicating that these protons were in a *trans* configuration. On the other hand, the other coupling constant ($J_{6\text{-}7}$= 4.2 Hz) enabled the elucidation of H-7's relative configuration to H-6 as *cis*. 2D NOESY confirms H-6/H-7's *cis* configuration (**Appendix IV.35**). 2D NOESY (**Figure 16**) also revealed key correlations between H-6/H-15 and H-7/H-15 which resolved C-15's configuration relative to C-6 and C-7. Indeed, these correlations indicated a *cis* configuration between C-15/C-6 and C-15/C-7 which agreed with the previous assignment of C-6/C-7 as *cis*.

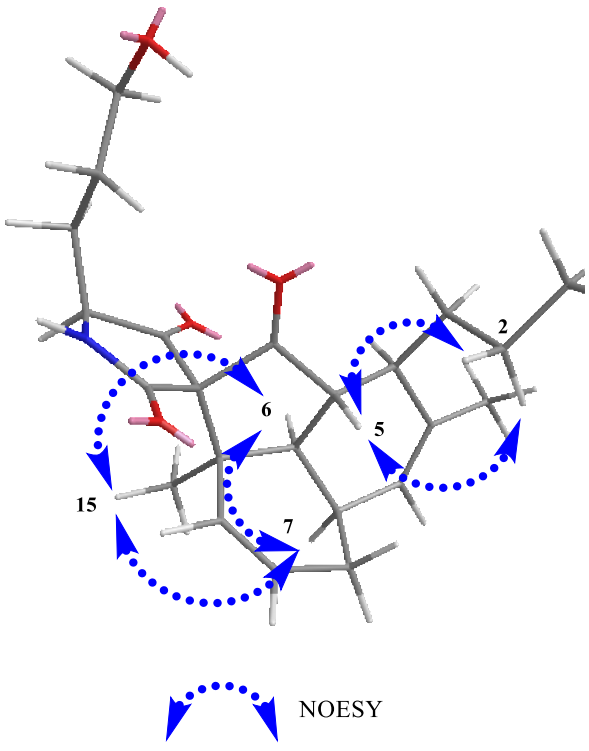

Figure 16. Key NOESY correlations of 31C

Finally, C-4's configuration was established and the relative configuration of the bottom moiety of 31C was solved. A coupling constant equal to 10.5 Hz was observed between H-4 and H-5. However, this could be equally indicative of a *trans*, or *cis* configuration and further analysis was needed. NOESY NMR provided a correlation between H-2 and H-5. 3D modeling with Chem3D was required to solve the configuration of C-4. The two possibilities ((*R**) C-4 and (*S**) C-4) are drawn below (**Figure 17**). This of course could also be drawn for C-5, C-6, C-7 and C-14 in the (*S**)-configuration. To simplify, the structures were only drawn with C-5, C-6, C-7 and C-14 in the (*R**)-configuration in the following figure and will be discussed as such in the next paragraphs.

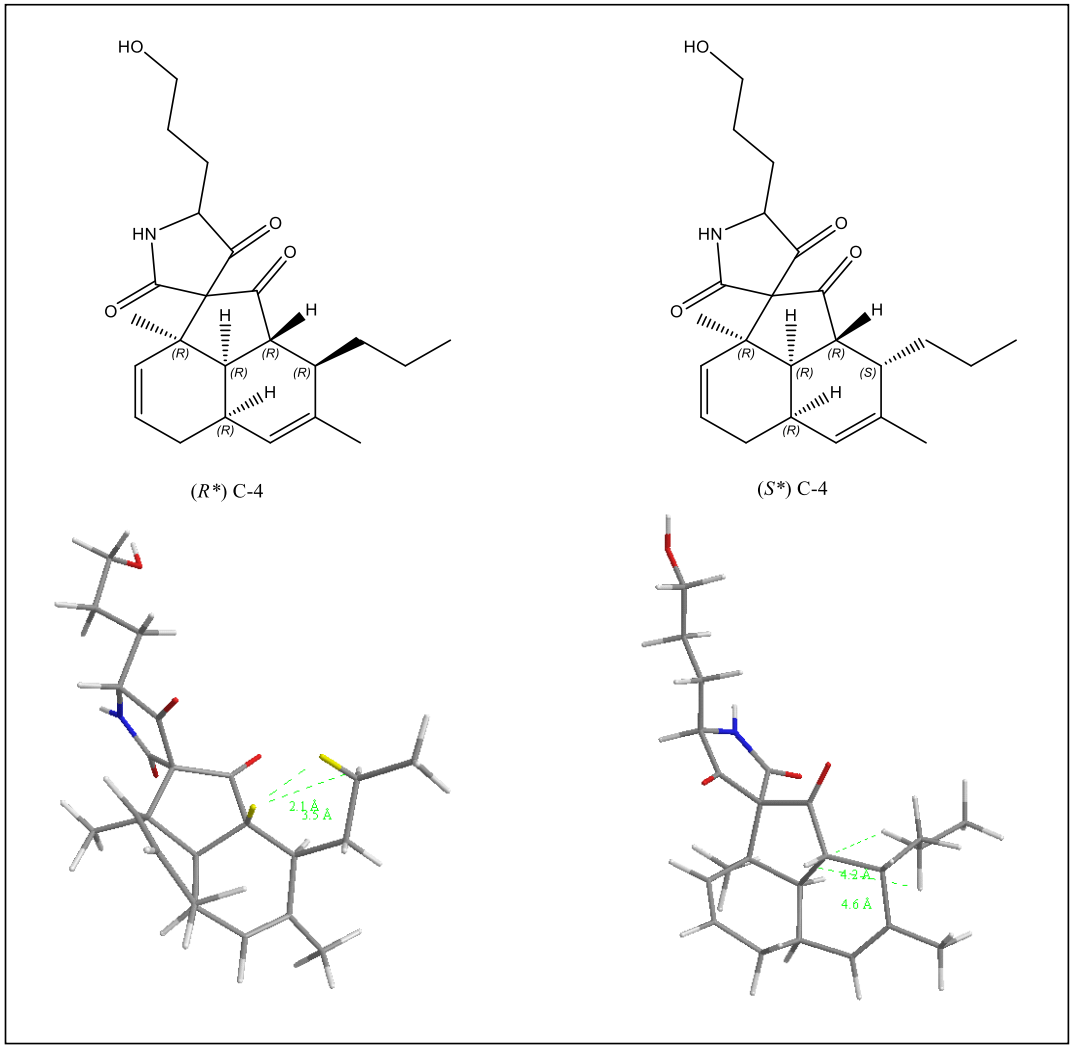

Figure 17. The two possibilities for C-4's configuration with their associated 3D models

The distances between H-2 and H-5 were also added in the above figure. When C-4 was in the (*S**)-configuration, the distances between H-2 and H-5 were too great (>3 Å) for proton coupling which meant that they would not correlate. Hence, a nuclear Overhauser effect (NOE) could not be observed in NOESY NMR. Therefore, it was established that H-5/H-4 were in a *trans* configuration. Moreover, this could also be confirmed if we were to expect that C-4 was in the (*S**)-configuration. Indeed, in the (*S**)-configuration, the dihedral angle between H-5 and H-4 was 35° ($J_{4\text{-}5}$= 4 Hz expected). The experimental coupling constant of $J_{4\text{-}5}$= 10.5 Hz invalidated the (*S**)-configuration. However, in the (R*)-configuration, the same dihedral angle equaled 130° ($J_{4\text{-}5}$= 9 Hz anticipated), therefore, C-4 was in a (R*)-configuration.

Five out of the seven stereocenters were assigned at this point. So far, 31C was either (*4R, 5R, 6R, 7R, 14R*)-31C or (*4S, 5S, 6S, 7S, 14S*)-31C. C-16 and C-20's configuration remained. The two unassigned carbons meant that were 2^n possibilities (n being the number of remaining carbons to assign) for the configuration of 31C. Hence, there were four possible stereoisomers (31C_1-4), and their structures are drawn in **Figure 18**. As mentioned previously, the same configurations of C-16 and C-20 exist with the bottom moiety (see **Figure 14**) having the opposite stereochemistry. Therefore, there were eight possible stereoisomers, half of which were drawn below.

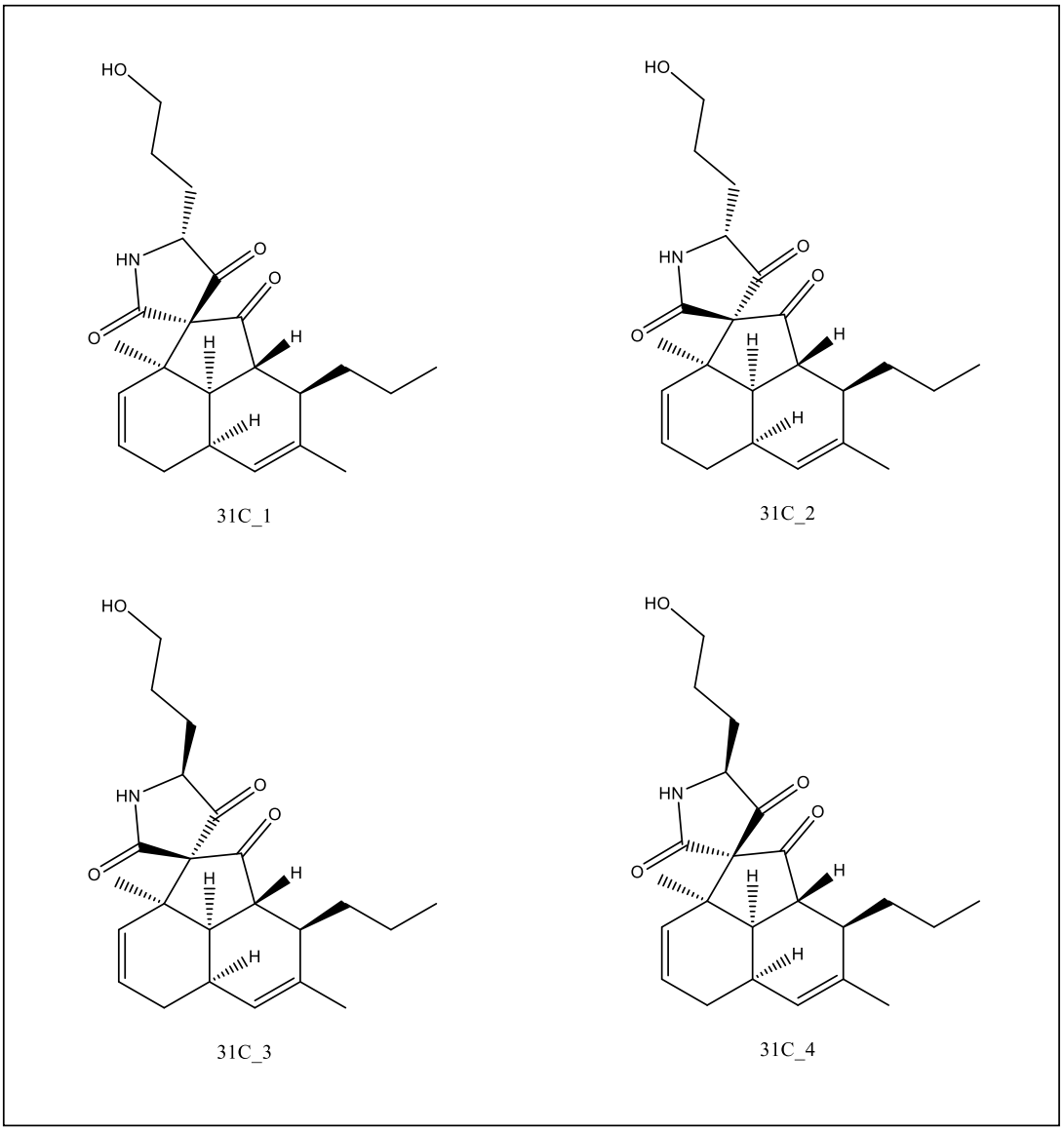

Figure 18. Possible conformers for 31C

The absolute configuration of C-16 and C-20 were determined by ECD. Specifically, 31C's experimental ECD spectrum was compared with the DFT quantum mechanical calculated ECD spectrum of the four previously drawn stereoisomers (**Figure 19**).

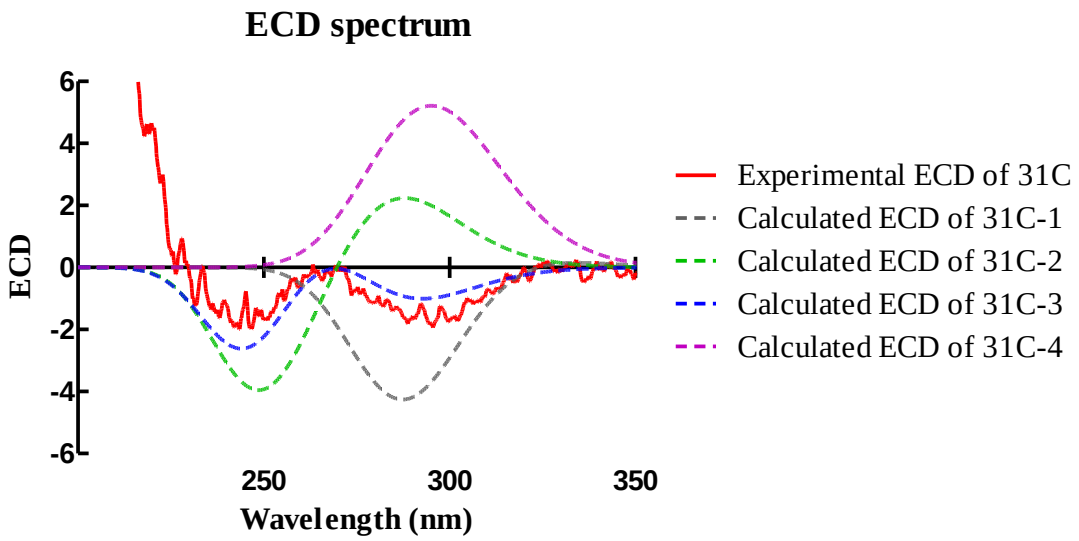

Figure 19. Experimental vs calculated ECD spectra of 31C

The calculated ECD spectrum of the 31C-3 isomer was matched with the experimental ECD of 31C, supporting the assignment of the absolute configuration of the top moiety of 31C as (*16R, 20S*)-31C. The two possible configurations (*4R*, 5R*, 6R*, 7R*, 14R*, 16R, 20S*)-31C and (*4S*, 5S*, 6S*, 7S*, 14S*, 16R, 20S*)-31C are represented below (**Figure 20**).

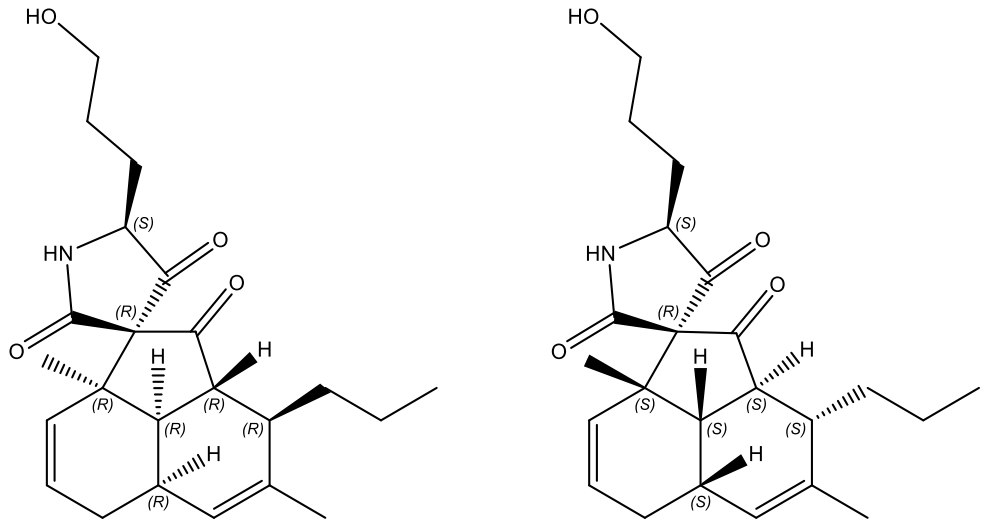

Figure 20. Structures of 31C

Further analysis was required to establish which one of the above configurations of 31C was correct. The absolute configuration of 31C will be established through VCD calculations at the same time as compound 52C (a stereoisomer of 31C) is characterized in the following paragraphs.

III.2.4.2 Characterization of 52C

Compound 52C was isolated from 31A's fractionation. NMR spectroscopic data **(**^{1}H 600 MHz, ^{13}C 150 MHz**)** for compound 52C in MeOH-d_4 was collected in the table below (**Table 7)** (**Appendix V.36-42**).

Position	δ_C, type	δ_H (*J* in Hz)	COSY	HMBC	NOESY
1	14.92, CH3	0.9, t	2	2, 3	
2	17.74, CH2	Hα: 1.03, m	1,3		
		Hβ: 1.26, m	1,3	4	5 b
3	31.96, CH2	Hα: 1.6, m	2,4		
		Hβ: 1.96, m	2,4		
4	42.42, CH	2.44, d (10.8)	3α, 3β, 5	5	
5	49.41, CH	2.53, dd (13.9, 10.8)	4,6	7, 17	2
6	45.91, CH	2.27, dd (13.9, 4.3)	5	11, 14	7, 15 b
7	29.67, CH	2.51, m	11α, 8	9, 11	6, 8, 15
8	130.67, CH	5.77, d (6.2)	7	4, 6, 10	10, 11
9	137.47, C			10	
10	20.77, CH3	1.68, s		4	8
11	28.97, CH2	Hα: 1.72, m	7	13	8, 12
		Hβ: 2.38, m	12		
12	125.51, CH	5.66, ddd (10.5, 5.1, 2.2)	11β, 13	11, 13	11
13	130.75, CH	5.73, d (10.7)			15
14	47.88, C				
15	24.18, CH3	1.21, s		6, 13, 14, 16	6, 7, 13
16	76.07, C				
17	211.03, C				
18	172.07, C				
19	210.79, C			21, 22	
20	64.65, CH	4.01, dd (6.4, 5)	21α, 21β	18, 19	21α, 21β
21	29.16, CH2	Hα: 1.72, m	20, 22	20, 23	20
		Hβ: 1.88, m	20, 22		
22	29.04, CH	1.63, m	21α, 21β, 23		
23	62.42, CH2	3.58, t (6)	22		21α, 21β
23-OH			23		
NH		a			

[a] Not observed

[b] 3D confirmed

Table 7. NMR Spectroscopic Data (^{1}H 500 MHz, ^{13}C 150 MHz) for 52C in MeOH-d$_4$

The molecular weight of 385 g/mol, along with the similar ^{1}H, ^{13}C (equal number of protons and carbons) and the fact that the correlations in 2D NMR were the same, led to believe

that this compound was a stereoisomer of previously characterized compound 31C. Protons that moved upfield or downfield from 31C to 52C were zoomed in on (**Figure 21**). Significant differences ($\Delta\delta_C$ > 0.5ppm) between 31C and 52C in ^{13}C NMR were highlighted in **Figure 22**.

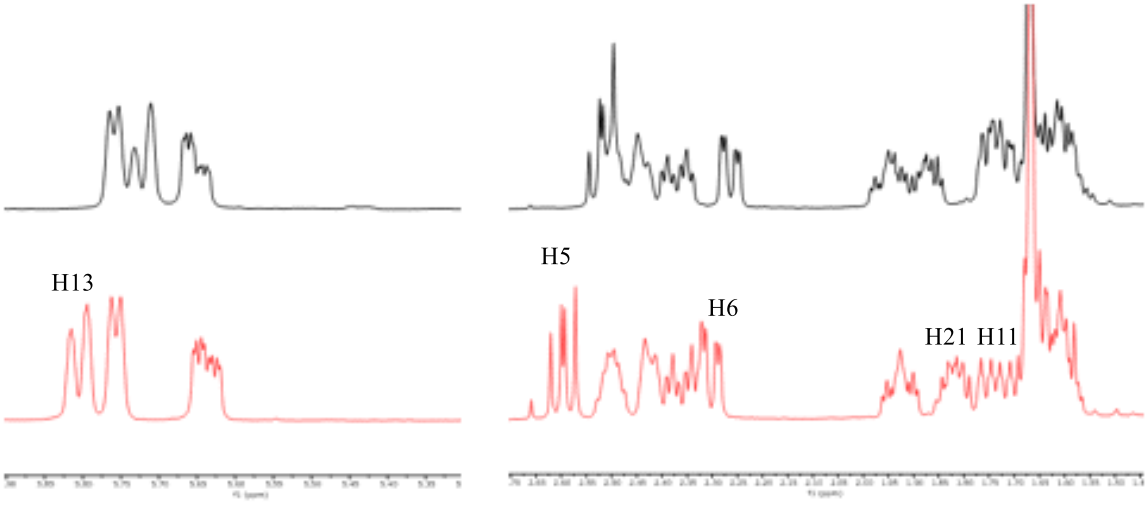

Figure 21. Zoom on the peaks that differ (labeled) between 31C and 52C in ^{1}H NMR

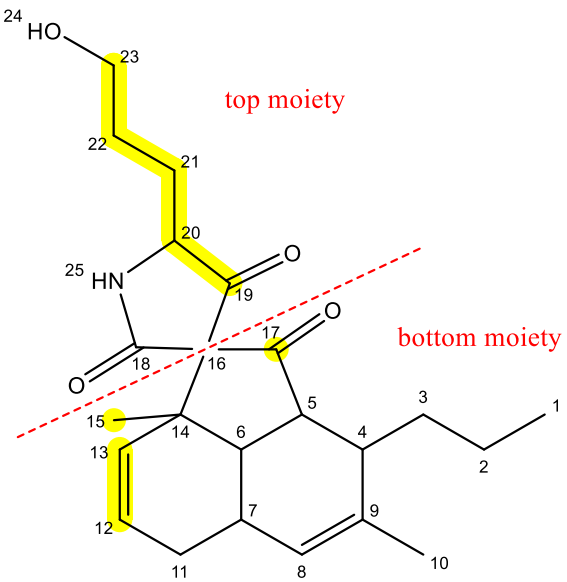

Figure 22. ^{13}C NMR signals that differ (highlighted) between 31C and 52C

The coupling constants between C-4, C-5, C-6, and C-7 of $J_{4\text{-}5}$= 10.7 Hz, $J_{5\text{-}6}$= 13.9 Hz, $J_{6\text{-}7}$= 4.3 Hz indicated that their relative configuration was *trans*, *trans* and *cis* respectively as

in 31C. This was further confirmed by NOESY NMR where the same three correlations were noted. This information, along with the carbon signals that shifted significantly between 31C and 52C being localized exclusively on the top moiety and around C-14 (**Figure 22**) indicated that either the stereocenters of the top moiety or those of the bottom moiety were inversed in 52C.

The ECD spectrum of 52C was measured. It's resemblance to 31C's ECD spectrum confirmed that C-16 and C-20 were in the same configuration (*16R* and *20S*) in 31C and 52C. As the ECD spectrum of 31C was first calculated for the (*4R**, *5R**, *6R**, *7R**, *14R**, *16R*, *20S*)-configuration, it was also calculated for the (*4S**, *5S**, *6S**, *7S**, *14S**, *16R*, *20S*)-configuration and was compared to 52C's experimental spectrum (**Figure 23**) to confirm whether the bottom moiety could have opposite stereochemistry and present the same ECD spectrum. It is important to note that the following ECD spectrum was calculated with only one optimized conformer and with a different method than for 31C.

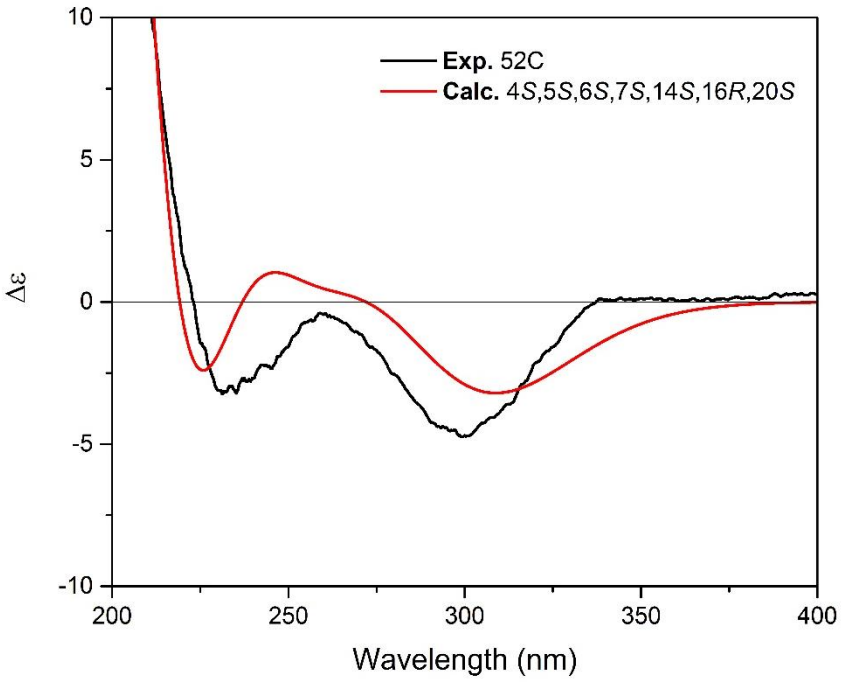

Figure 23. Experimental ECD of 52C and calculated ECD of (4S, 5S, 6S, 7S, 14S, 16R, 20S)-31C

The sign and intensity of the Cotton effects were very similar in both configurations. It was concluded that the Cotton effects produced by the stereocenters in the bottom moiety were either buried in the signals produced by C-16 and C-20 or they were not observable. ECD data was not sufficient to differentiate the two stereoisomers 31C and 52C which are both represented in **Figure 20**. The specific optical rotations of both compounds were determined: +350° for 31C and +24° for 52C. Comparison to the literature did not allow for elucidation.

The remaining known methods to attribute 31C and 52C's configuration were: VCD calculations or X-ray crystallography. Two separate attempts at crystallization did not produce suitable crystals for X-ray crystallography. Due to the VCD equipment malfunctioning, experimental data could not be collected, and calculations were not carried out. Therefore, the (*4R*, *5R*, *6R*, *7R*, *14R*, *16R*, *20S*) and (*4S*, *5S*, *6S*, *7S*, *14S*, *16R*, *20S*) configurations were not attributed to their respective compounds 31C and 52C.

During this fractionation process, two compounds, 31C and 52C were discovered. These two compounds, which were not described in the literature, possessed a novel scaffold. Indeed, only select parts of the molecule were described. The spiro structure of 31C and 52C was related to the spiro architecture of Altercrasin A whereas the acenaphthylene moiety was related to acenaphthylenone (**Figure 24**).[45-46]

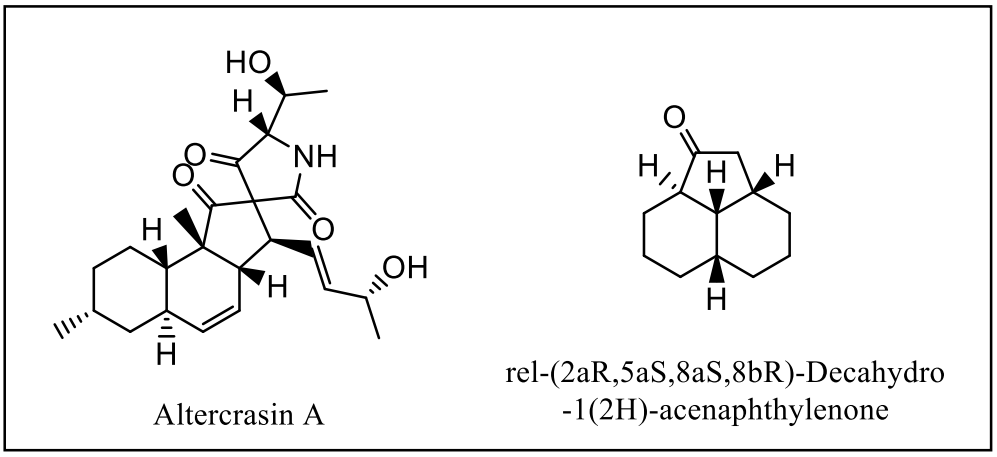

Figure 24. Similar scaffolds in CAS

However, a combination of these two subunits with the significant propane and propanol group substitutions as well as the two alkenes present in the acenaphthylene moiety distinguish this compound as containing a novel structural scaffold.

III.2.5 Conclusions

This chapter serves as a blueprint for future reference when proceeding with further fractionations of *Remersonia thermophila*. Indeed, since characterization of the active compounds produced by the fungus was not achieved, the beginning of this chapter details the methods that were developed for the isolation of active compounds with excellent activities 41D and 42E (<400 Live trichomonads) as well as the other active metabolites produced by the fungus. Both 41D and 42E showed great promise with activity levels below the 400 live trichomonads mark. Moreover, the active compounds from *R. thermophila* could not be dereplicated and this could point to the discovery of new active compounds which was further encouraged by the discovery of new chemistry. Further investigation with a scale-up to six bags or more is therefore highly recommended.

Within this chapter, the isolation and structural elucidation of two new compounds possessing seven stereocenters from *Remersonia thermophila* was described. The structural characterization was achieved through the combination of mass data with extensive 1D and 2D NMR spectroscopy. The relative configurations of 31C and 52C were established through NOESY NMR and 3D modeling. ECD calculations enabled the elucidation of the absolute configurations of two stereocenters. It is expected that VCD calculations enable the elucidation of the absolute configuration of the other five stereocenters in the bottom moiety, consequently allowing each configuration to be attributed to 31C or 52C. Therefore, in this chapter, a novel molecular scaffold which combined two previously described scaffolds with significant substitutions was found and reported for the first time. The inhibitory activities of these compounds remain to be tested and should be carried out on *T. vaginalis* as well as other diseases to determine if the scaffold shows promise in medicinal chemistry.

III.3 Materials and Methods

III.3.1 General Experimental Procedure

Column chromatography was conducted using silica gel and HP20SS. Preparative HPLC was performed using SCL-10A VP pumps and system controller with a Phenomenex Luna 5µm C_{18}(2) column (100Å, 250 mm x 21.2 mm) with a flow rate of 10 mL/min. Semi-preparative HPLC purification were performed using Waters 1525 binary pumps with a Waters 2998 PDA detector and either a Gemini 5µm C_{18} column (110Å, 250 mm x 10 mm), a Kinetex 5 µm F5 column (100 Å, 250 x 10 mm) or a Luna 5 µm C_{18} column (100 Å, 250 mm x 10 mm) with a flow rate of 4 mL/min.

All solvents were used as purchased without further purification unless mentioned. HPLC solvents for fractionation were of ACS grade or better (≥ 99.5%). NMR spectra were recorded on a Varian VNMRS DirectDrive spectrometer equipped with an indirect observe probe at 500 MHz for ^{1}H and at 150 MHz for ^{13}C. All 2D-NMR experiments were acquired with nonuniform sampling (NUS) set to 50%. Chemical shifts for proton and carbon resonances are reported in ppm (δ) relative to the residual protons in chloroform (δ 7.26), in DMSO (δ 2.5) and in methanol (δ 3.31, δ 4.78) as references. The LC-ESIMS analyses were conducted on a Shimadzu UFLC system with a quadrupole mass spectrometer using a Phenomenex Kinetex C18 column (3.0 mm × 75 mm, 2.6 µm) and MeOH-H2O (0.1% HCOOH) gradient solvent system. ECD spectra were obtained on a JASCO J-715 circular dichroism spectrometer. VCD spectra were obtained on a Biotools ChiralIR 2X vibrational circular dichroism spectrometer.

III.3.2 Fungal Material

The fungal isolate (internal designation MN4085 RBM-3) was obtained from a soil sample collected in a vegetable garden in Minneapolis, Minnesota. The isolate was identified as belonging to the species *Remersonia thermophila*.

The fungus was grown on Cheerios breakfast cereal supplemented with a 0.3% sucrose solution and 0.005% chloramphenicol in three large mycobags (Unicorn Bags, Plano, TX, USA). The fungus was grown for 4 weeks, whereupon it had achieved complete coverage of the solid substrate.

The fungal biomass was extracted by soaking overnight in ethyl acetate. The organic extract was subjected to partitioning two times against water (1:1, vol/vol). The ethyl acetate layer was retained, and the solvent removed by evaporation in vacuo, yielding 32 g of dark red organic-soluble material for the RT (174MM4A) colonized cheerios. A regrowth of RT, consisting of six large mycobags, which originally consisted of six large mycobags, of which three were unusable, yielded 18.4g of material (174MM34A). Due to previously mentioned contamination, a second regrowth of RT, consisting of two large mycobags, yielded 8.5g of material (174MM43A).

III.3.3 Large-scale extract pre-fractionation

III.3.3.1 Standard Procedure

The crude material obtained beforehand was subjected to silica gel chromatography using step-wide gradient consisting of (1) 50% Hexane-50% DCM; (2) 100% DCM; (3) 90% DCM-10% MeOH; and (4) 100% MeOH to give four fractions (Fractions B-E). Solvents were evaporated in vacuo and the remaining residues were transferred into pre-weighed vials.

Fraction D was further fractionated on a HP20 VLC column using the following series of solvents completed with water: (1) 30% MeOH; (2) 50% MeOH; (3) 70% MeOH; (4) 90% MeOH; (5) 100% MeOH; (6) 50% MeOH-50% DCM to give six fractions (Fractions F-K). The above procedure was also applied to fraction E when it was the active fraction.

III.3.3.2 Pre-fractionation of *Remersonia thermophila*

Through silica VLC, 174MM4A yielded fractions 174MM4B (16.643 g), 174MM4C (1.2643 g), 174MM4D (8.8 g), and 174MM4E (861 mg). The second fractionation with HP20 VLC of 174MM4D provided the following fractions: 174MM4F (521.1 mg), 174MM4G (416.3 mg), 174MM4H (830.4 mg), 174MM4I (1.3213 g), 174MM4J (957 mg), 174MM4K (2.9482 g).

Fractions 4I, 4J and 4K were biologically active in the *Trichomonas* assay with the highest activity for 4J (**Appendix II.6**).

For the regrowth, 174MM34A yielded fractions 174MM34B (9.515 g), 174MM34C (3.242 mg), 174MM34D (3 g), and 174MM34E (962.2 mg) through silica gel chromatography. HP20 VLC of 174MM34D provided the following fractions: 174MM34F (217.1 mg), 174MM34G (171.3 mg), 174MM34H (250.1 mg), 174MM34I (348.6 mg), 174MM34J (1.163 g) and 174MM34K (585.4 mg). HP20 VLC of 174MM34E yielded fractions: 174MM36A (451.9 mg), 174MM36B (113 mg), 174MM36C (62.8 mg), 174MM36D (110.5 mg), 174MM36E (60 mg) and 174MM36F (76.2 mg). An additional silica VLC of 174MM34K gave 7 fractions 174MM39A (27.4 mg), 174MM39B (55.3 mg), 174MM39C (79.9 mg), 174MM39D (96.3 mg), 174MM39E (66.4 mg), 174MM39F (125.7 mg) and 174MM39G (78.2 mg).

Fractions 34K, 34E, 36D, 36E and 36F showed trichomonas inhibitory activity (**Appendix II.14,15**). 34E, 36E and 36F showed the best inhibitory activity levels with the lowest number of live trichomonads (under 500).

III.3.4 LC-MS analysis

For every fraction, two sets of Eppendorf tubes were prepared. The first set was weighed empty and was sent for bioassay whereas the second one was used for LC-MS analysis.

Fractions were analyzed by LC-MS. The organic residues were solubilized in MeOH (5 mg/mL). The material was completely solubilized using a Branson 5510 sonicator. Further dilution in MeOH (0.5 mg/mL) was carried out in the second set of Eppendorf tubes. The samples are vortexed and centrifuged (14,800 rpm, 10 min) at room temperature. Aliquots consisting of 100 µL of samples prepared at 0.5 mg/mL were transferred to HPLC vials for LC-MS analysis. LC-MS instrument parameters can be found as follows below (**Table 8)**.

MS	
Acquisition Time (min)	15 min
Acquisition Mode	Scan
m/z Range	200-2000
Voltage (kV)	1.55
Interface	
DL Temperature (°C)	250
Heat Block Temperature (°C)	200
Nebulizing Gas Flow (mL/min)	1.5
Drying Gas Flow (mL/min)	10
Pump	
Solvent A	Methanol (MeOH)
Solvent B	Water + 0.1% Formic Acid
Total Flow (mL/min)	0.4
Mode	Binary Gradient

Table 8. LC-MS Instrument Parameters

LC gradient was set according to **Table 9**.

Time (min)	%MeOH
0	10
15	100

Table 9. LC-MS Gradient

III.3.5 Bioassay sample preparation

LCMS sample preparation was carried out at the same time as samples were prepared for bioassay. A portion of the previously prepared solutions were added to pre-weighed sets of Eppendorf tubes so that the mass after solvent evaporation is in the following ranges for the assay: 0.3 – 2 mg for the *Mycoplasma* assay.

The solvent was evaporated with the Genevac EZ-2 Elite centrifugal evaporator. Eppendorf tubes were weighed to verify that the mass was sufficient to proceed to bioassay. Samples for the *Mycoplasma* assay were shipped dry.

For very small fractions, solutions of 1 mg/mL were prepared directly in the vials. In weighed Eppendorf tubes, the appropriate quantity of material for LC-MS analysis and bioassay was collected. The samples were vortexed and centrifuged like previously. For LCMS analysis, 100 µL of each sample was collected. Bioassays required 0.1 mg (minimum mass measurable on the scale).

III.3.6 Fractionation

Fractions that showed inhibitory activity were subjected to further purification on a C_{18} HPLC column (5µm, 250 × 21.2 mm) at a flow rate of 10 mL/min with the linear gradients that are described for each fraction in the following paragraphs. Every run was completed with a 100% MeOH wash, followed by a 5-minute column reconditioning to set MeOH/H_2O concentrations at the starting values for the next run. Each fraction was prepared for preparative HPLC by adding a volume of MeOH such that the concentration was 100 mg/mL. Concentrations were lowered to 50 mg/mL when saturation occured.

Fractions 4I, 4J and 4K were respectively fractionated into :

- 7 fractions 174MM29A-G
- 7 fractions 174MM16A-G
- 6 fractions 174MM17A-F and 10 fractions 174MM30B-K through silica column chromatography

The methods used for separation are described below (**Table 10**).

Fraction	Time (min)	%MeOH start	%MeOH end	Duration of 100% MeOH rinse (min)
4I	25	70	100	4
4J	25	80	100	10
4K	20	85	100	10

Table 10. Preparative HPLC Gradients for purification of 174MM4I-K

Fraction 4I yielded subfractions 29A (282.5 mg), 29B (49.2 mg), 29C (285.1 mg), 29D (157.7 mg), 29E (207.4 mg), 29F (111.8 mg), and 29G (11.5 mg). 4J was fractionated into subfractions 16A (73.2 mg), 16B (50.5 mg), 16C (31.5 mg), 16D (79.8 mg), 16E (251.4 mg), 16F (295.3 mg) and 16H (28.7 mg). Fraction 4K provided subfractions 17A (148.6 mg), 17B (11.8 mg), 17C (108.1 mg), 17D (60.5 mg), 17E (68.3 mg) and 17F (13.3 mg).

Through silica VLC, the remaining 2.1g of 174MM4K yielded the fractions 174MM30B (6.8 mg), 174MM30C (541.1 mg), 174MM30D (1.5 g), and 174MM30E (312.8 mg). The second fractionation with HP20 VLC of 174MM30D provided the following fractions: 174MM30F (8.1 mg), 174MM30G (3.6 mg), 174MM30H (5.6 mg), 174MM30I (13.9 g), 174MM30J (62.2 mg), 174MM30K (928.1 mg).

The fractions from 4J and 4K that showed the best inhibitory activity in the trichomonas assay were 17A, 16A and 16B from most active to least active (**Appendix II.7, 8**). The most active fractions from 4I and the second fractionation of 4K (with the silica column) were fractions 29C and 30I (**Appendix II.9, 10**).

For the regrowth, fractions 36D, 36E and 36F were fractionated into 10 fractions 174MM41A-J, 11 fractions 174MM38A-K, and 9 fractions 174MM40A-I respectively. The methods used for separation are described below (**Table 11**).

Fraction	Time (min)	%MeOH start	%MeOH end
36D	20	60	100
36E	20	65	100
36F	20	65	100

Table 11. Preparative HPLC Gradients for purification of 174MM36D-F

Fraction 36D yielded subfractions 41A (3.1 mg), 41B (4.3 mg), 41C (3.4 mg), 41D (2.9 mg), 41E (29.6 mg), 41F (2.9 mg), 41G (9.8 mg), 41H (2.8 mg), 41I (25.3 mg) and 41J (15.4 mg). 36E was fractionated into subfractions 38A (5.3 mg), 38B (0.7 mg), 38C (1.1 mg), 38D (0.8 mg), 38E (2.3 mg), 38F (2.1 mg), 38G (2 mg), 38H (1.4 mg), 38I (6.5 mg), 38J (1.6 mg) and 38K (28.1 mg). Fraction 36F provided subfractions 40A (3.5 mg), 40B (0.4 mg), 40C (1.1 mg), 40D (0.6 mg), 40E (2.3 mg), 40F (0.8 mg), 40G (2.8 mg), 40H (14.1 mg), and 40I (38.9 mg).

The most active fractions from 36D, 36E and 36F in the trichomonas assay were 38I, 40H, 40I, 41C and 41I (**Appendix II.16, 18, 20**). Due to fraction purity and available material, only fractions 38H and 38K were further fractionated.

III.3.7 Further fractionation and isolation

The fractions with the best activity were further purified with HPLC semi-preparative columns. Pure compounds were collected after this step and structural characterization could begin.

Considering the quantities of each fraction and the number of peaks observed in the LC-MS chromatograms, fractions 16A and 17A could be further fractionated. 29C, 29D, 29E, and 31A although not active, were fractionated to obtain pure compounds in sufficient quantities

for structural characterization. Fractionation was conducted on semi-preparative HPLC columns according to **Table 12**.

Fraction	Time (min)	%CH3CN	Column
16A	16	60	Gemini 5 µm C18, 250 x 10mm
17A	14	100	Gemini 5 µm C18, 250 x 10mm
29C	15	60	Gemini 5 µm C18, 250 x 10mm
29D	15	60	Gemini 5 µm C18, 250 x 10mm
29E	13	60	Gemini 5 µm C18, 250 x 10mm
31A	50	50	Luna 5 µm C18, 250 x 10mm

Table 12. Semi-preparative HPLC isocratic methods used for RT

Fraction 16A yielded fractions 24A (44.8 mg), 24B (1.6 mg), 24C (1.8 mg), 24D (0.9 mg) and 24E (1.2 mg). Fraction 17A gave fractions 23A (51.7 mg), 23B (24.1 mg), and 23C (8.1 mg). The most active fractions were 24C and 24E (**Appendix II.12**).

Fraction 29C yielded 33A (224.8 mg), 33B (15.4 mg), 33C (27.2 mg), 33D (17.6 mg), 33E (8.2 mg) and 33F (9.5 mg). Fraction 29D was separated into 32A (119.4 mg), 32B (5.6 mg, tR = 7.8 min), 32C (6.7 mg) and 32D (18.3 mg). Fraction 29E was fractionated into 31A (70.7 mg), 31B (7 mg), 31C (47.8 mg, tR = 9.71 min), 31D (3.6 mg), 31E (3.3 mg) and 31F (2.2 mg). Fraction 31A yielded 52A (1.1 mg), 52B (0.7 mg), 52C (6.3 mg, tR = 9.59 min), 52D (0.4 mg), 52E (18.9 mg),52F (25.7 mg), and 52G (5.7 mg).

Fractionation of the material from the regrowth was carried out according to **Table 13**.

Fraction	Time (min)	%CH3CN	Column
38K	19	70	Gemini 5 µm C18, 250 x 10mm
38H	40	55	Gemini 5 µm C18, 250 x 10mm

Table 13. Semi-preparative HPLC isocratic methods used for RT regrowth

Fraction Fraction 38H yielded fractions 45A (4.3 mg), 45B (1 mg), 45C (0.6 mg), 45D (0.3 mg), 45E (1 mg), 45F (1 mg), 45G (0.6 mg), 45H (2 mg), 45I (0.9 mg), and 45J (3.2 mg). Fraction 38K gave fractions 42A (51.7 mg), 42B (5.9 mg), 42C (1 mg), 42D (2.3 mg), 42E (0.3 mg), and 42F (5.4 mg) . The most active fractions were 45I, 42E and 42F (**Appendix II.19, 22**).

III.3.8 Trichomonas Assay

A 250 µL aliquot of *T. vaginalis* cryopreserved in liquid N_2 with 5% DMSO was thawed rapidly at 37 °C and put into a screw cap tube containing 12 mL of prewarmed modified TYI-S-33 medium. The sample was incubated for 24 h at which point confluent growth of the parasite had occurred, and live trichomonads were counted (above 3.0×10^7 cells per tube). Stock cultures were diluted in fresh medium to achieve 40 000 trichomonads per 100 µL of medium in each well of a 96-well microtiter plate. Trichomonads were not exposed to normal atmospheric conditions for any longer than 30 min throughout setting up the assay. All experiments were conducted so that the amount of DMSO did not exceed 1% by volume. Assay consistency is established through vehicle-only (DMSO) and positive (25 µM metronidazole) controls. After 18 h of incubation, microtiter plates were removed and 100 µL of room temperature fixation solution was added to each well. The fixing solution (PBS-based) contains 1% glutaraldehyde, 5 µM propidium iodide, and 5 µM acridine orange (HCl salt). Treated plates were placed on an orbital shaker for 30 s to disperse cell agglomerations and were then moved

to an incubator for 3 h for staining and fixation. Quantitative imaging was carried out using the PerkinElmer Operetta and analysis using the Harmony 3.5.1 software package. Automated quantification involved the software identifying all trichomonads and subtracting live (green only) from dead (green and red) cells using a propidium iodide threshold of less than 6500 units (which enables assessment of membrane integrity, thus differentiation between live and dead cells).[6]

III.3.9 Computational Details

For 31C, a preliminary conformational search was carried out by using ComputeVOA (BioTools, Inc.) at the molecular mechanics level (MMFF). The conformers obtained were further optimized at the B3LYP/6-31G (d,p) level with Gaussian 09 (Gaussian Inc.). Stable conformers with populations greater than 1% were submitted to ECD calculation by time-dependent DFT at the B3LYP/6-311+g(d,p) level. The ECD spectra were added together after a Boltzmann statistical weighting using SpecDis 1.71 (sigma value of 0.3 eV). After applying a UV-shift correction, the computed ECD spectra were compared with the experimentally derived ECD curves.

III.3.10 Compound data summary

31C: (1R,2aR,2a1R,3R,5aR,5'S,8aR)-5'-(3-hydroxypropyl)-4,8a-dimethyl-3-propyl-2a,2a1,3,5a,6,8a-hexahydro-2H-spiro[acenaphthylene-1,3'-pyrrolidine]-2,2',4'-trione

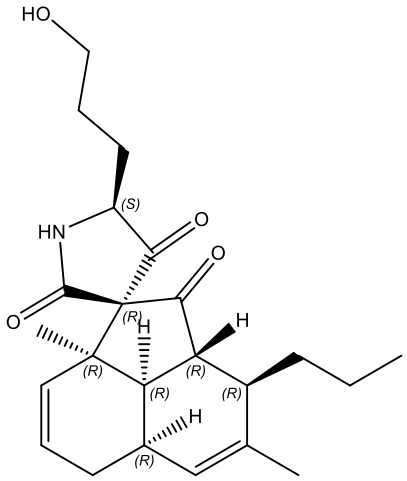

Brown amorphous solid; $[\alpha]^{20}_{D}$ +350 (*c* 1 mg/mL, MeOH); UV (MeOH) λ_{max} (log ε) 239 (2.13) nm; ECD (*c* 8.7 × 10^{-5} M, MeOH) λ_{max} (Δε) 295 (-1.93), and 243 (−1.98) nm; ^{1}H and ^{13}C NMR, **Table 6**; LRESIMS m/z 386 $[M + H]^+$, 771 $[2M + H]^+$; HRESIMS m/z 386.2333 $[M + H]^+$ (calcd for $C_{23}H_{32}NO_4$, 386.2331).

52C: (1R,2aS,2a1S,3S,5aS,5'S,8aS)-5'-(3-hydroxypropyl)-4,8a-dimethyl-3-propyl-2a,2a1,3,5a,6,8a-hexahydro-2H-spiro[acenaphthylene-1,3'-pyrrolidine]-2,2',4'-trione

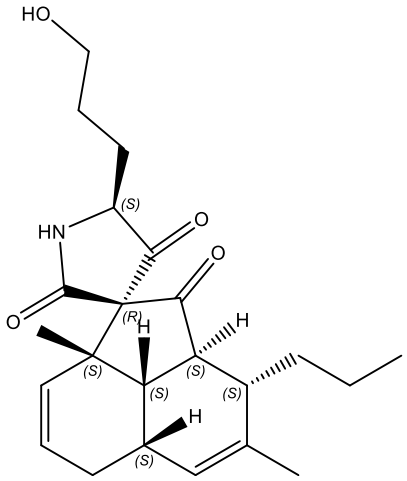

Brown amorphous solid; $[\alpha]^{20}_{D}$ +24 (*c* 1 mg/mL, MeOH); UV (MeOH) λ_{max} (log ε) 239 (0.96) nm; ECD (*c* 2.6 × 10^{-4} M, MeOH) λ_{max} (Δε) 299 (-4.74), and 231 (-3.21) nm; ^{1}H and ^{13}C NMR, **Table 7**; LRESIMS m/z 386 $[M + H]^{+}$, 771 $[2M + H]^{+}$.

References

1. Sexually transmitted infections (STIs). https://www.who.int/news-room/fact-sheets/detail/sexually-transmitted-infections-(stis).

2. Ona, S., Molina, R. L. & Diouf, K. Mycoplasma genitalium: An Overlooked Sexually Transmitted Pathogen in Women? *Infectious Diseases in Obstetrics and Gynecology* **2016**, e4513089 (2016).

3. Manhart, L. E., Holmes, K. K., Hughes, J. P., Houston, L. S. & Totten, P. A. Mycoplasma genitalium Among Young Adults in the United States: An Emerging Sexually Transmitted Infection. *Am J Public Health* **97**, 1118–1125 (2007).

4. Ross, J. D. C. & Jensen, J. S. Mycoplasma genitalium as a sexually transmitted infection: implications for screening, testing, and treatment. *Sexually Transmitted Infections* **82**, 269–271 (2006).

5. Sutton, M. *et al.* The Prevalence of Trichomonas vaginalis Infection among Reproductive-Age Women in the United States, 2001-2004. *Clinical Infectious Diseases* **45**, 1319–1326 (2007).

6. King, J. B. *et al.* Design and Application of a High-Throughput, High-Content Screening System for Natural Product Inhibitors of the Human Parasite Trichomonas vaginalis. *ACS Infect. Dis.* **5**, 1456–1470 (2019).

7. Mann, J. R. *et al.* Trichomoniasis in Pregnancy and Mental Retardation in Children. *Annals of Epidemiology* **19**, 891–899 (2009).

8. Gabriel, G., Robertson, E. & Thin, R. N. T. Single Dose Treatment of Trichomoniasis. *J Int Med Res* **10**, 129–130 (1982).

9. CDC - Trichomoniasis Treatment. https://www.cdc.gov/std/trichomonas/treatment.htm (2021).

10. He, W., Van Puyvelde, L., Maes, L., Bosselaers, J. & De Kimpe, N. Antitrichomonas In Vitro Activity of Cussonia Holstii Engl. *Natural Product Research* **17**, 127–133 (2003).

11. Kaneda, Y., Tanaka, T. & Saw, T. Effects of berberine, a plant alkaloid, on the growth of anaerobic protozoa in axenic culture. *Tokai J Exp Clin Med* **15**, 417–423 (1990).

12. Hwang-Huei, W. Antitrichomonal action of emodin in mice. *Journal of Ethnopharmacology* **40**, 111–116 (1993).

13. Yuan, H., Ma, Q., Ye, L. & Piao, G. The Traditional Medicine and Modern Medicine from Natural Products. *Molecules* **21**, 559 (2016).

14. Discovery of Camptothecin and Taxol - National Historic Chemical Landmark. *American Chemical Society* https://www.acs.org/content/acs/en/education/whatischemistry/landmarks/camptothecintaxol.html.

15. Klockgether-Radke, A. P. F. W. Sertürner und die Entdeckung des Morphins. *Anästhesiol Intensivmed Notfallmed Schmerzther* **37**, 244–249 (2002).

16. Salicin - an overview | ScienceDirect Topics. https://www.sciencedirect.com/topics/chemistry/salicin.

17. Li, J. W.-H. & Vederas, J. C. Drug Discovery and Natural Products: End of an Era or an Endless Frontier? *Science* **325**, 161–165 (2009).

18. Newman, D. J. & Cragg, G. M. Natural Products as Sources of New Drugs from 1981 to 2014. *J. Nat. Prod.* **79**, 629–661 (2016).

19. Veeresham, C. Natural products derived from plants as a source of drugs. *J Adv Pharm Technol Res* **3**, 200–201 (2012).

20. Blackwell, M. The Fungi: 1, 2, 3 … 5.1 million species? *American Journal of Botany* **98**, 426–438 (2011).

21. Arslan, I. Trends in Antimicrobial Resistance in Healthcare-Associated Infections: A Global Concern. in *Reference Module in Biomedical Sciences* (Elsevier, 2021). doi:10.1016/B978-0-12-818731-9.00111-7.

22. Sanchez, S. & Demain, A. L. Bioactive Products from Fungi. in *Food Bioactives: Extraction and Biotechnology Applications* (ed. Puri, M.) 59–87 (Springer International Publishing, 2017). doi:10.1007/978-3-319-51639-4_3.

23. Bérdy, J. Bioactive Microbial Metabolites. *J Antibiot* **58**, 1–26 (2005).

24. Fleming, A. On the antibacterial action of cultures of a penicillium, with special reference to their use in the isolation of B. influenzae. 1929. *Bull World Health Organ* **79**, 780–790 (2001).

25. Hoeksma, J. *et al.* A new perspective on fungal metabolites: identification of bioactive compounds from fungi using zebrafish embryogenesis as read-out. *Sci Rep* **9**, 17546 (2019).

26. About. *The University of Oklahoma Citizen Science Soil Collection Program* https://whatsinyourbackyard.org/about/.

27. Lass-Flörl, C., Dietl, A.-M., Kontoyiannis, D. P. & Brock, M. Aspergillus terreus Species Complex. *Clinical Microbiology Reviews* **34**, e00311-20.

28. Lass-Flörl, C. Treatment of Infections Due to Aspergillus terreus Species Complex. *Journal of Fungi* **4**, 83 (2018).

29. Subhan, M., Faryal, R. & Macreadie, I. Exploitation of Aspergillus terreus for the Production of Natural Statins. *Journal of Fungi* **2**, 13 (2016).

30. Ghanem, N. B., Yusef, H. H. & Mahrouse, H. K. Production of Aspergillus terreus xylanase in solid-state cultures: application of the Plackett–Burman experimental design to evaluate nutritional requirements. *Bioresource Technology* **73**, 113–121 (2000).

31. Nadumane, V. K., Venkatachalam, P. & Gajaraj, B. Chapter 19 - Aspergillus Applications in Cancer Research. in *New and Future Developments in Microbial Biotechnology and Bioengineering* (ed. Gupta, V. K.) 243–255 (Elsevier, 2016). doi:10.1016/B978-0-444-63505-1.00020-8.

32. McPhillips, K. *et al.* Purification and Characterisation of a β-1,4-Xylanase from Remersonia thermophila CBS 540.69 and Its Application in Bread Making. *Appl Biochem Biotechnol* **172**, 1747–1762 (2014).

33. Seifert, K. A., Louis-Seize, G., Samson, R. A. & Boekhout, T. Remersonia, a new genus for Stilbella thermophila, a thermophilic mould from compost. *Can. J. Bot.* **75**, 1158–1165 (1997).

34. Marson, C. M. New and unusual scaffolds in medicinal chemistry. *Chem. Soc. Rev.* **40**, 5514–5533 (2011).

35. Dahms, H.-U. Challenges in Medicinal Chemistry. *Journal of Pharmacology and Medicinal Chemistry* **1**, (2017).

36. Wess, G. Challenges for medicinal chemistry. *Drug Discovery Today* **1**, 529–532 (1996).

37. Wess, G., Urmann, M. & Sickenberger, B. Medicinal Chemistry: Challenges and Opportunities. *Angewandte Chemie International Edition* **40**, 3341–3350 (2001).

38. Hu, Y., Stumpfe, D. & Bajorath, J. Recent Advances in Scaffold Hopping. *J. Med. Chem.* **60**, 1238–1246 (2017).

39. Barreiro, E. J. Chapter 1 Privileged Scaffolds in Medicinal Chemistry: An Introduction. 1–15 (2015) doi:10.1039/9781782622246-00001.

40. Venkanna, A. *et al.* Pharmacological use of a novel scaffold, anomeric N,N-diarylamino tetrahydropyran: molecular similarity search, chemocentric target profiling, and experimental evidence. *Sci Rep* **7**, 12535 (2017).

41. Zhao, H. & Akritopoulou-Zanze, I. When analoging is not enough: scaffold discovery in medicinal chemistry. *Expert Opinion on Drug Discovery* **5**, 123–134 (2010).

42.Penning, T. D. *et al.* Synthesis and Biological Evaluation of the 1,5-Diarylpyrazole Class of Cyclooxygenase-2 Inhibitors: Identification of 4-[5-(4-Methylphenyl)-3- (trifluoromethyl)-1H-pyrazol-1-yl]benzenesulfonamide (SC-58635, Celecoxib). *J. Med. Chem.* **40**, 1347–1365 (1997).

43. Wenglowsky, S. *et al.* Pyrazolopyridine Inhibitors of B-RafV600E. Part 1: The Development of Selective, Orally Bioavailable, and Efficacious Inhibitors. *ACS Med. Chem. Lett.* **2**, 342–347 (2011).

44. Zhang, C. & Bollag, G. Scaffold-based design of kinase inhibitors for cancer therapy. *Current Opinion in Genetics & Development* **20**, 79–86 (2010).

45. Yamada, T., Kikuchi, T. & Tanaka, R. Altercrasin A, a novel decalin derivative with spirotetramic acid, produced by a sea urchin-derived Alternaria sp. Tetrahedron Letters 56, 1229–1232 (2015).

46. Boldt, P. et al. Synthesis of Stereoisomeric Ufolanes. Chemische Berichte 125, 1147–1157 (1992).

Appendix Contents

Appendix I. Bioassay results for *A. terreus*

Appendix I.1. Bioassay results for 174MM6A-K

Sample ID	Sample Information	MIC90 (µg/ml)
174MM6A	Crude material	25
174MM6B	Si VLC of 174MM6A	>25
174MM6C	Si VLC of 174MM6A	>25
174MM6D	Si VLC of 174MM6A	25
174MM6E	Si VLC of 174MM6A	>25
174MM6F	HP20 VLC of 174MM6D	>25
174MM6G	HP20 VLC of 174MM6D	>25
174MM6H	HP20 VLC of 174MM6D	>25
174MM6I	HP20 VLC of 174MM6D	12.5
174MM6J	HP20 VLC of 174MM6D	12.5
174MM6K	HP20 VLC of 174MM6D	12.5

Appendix I.2. Bioassay results for 174MM44A-K

Sample ID	Sample Information	MIC90 (µg/mL)
174MM44A	Crude (EtOAc extract)	12.5
174MM44B	Si VLC of 174MM44A	>50
174MM44C	Si VLC of 174MM44A	25
174MM44D	Si VLC of 174MM44A	12.5
174MM44E	Si VLC of 174MM44A	6.3
174MM44F	HP20 VLC of 174MM44D	>50
174MM44G	HP20 VLC of 174MM44D	>50
174MM44H	HP20 VLC of 174MM44D	>50
174MM44I	HP20 VLC of 174MM44D	12.5
174MM44J	HP20 VLC of 174MM44D	12.5
174MM44K	HP20 VLC of 174MM44D	3.1

Appendix I.3. Bioassay results for 174MM9A-G, 174MM11A-J and 174MM12A-H

Sample ID	Sample Information	MIC90 (µg/ml)
174MM9A	Prep HPLC of 174MM6I	25
174MM9B	Prep HPLC of 174MM6I	50
174MM9C	Prep HPLC of 174MM6I	25
174MM9D	Prep HPLC of 174MM6I	25
174MM9E	Prep HPLC of 174MM6I	12.5
174MM9F	Prep HPLC of 174MM6I	25
174MM9G	Prep HPLC of 174MM6I	6.3
174MM11A	Prep HPLC of 174MM6J	50
174MM11B	Prep HPLC of 174MM6J	12.5
174MM11C	Prep HPLC of 174MM6J	12.5
174MM11D	Prep HPLC of 174MM6J	3.2
174MM11E	Prep HPLC of 174MM6J	3.2
174MM11F	Prep HPLC of 174MM6J	3.2
174MM11G	Prep HPLC of 174MM6J	3.2
174MM11H	Prep HPLC of 174MM6J	3.2
174MM11I	Prep HPLC of 174MM6J	6.3
174MM11J	Prep HPLC of 174MM6J	12.5
174MM12A	Prep HPLC of 174MM6K	12.5
174MM12B	Prep HPLC of 174MM6K	50
174MM12C	Prep HPLC of 174MM6K	50
174MM12D	Prep HPLC of 174MM6K	25
174MM12E	Prep HPLC of 174MM6K	12.5
174MM12F	Prep HPLC of 174MM6K	6.3
174MM12G	Prep HPLC of 174MM6K	6.3
174MM12H	Prep HPLC of 174MM6K	12.5

Appendix I.4. Bioassay results for 174MM19A-B, 174MM20A-B, 174MM21A-C and 174MM22A-E

Sample ID	Sample Information	MIC90 (µg/ml)
174MM22A	Semi prep HPLC of 174MM11G	10
174MM22B	Semi prep HPLC of 174MM11G	10
174MM22C	Semi prep HPLC of 174MM11G	2.5
174MM22D	Semi prep HPLC of 174MM11G	10
174MM22E	Semi prep HPLC of 174MM11G	5
174MM21A	Semi prep HPLC of 174MM11H	10
174MM21B	Semi prep HPLC of 174MM11H	5
174MM21C	Semi prep HPLC of 174MM11H	10
174MM20A	Semi prep HPLC of 174MM12G	5
174MM20B	Semi prep HPLC of 174MM12G	>10
174MM19A	Semi prep HPLC of 174MM11F	2.5
174MM19B	Semi prep HPLC of 174MM11F	10

Appendix I.5. Bioassay results for 174MM46A-F

Sample ID	Sample Information	MIC90 (µg/mL)
174MM46A	HP20 VLC of 174MM44E	>25
174MM46B	HP20 VLC of 174MM44E	>25
174MM46C	HP20 VLC of 174MM44E	>25
174MM46D	HP20 VLC of 174MM44E	>25
174MM46E	HP20 VLC of 174MM44E	25
174MM46F	HP20 VLC of 174MM44E	0.2

Appendix II. Bioassay results for *R. thermophila*

Appendix II.6. Bioassay results for 174MM4A-K

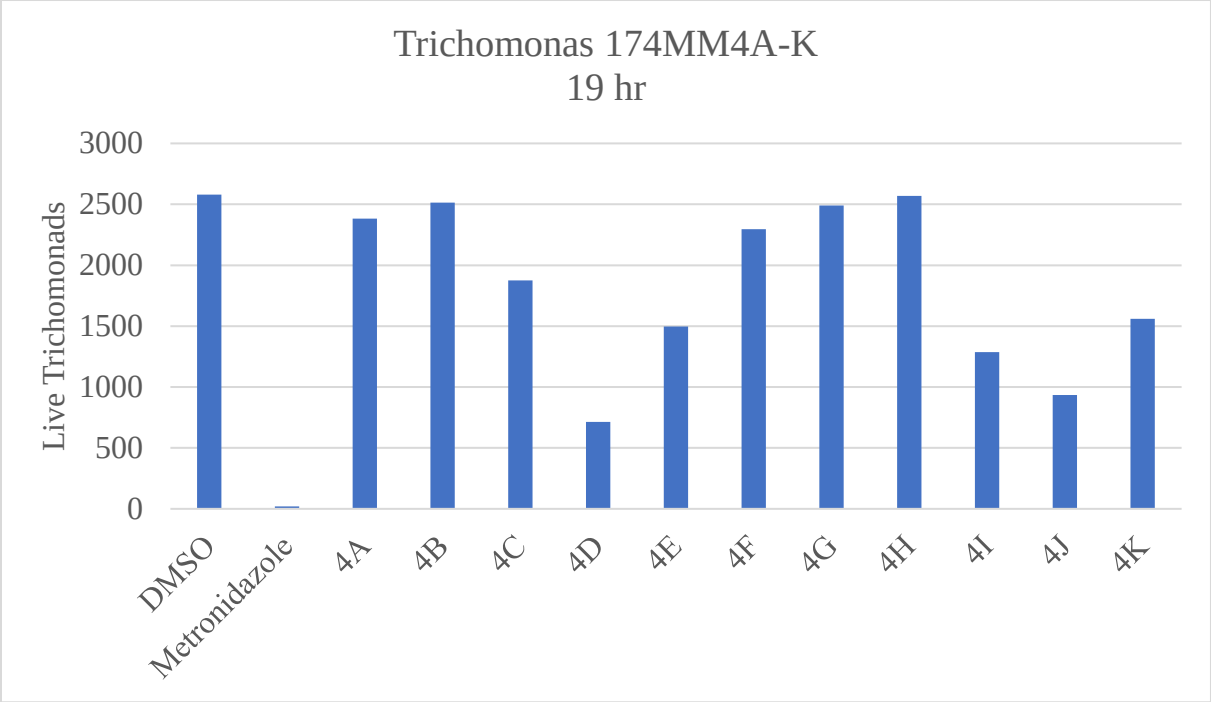

Appendix II.7. Bioassay results for 174MM16A-G

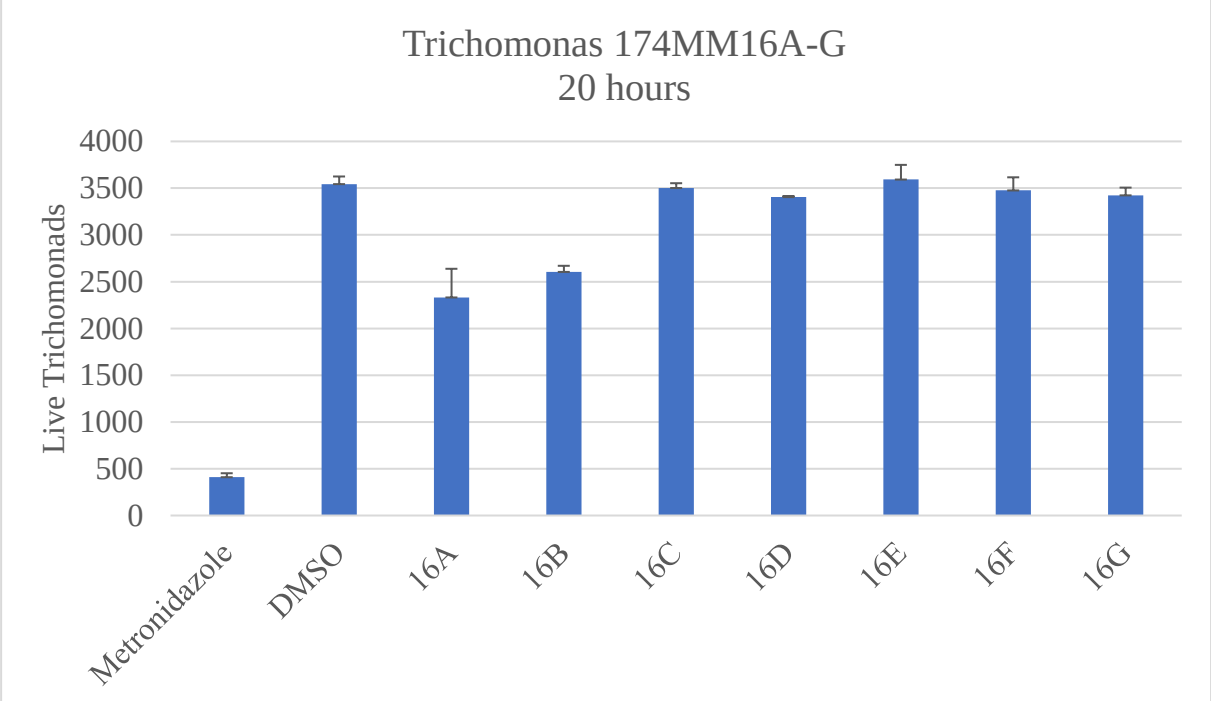

Appendix II.8. Bioassay results for 174MM17A-F

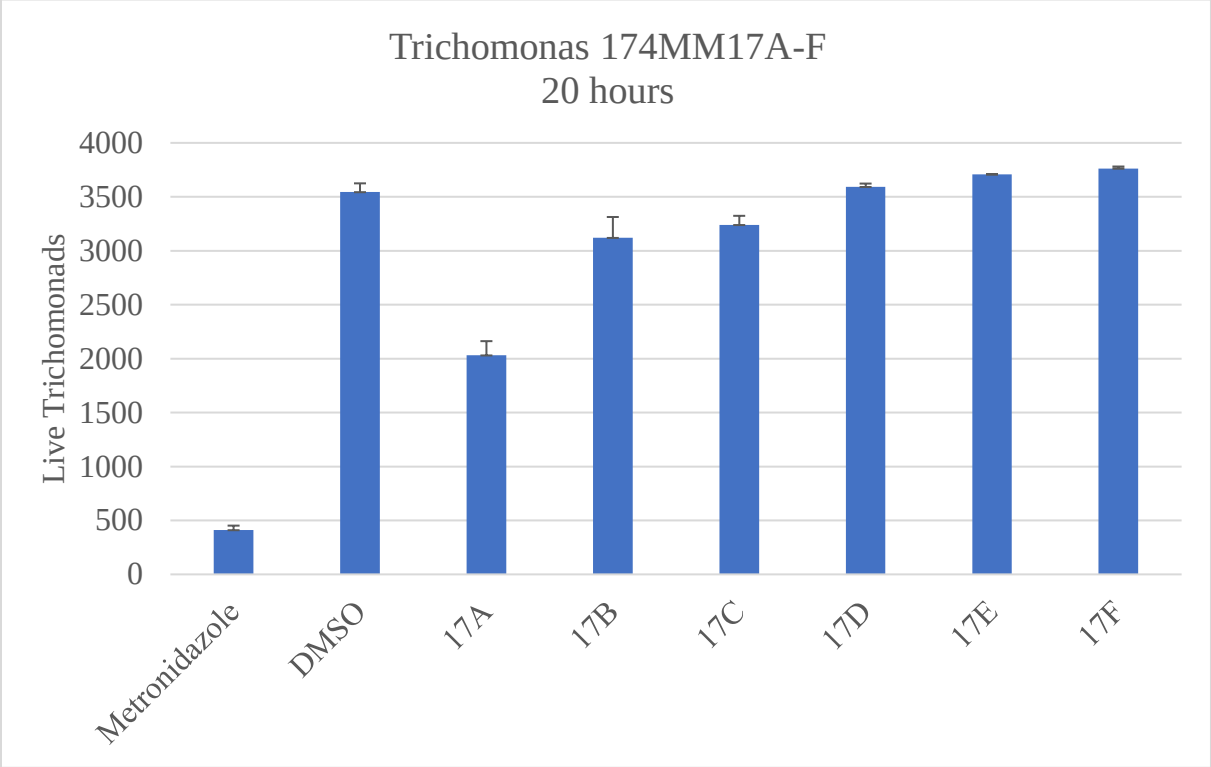

Appendix II.9. Bioassay results for 174MM29A-G

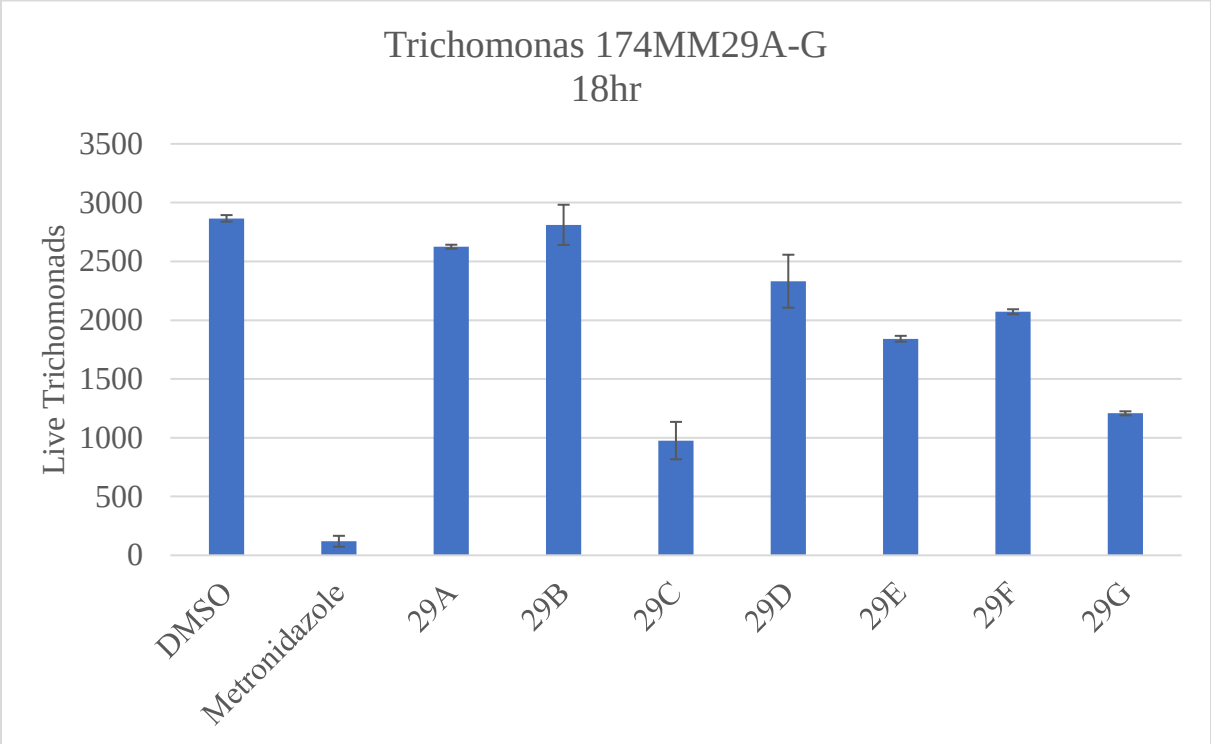

Appendix II.10. Bioassay results for 174MM30B-K

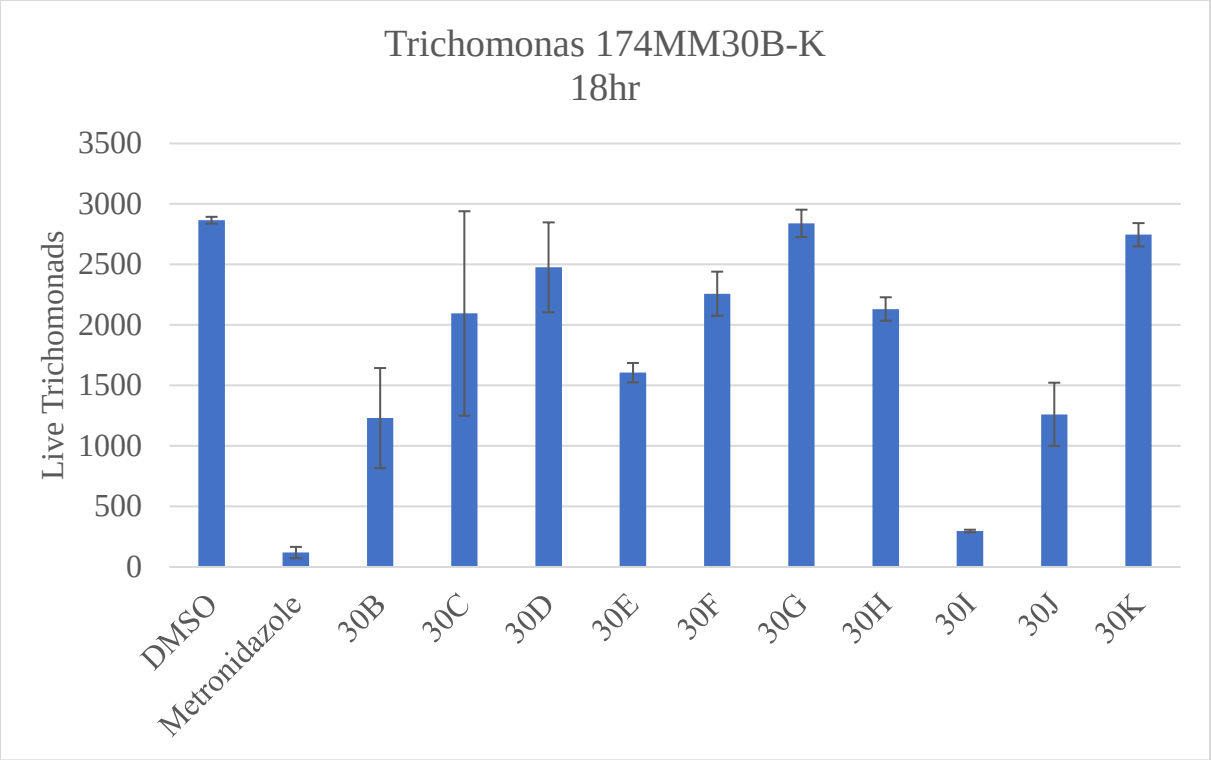

Appendix II.11. Bioassay results for 174MM23A-C

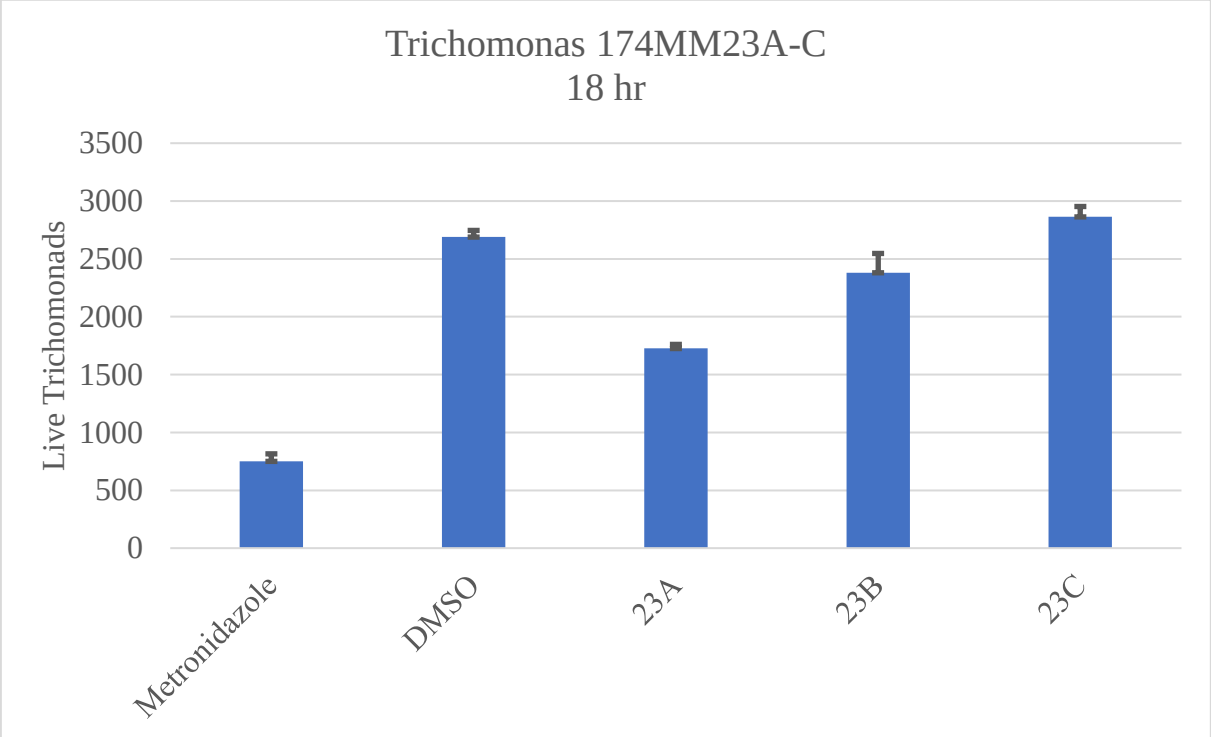

Appendix II.12. Bioassay results for 174MM24A-E

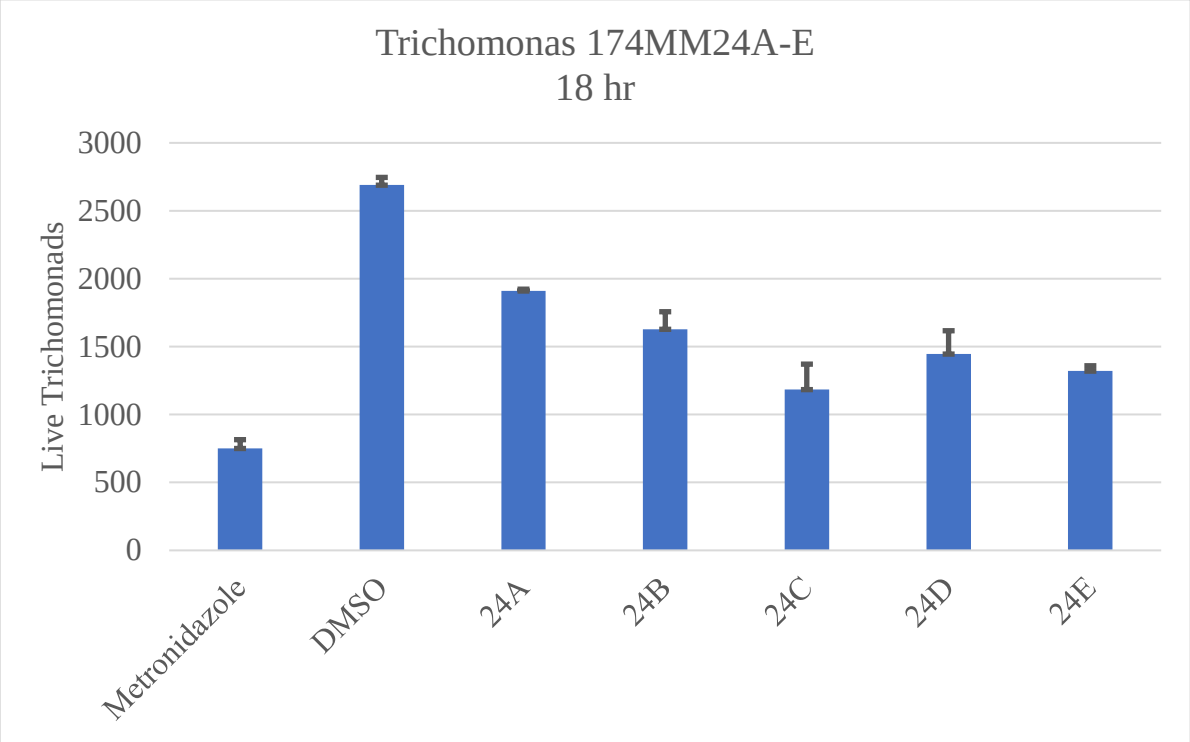

Appendix II.13. Bioassay results for 174MM33A-F

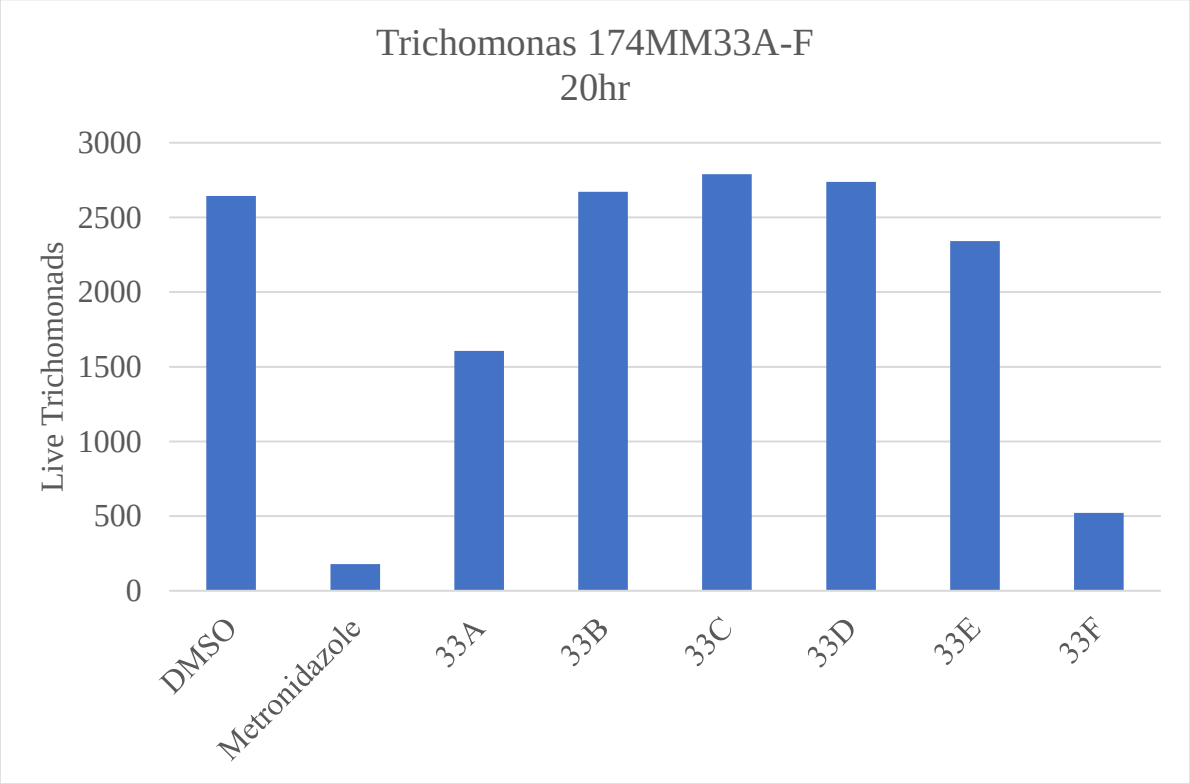

Appendix II.14. Bioassay results for 174MM34A-K

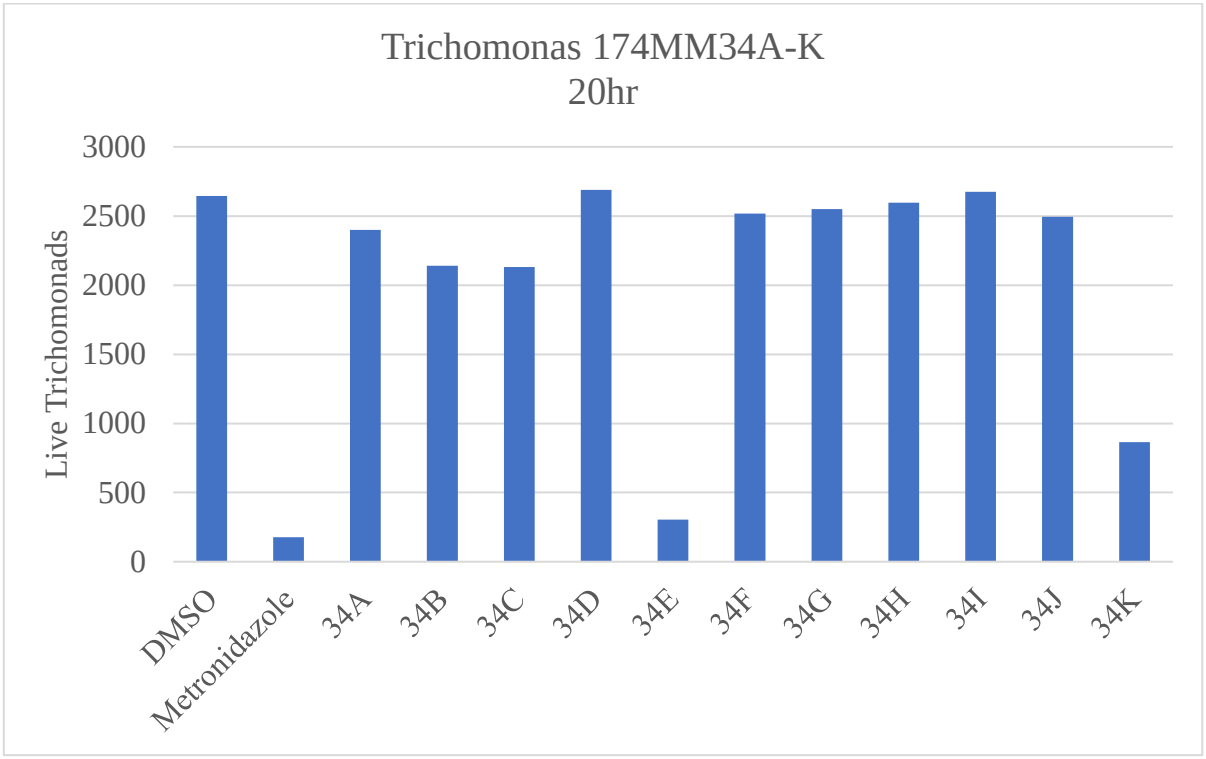

Appendix II.15. Bioassay results for 174MM36A-F

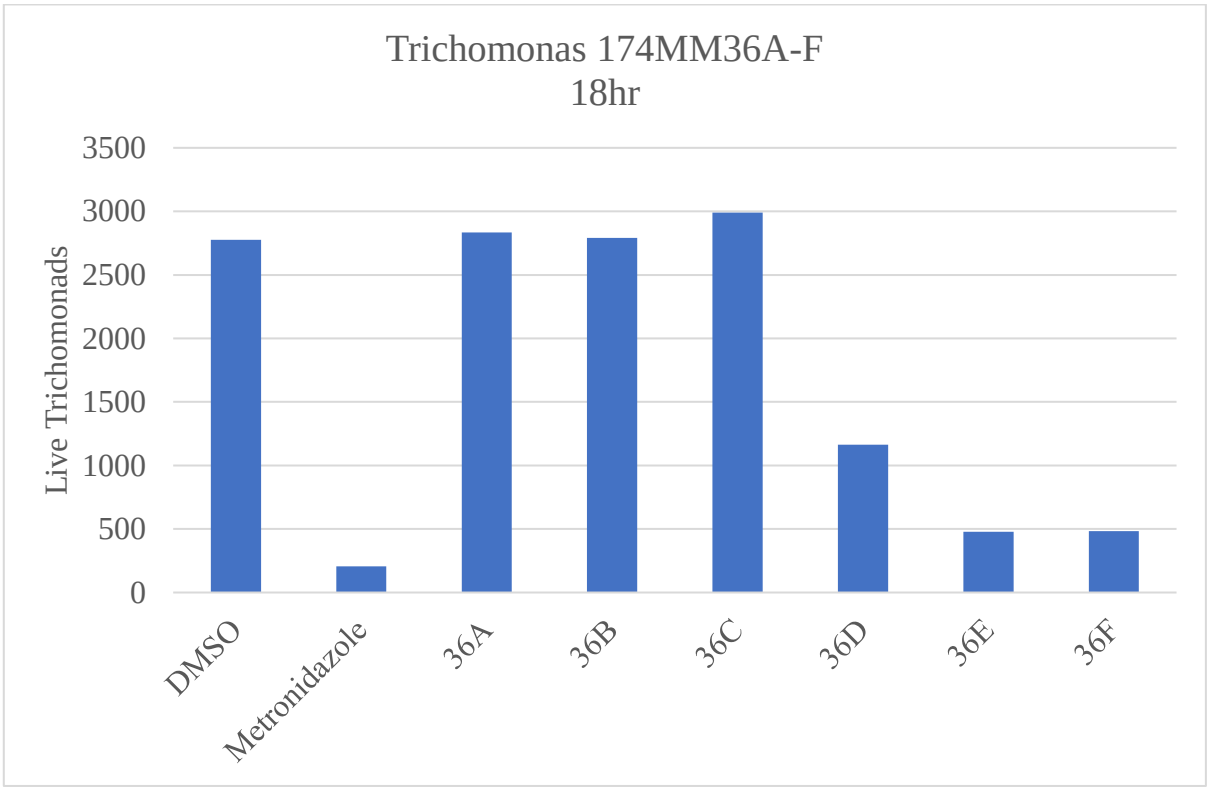

Appendix II.16. Bioassay results for 174MM38A-K

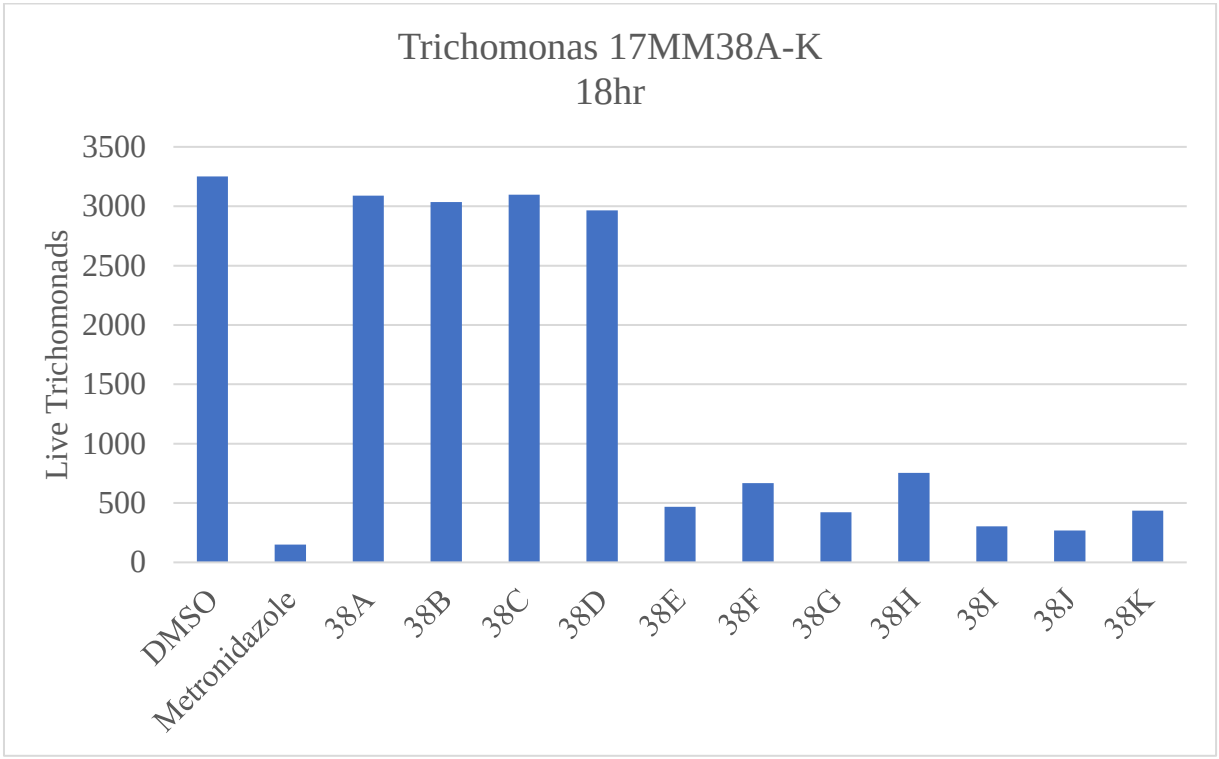

Appendix II.17. Bioassay results for 174MM39A-G

Appendix II.18. Bioassay results for 174MM40A-I

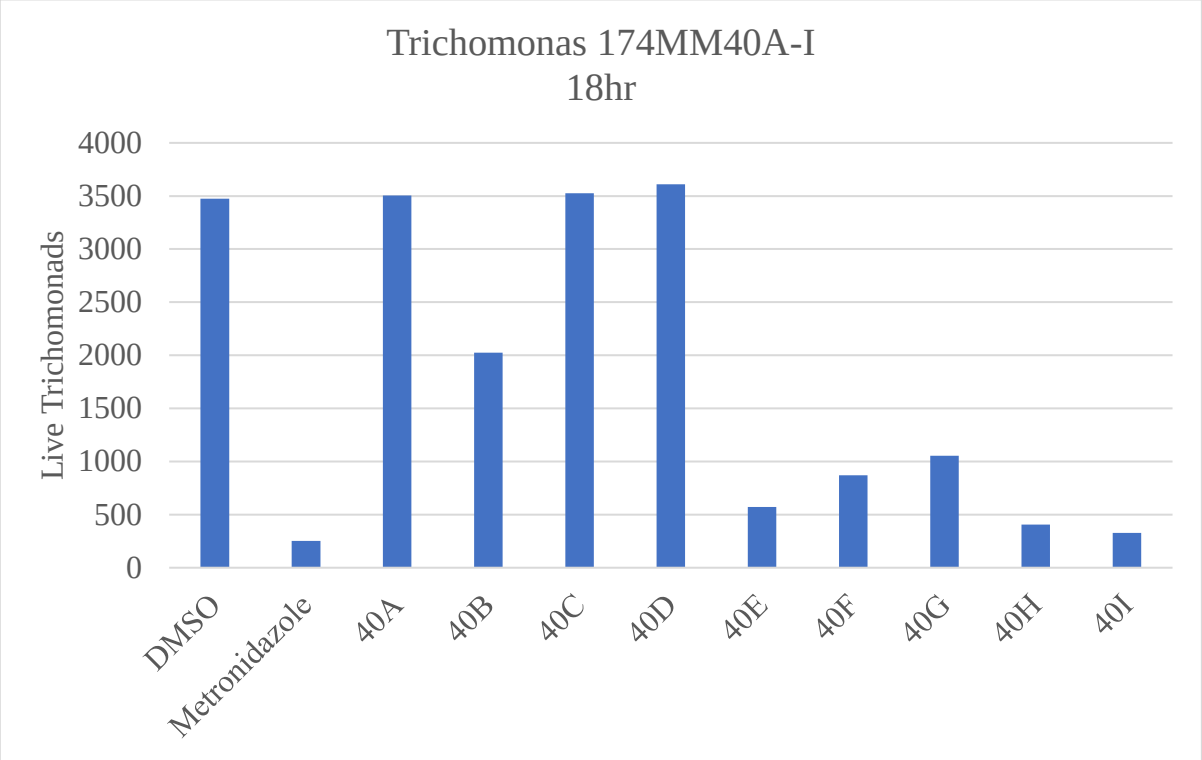

Appendix II.19. Bioassay results for 174MM42A-F

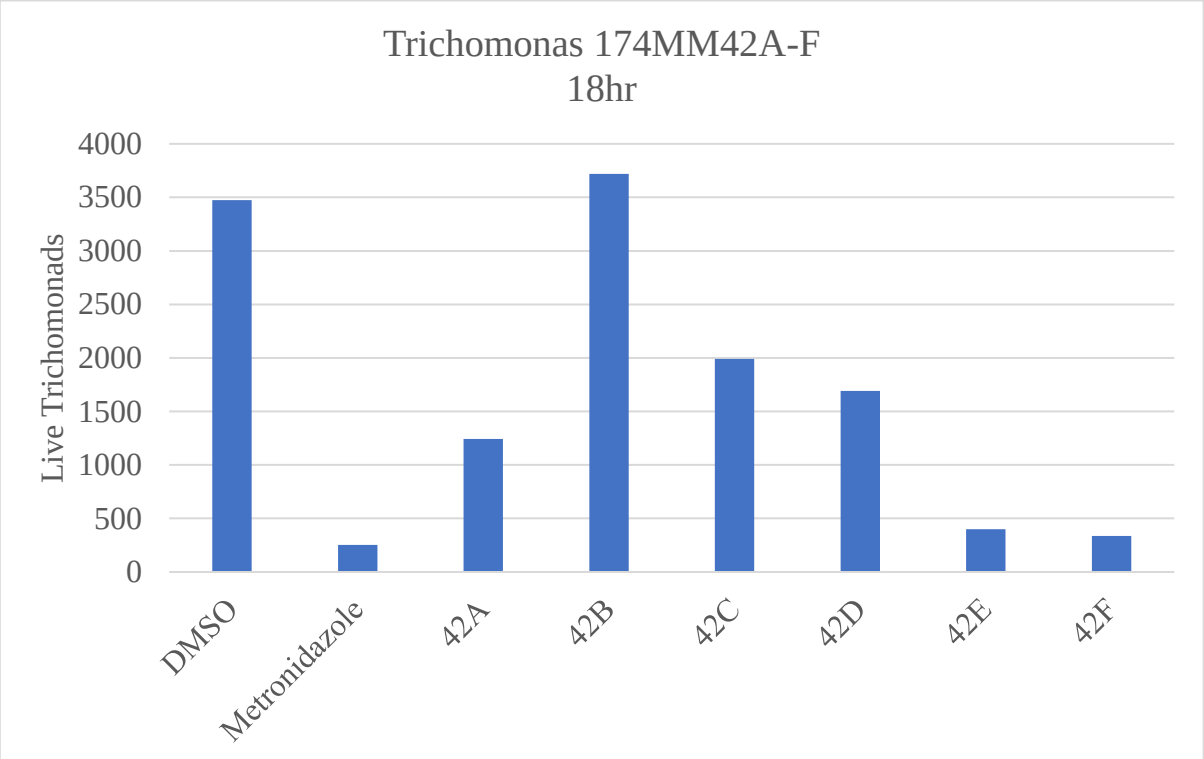

Appendix II.20. Bioassay results for 174MM41A-J

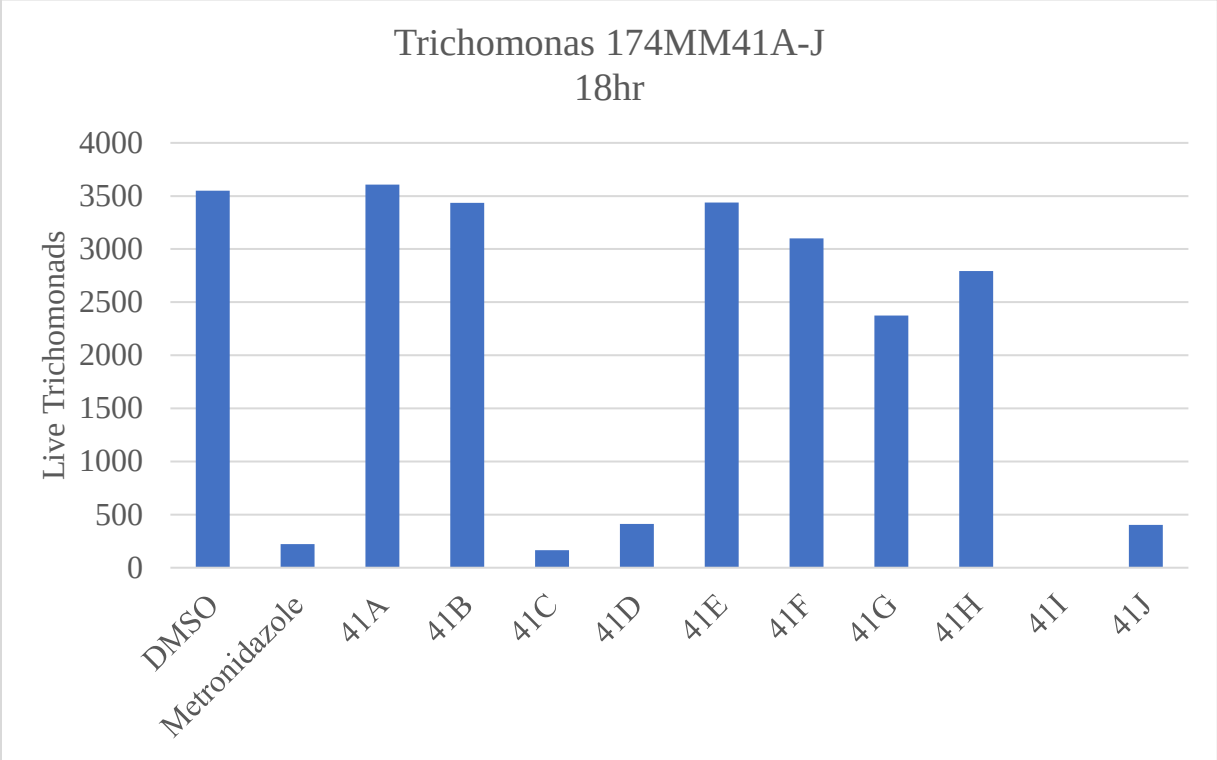

Appendix II.21. Bioassay results for 174MM43A-E

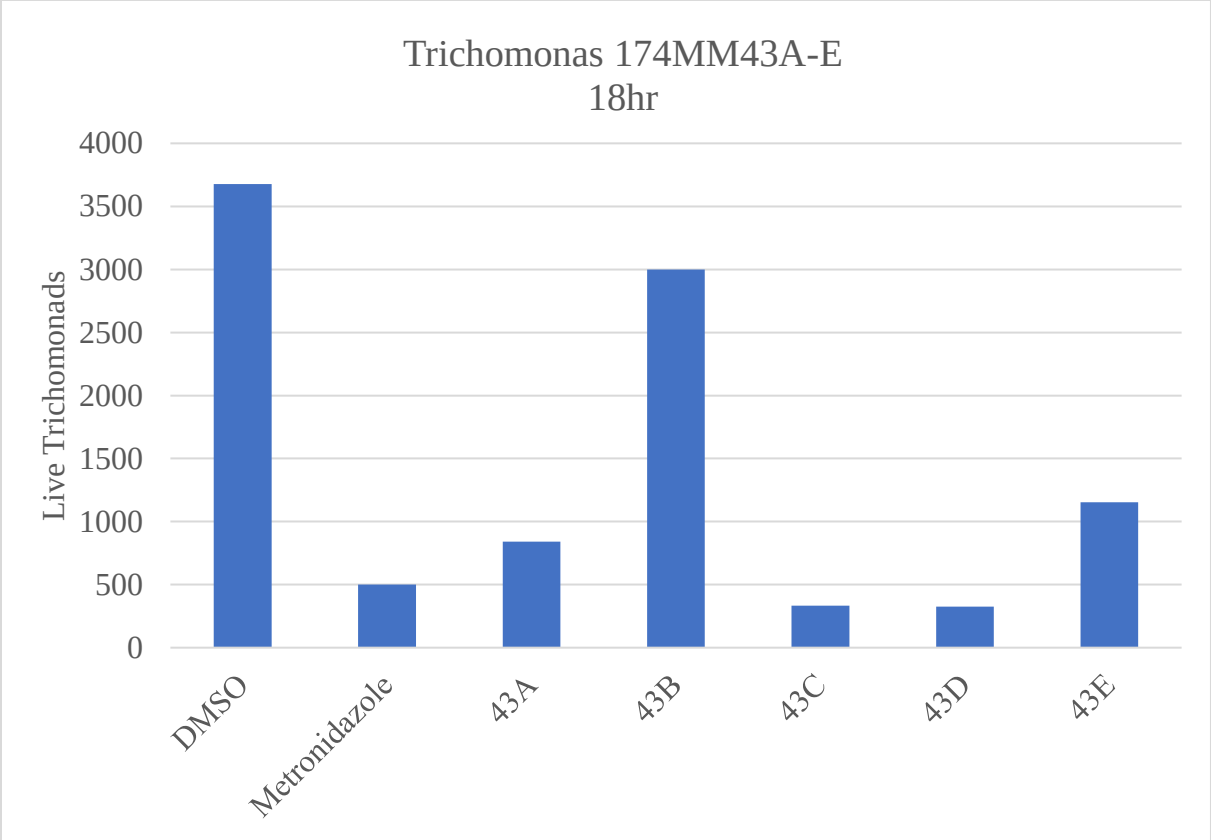

Appendix II.22. Bioassay results for 174MM45A-J

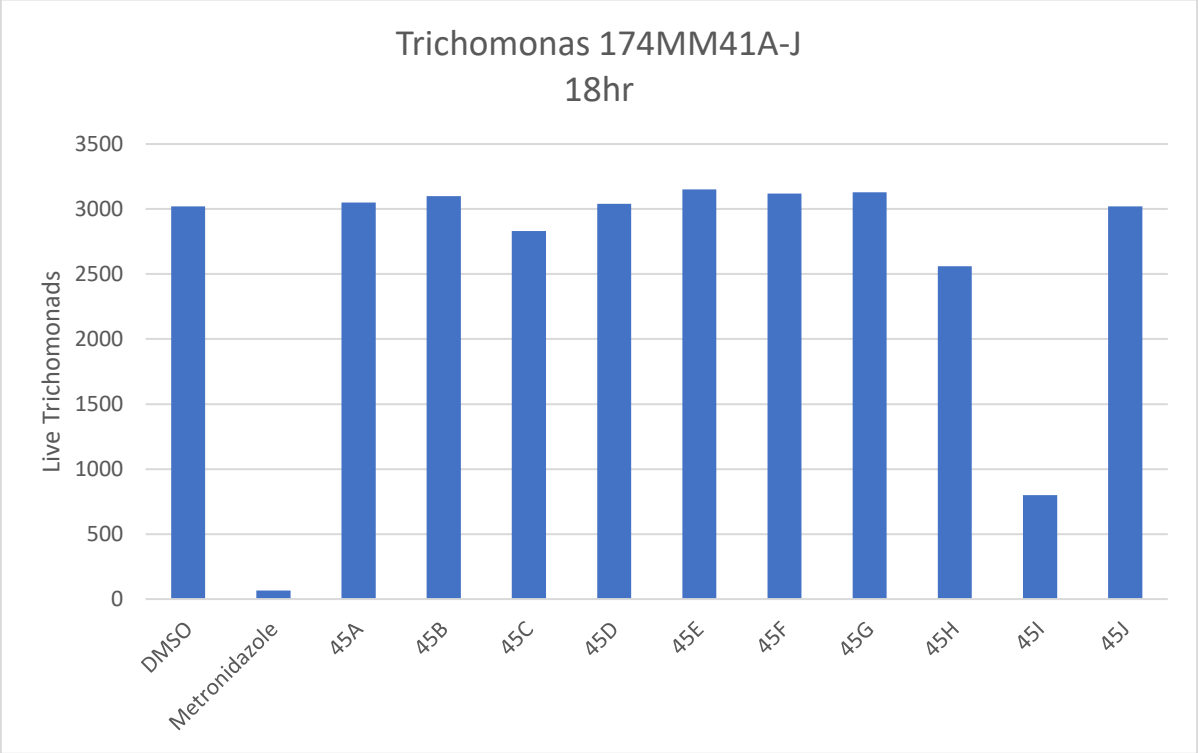

Appendix III. TLC plates

Appendix III.23. TLC of 16A tested with different elution conditions (left to right: 100% MeOH, 3:1 DCM:MeOH and 9:1 DCM:MeOH)

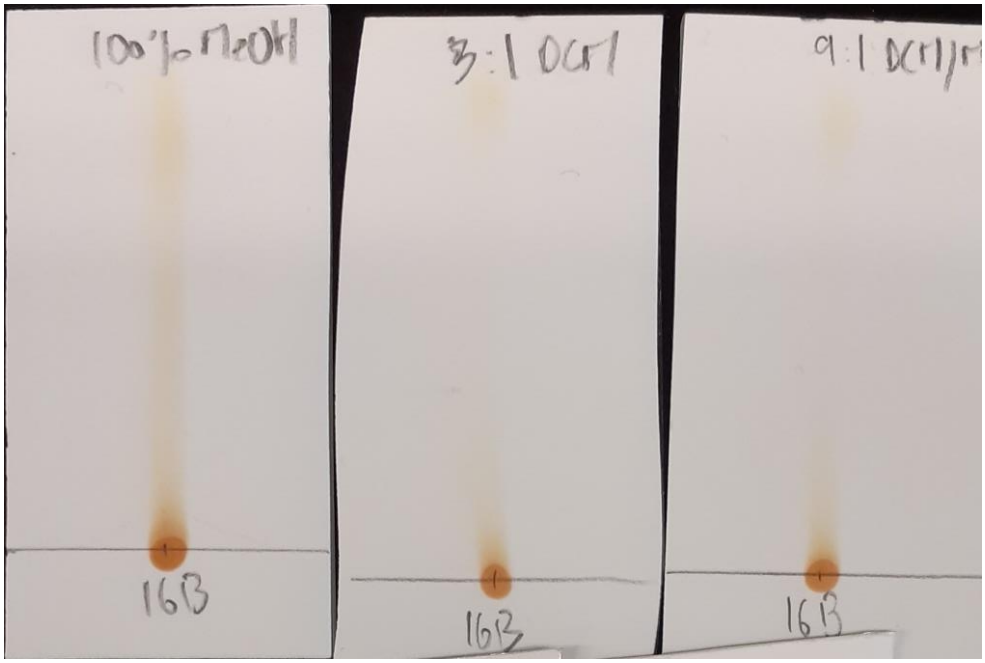

Appendix III.24. TLC of 16A tested with different elution conditions (left to right : 60% CH3CN and 100% CH3CN with water)

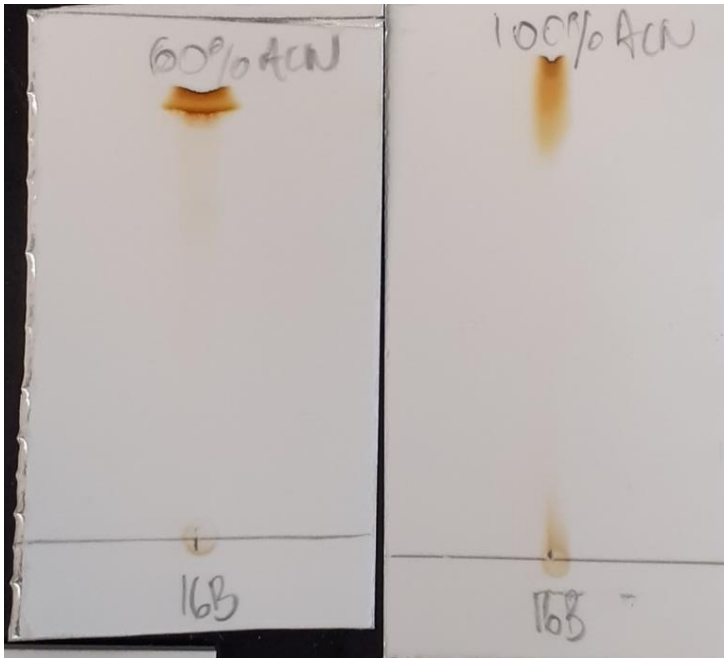

Appendix III.25. TLC of 16A tested with different elution conditions (left to right with 1% AcOH: 8:2 Toluene: EtOAc, 1:1 Toluene: EtOAc and 2:8 Toluene: EtOAc)

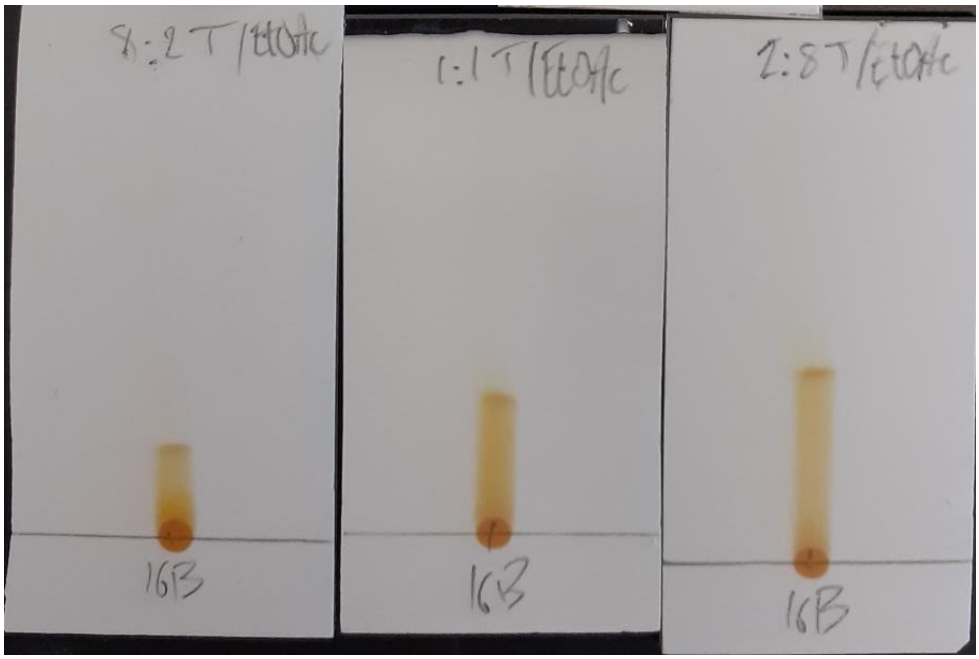

Appendix III.26. TLCs for method development for separation of 34K (DCM 100%, DCM:MeOH 100:1, DCM:MeOH 50:1, DCM:MeOH 20:1, DCM:MeOH 10:1, DCM:MeOH 5:1, and DCM:MeOH 1:1)

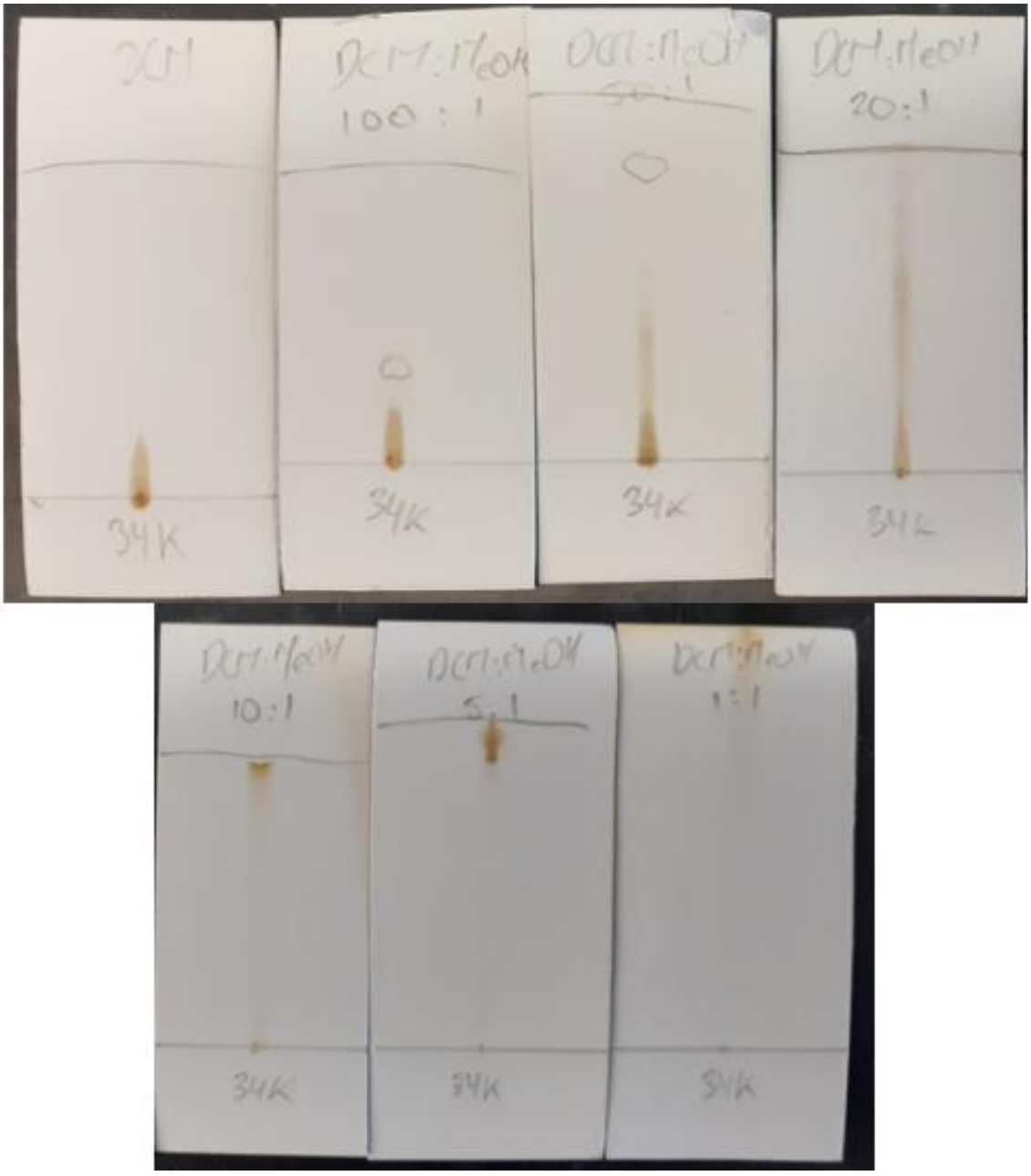

Appendix IV. Data for 31C

Appendix IV.27. LCMS chromatogram of 174MM31C

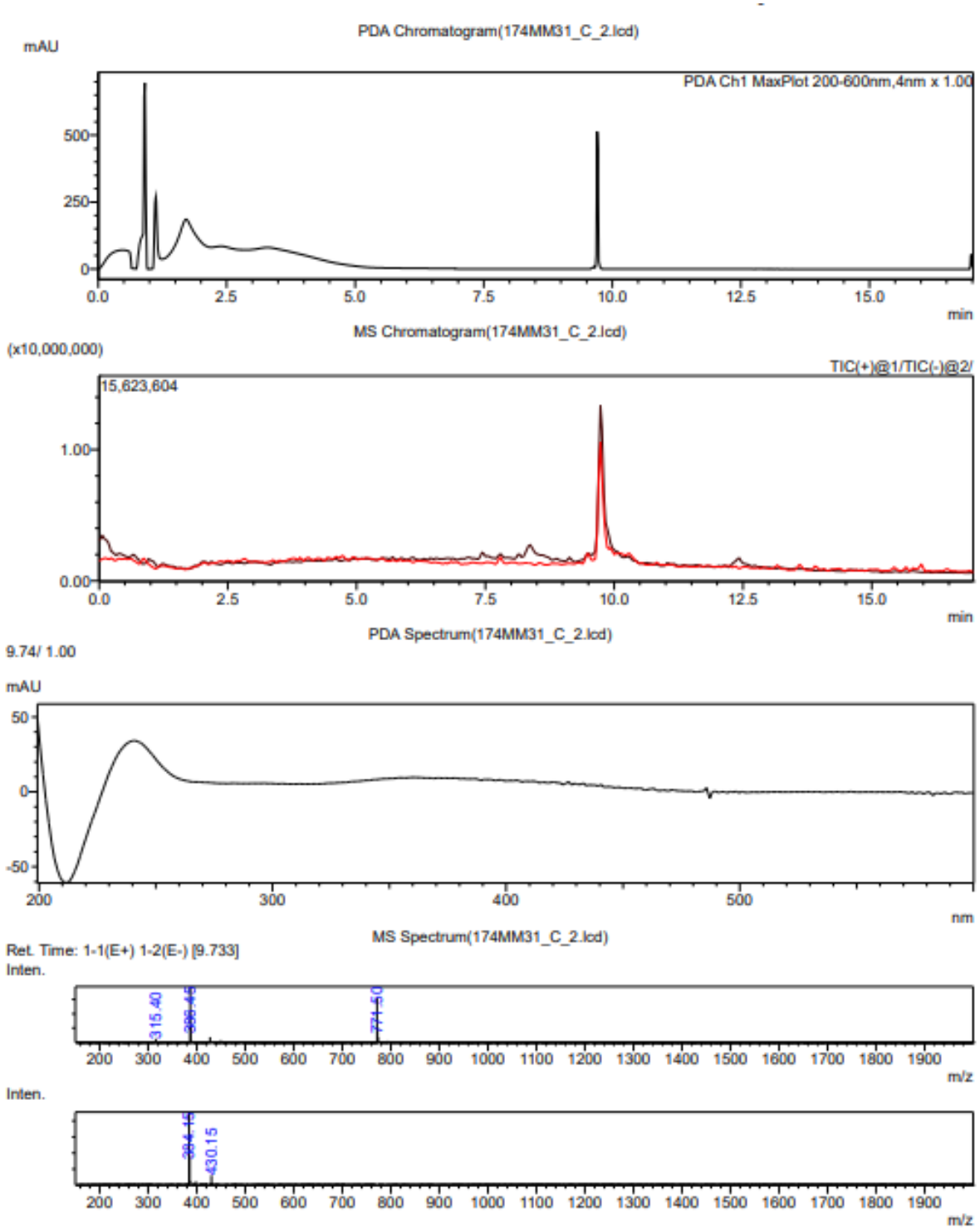

Appendix IV.28. HRESIMS of 174MM31C with a zoom on the peaks of interest

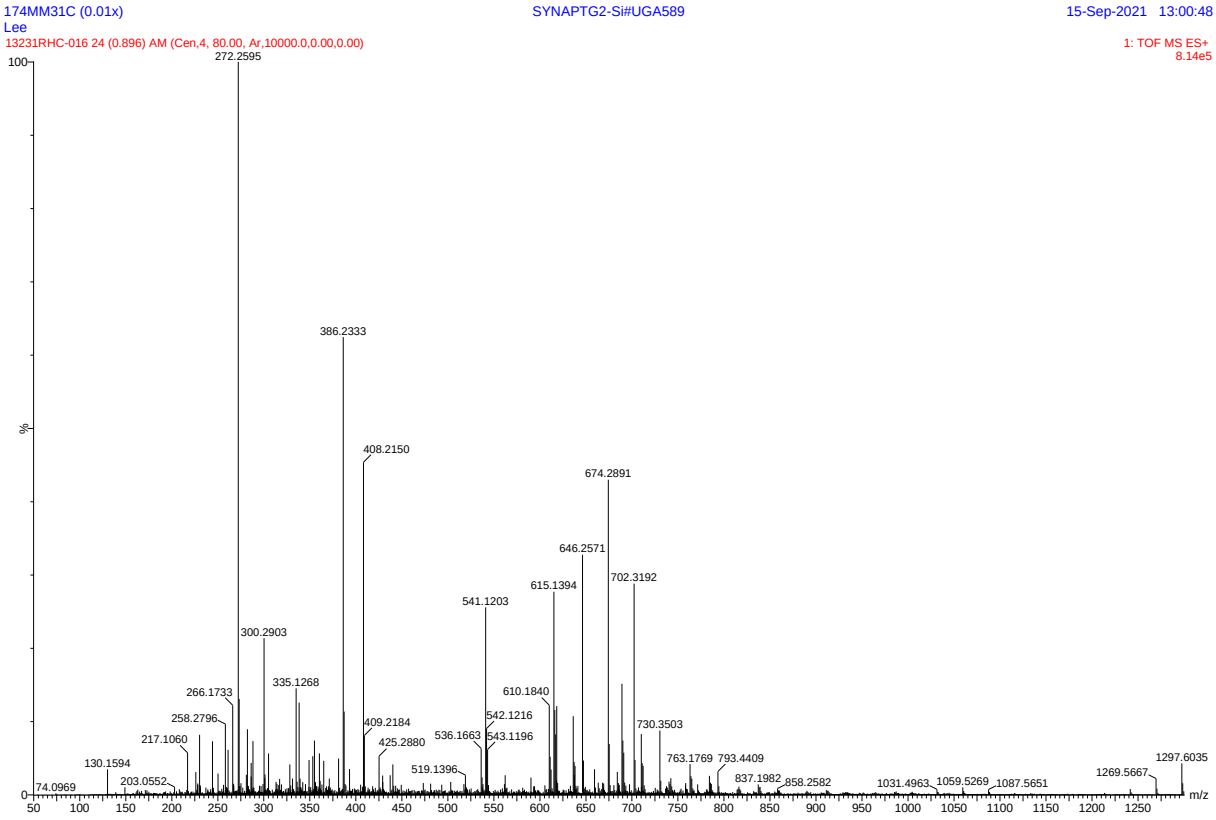

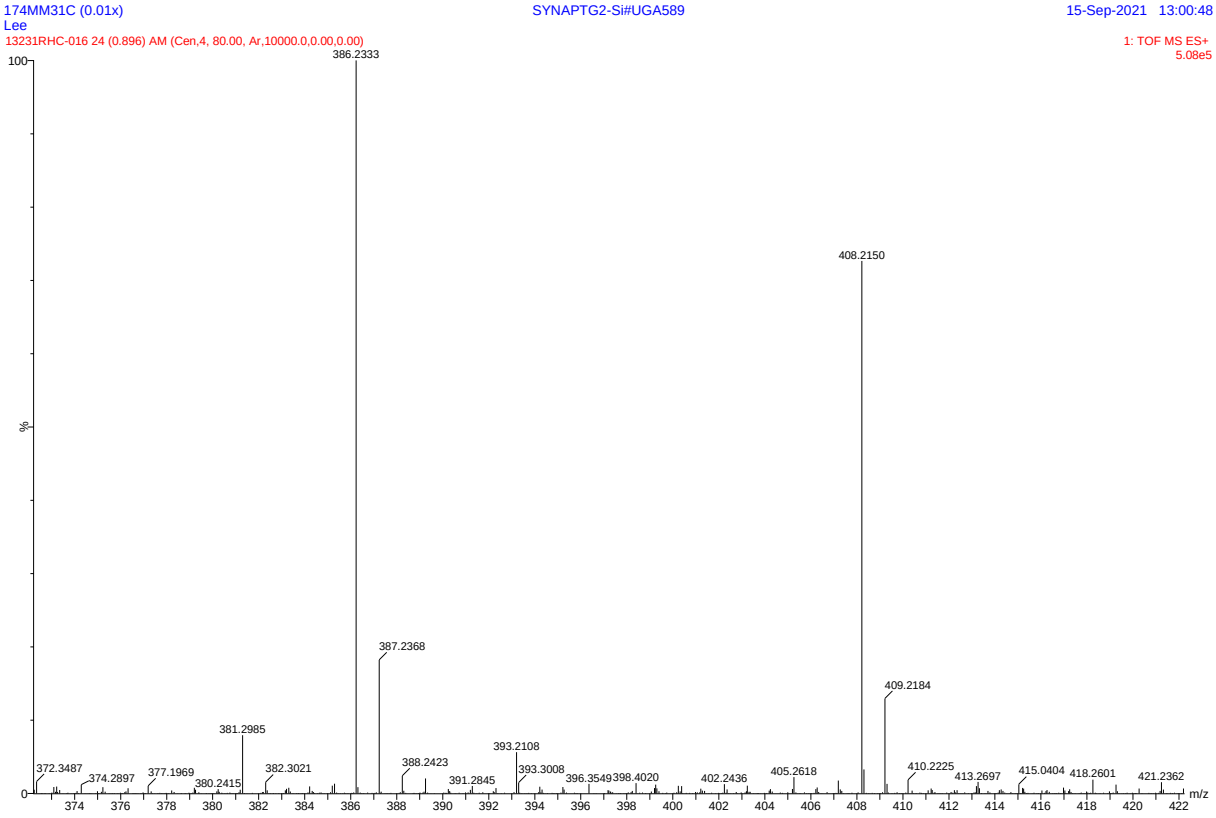

Appendix IV.29. ^{1}H-NMR in MeOH of 174MM31C

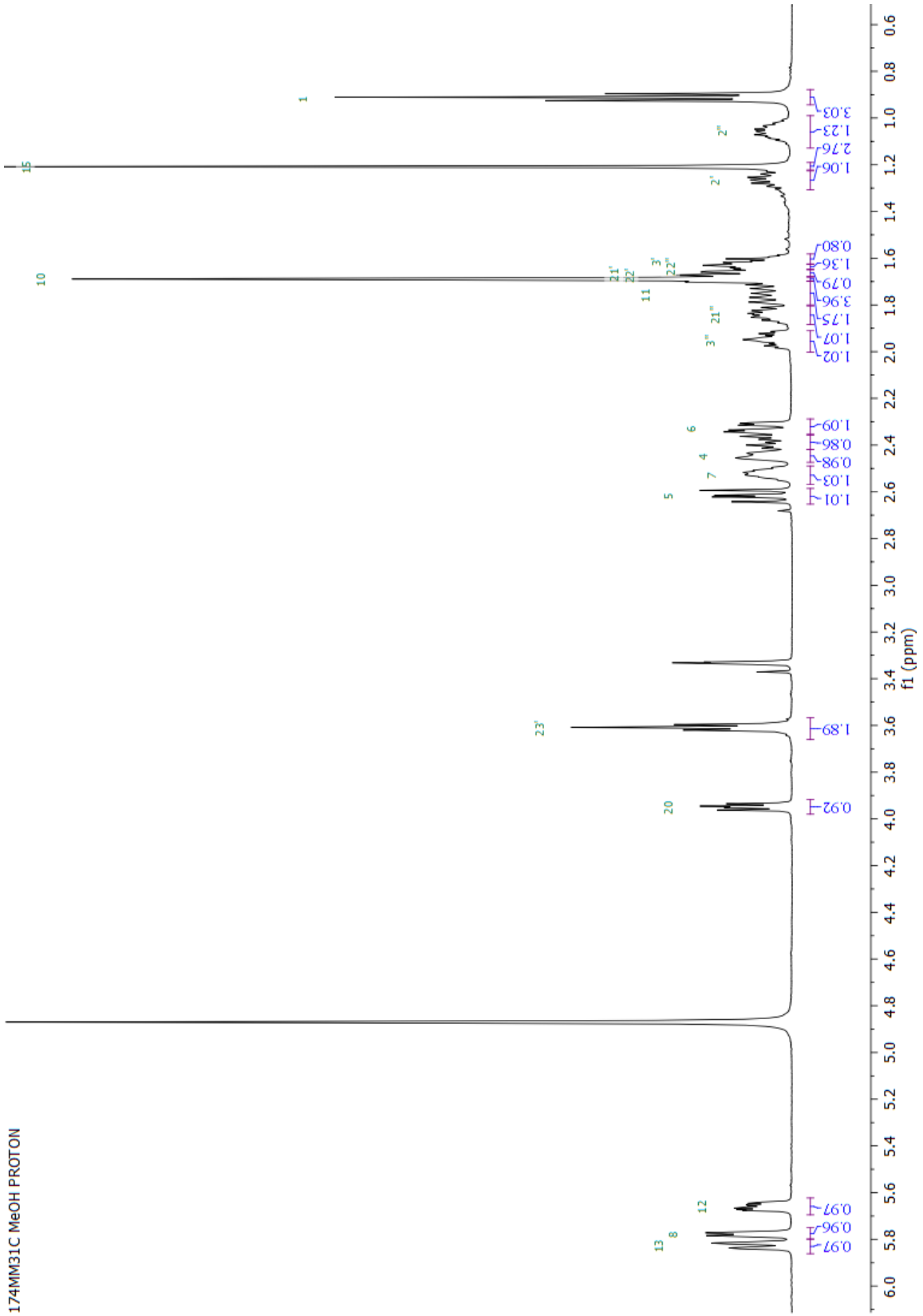

Appendix IV.30. ^{1}H-NMR in DMSO of 174MM31C

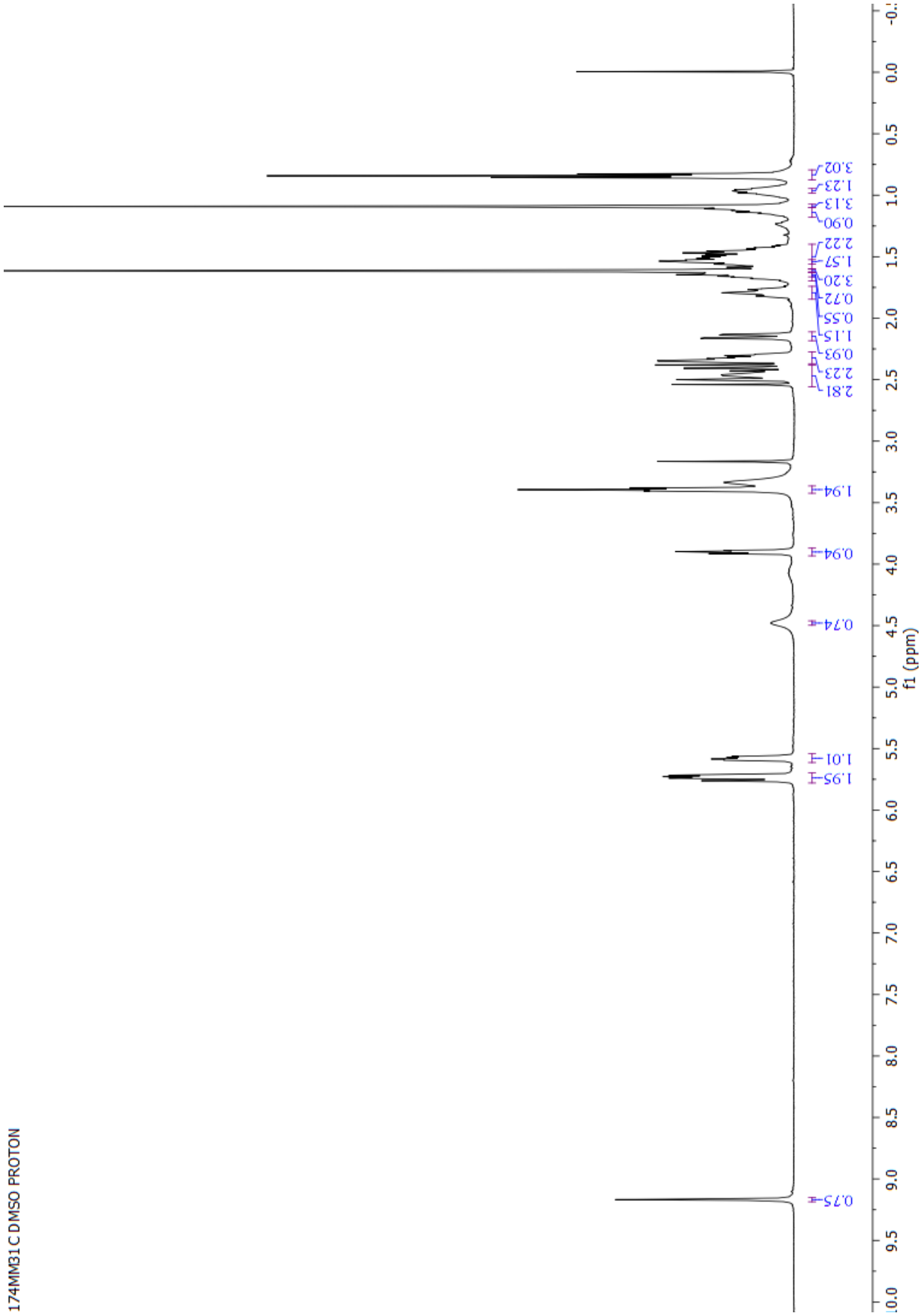

Appendix IV.31. ^{13}C-NMR in MeOH of 174MM31C

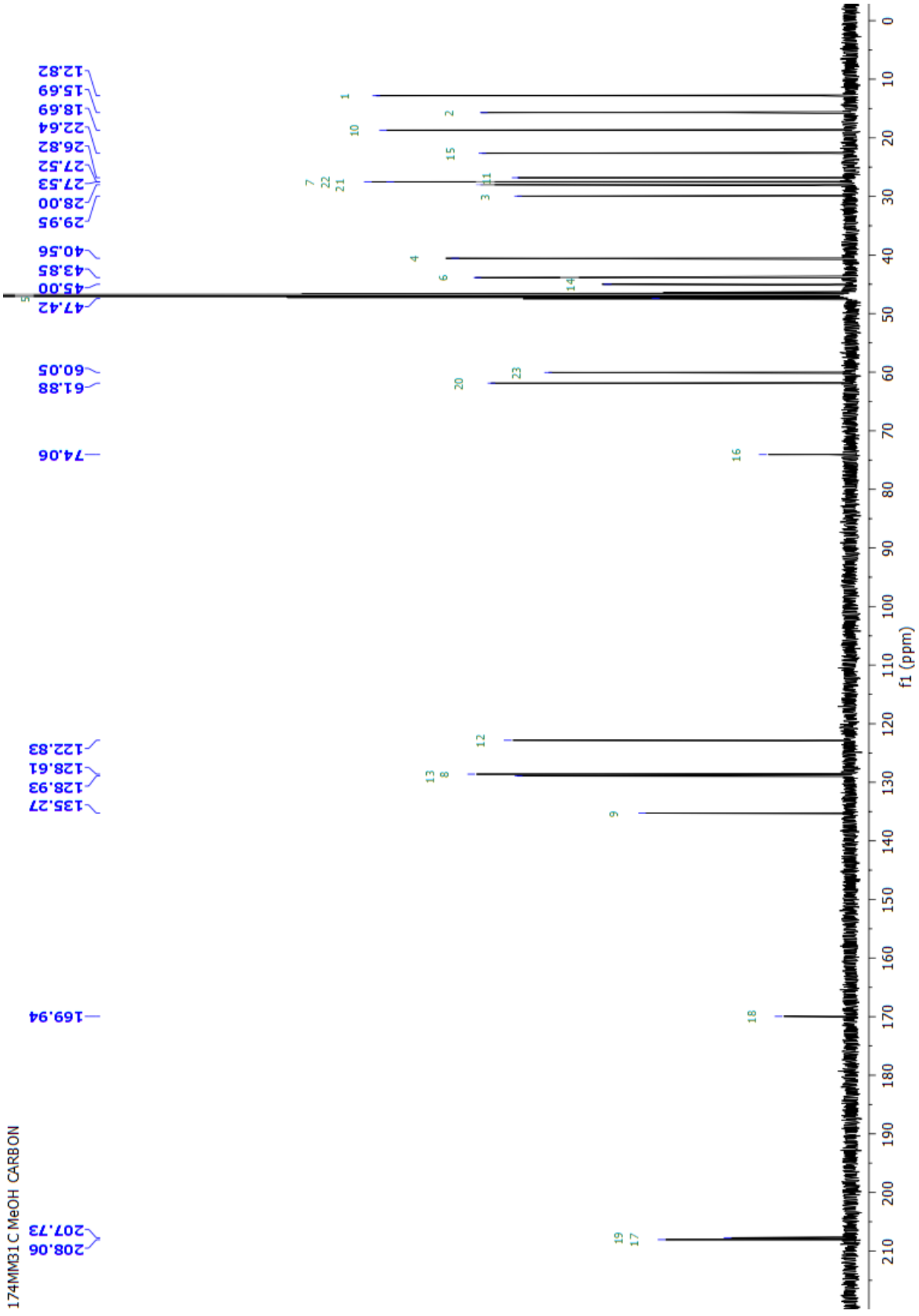

Appendix IV.32. HSQCAD NMR in MeOH of 174MM31C

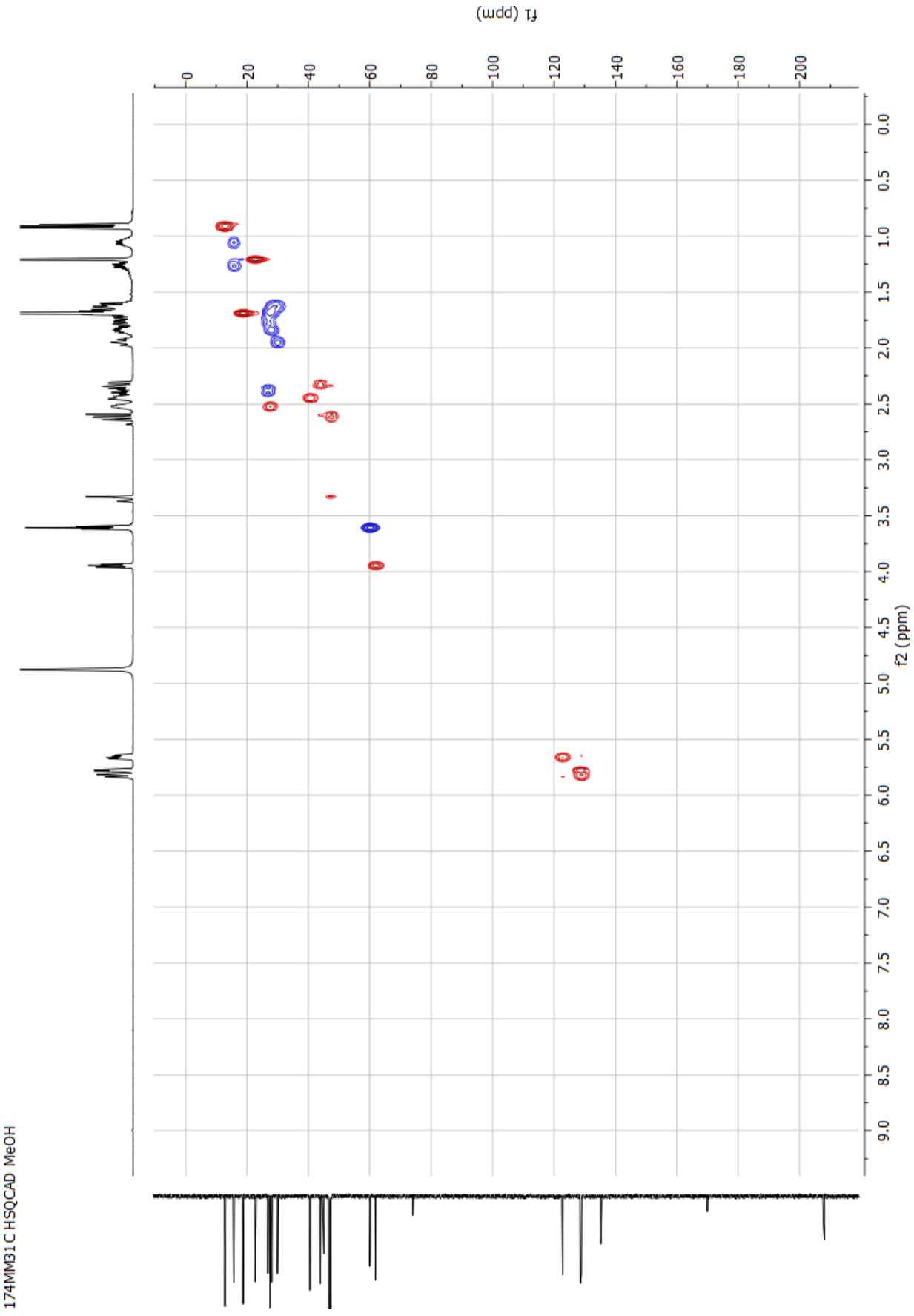

Appendix IV.33. gHMBCAD NMR in MeOH of 174MM31C

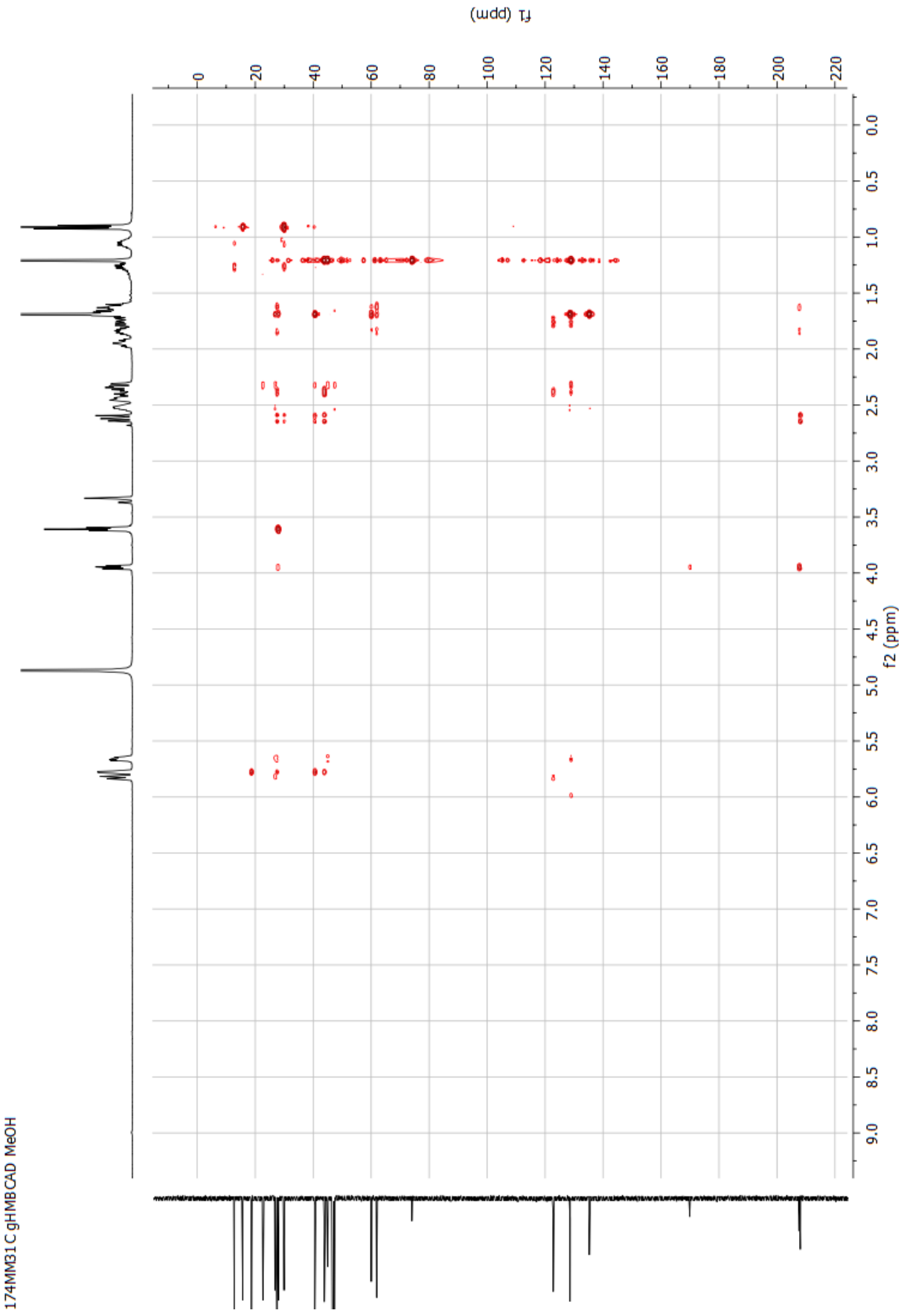

Appendix IV.34. gCOSY NMR in MeOH of 174MM31C

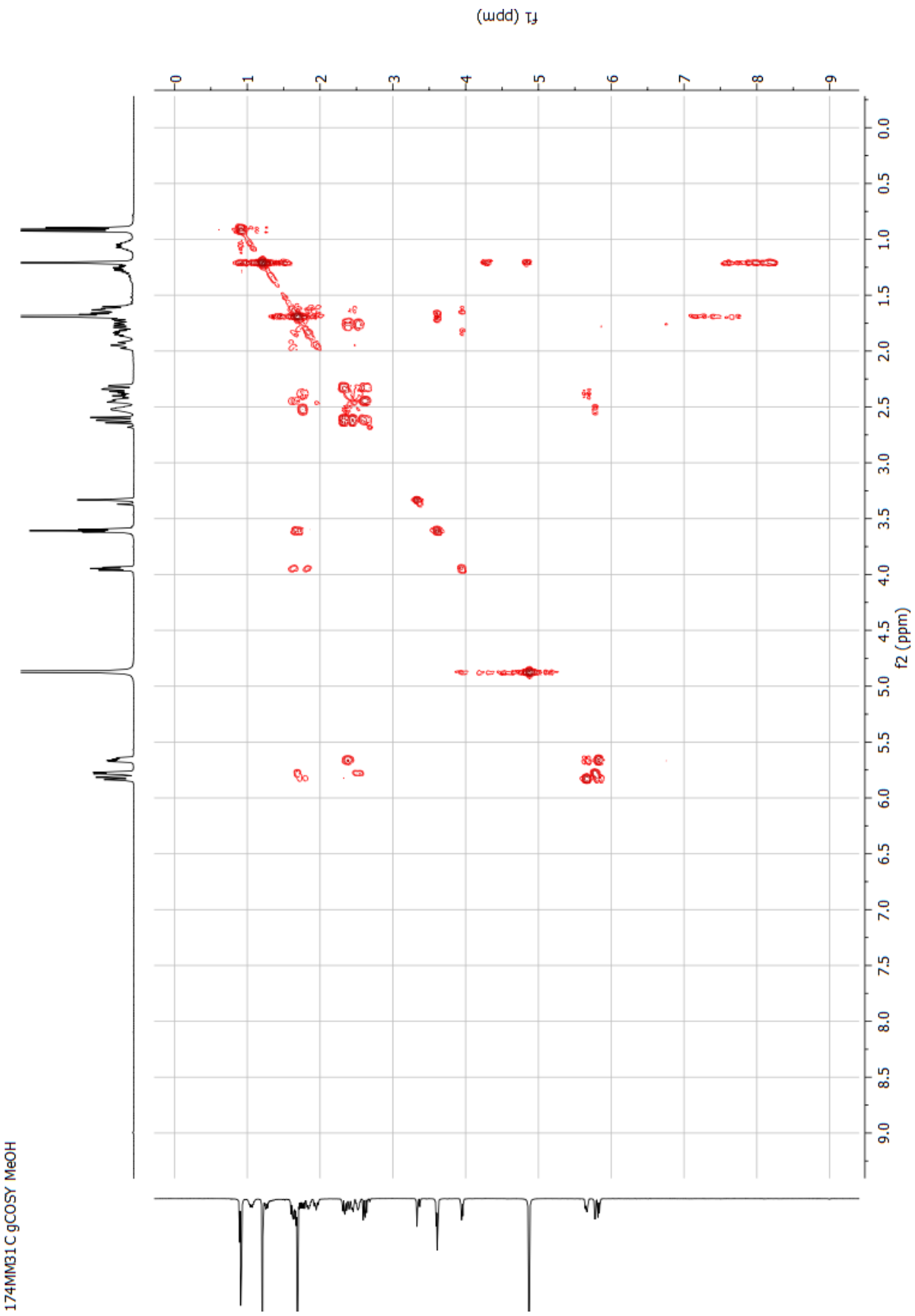

Appendix IV.35. NOESY NMR in MeOH of 174MM31C

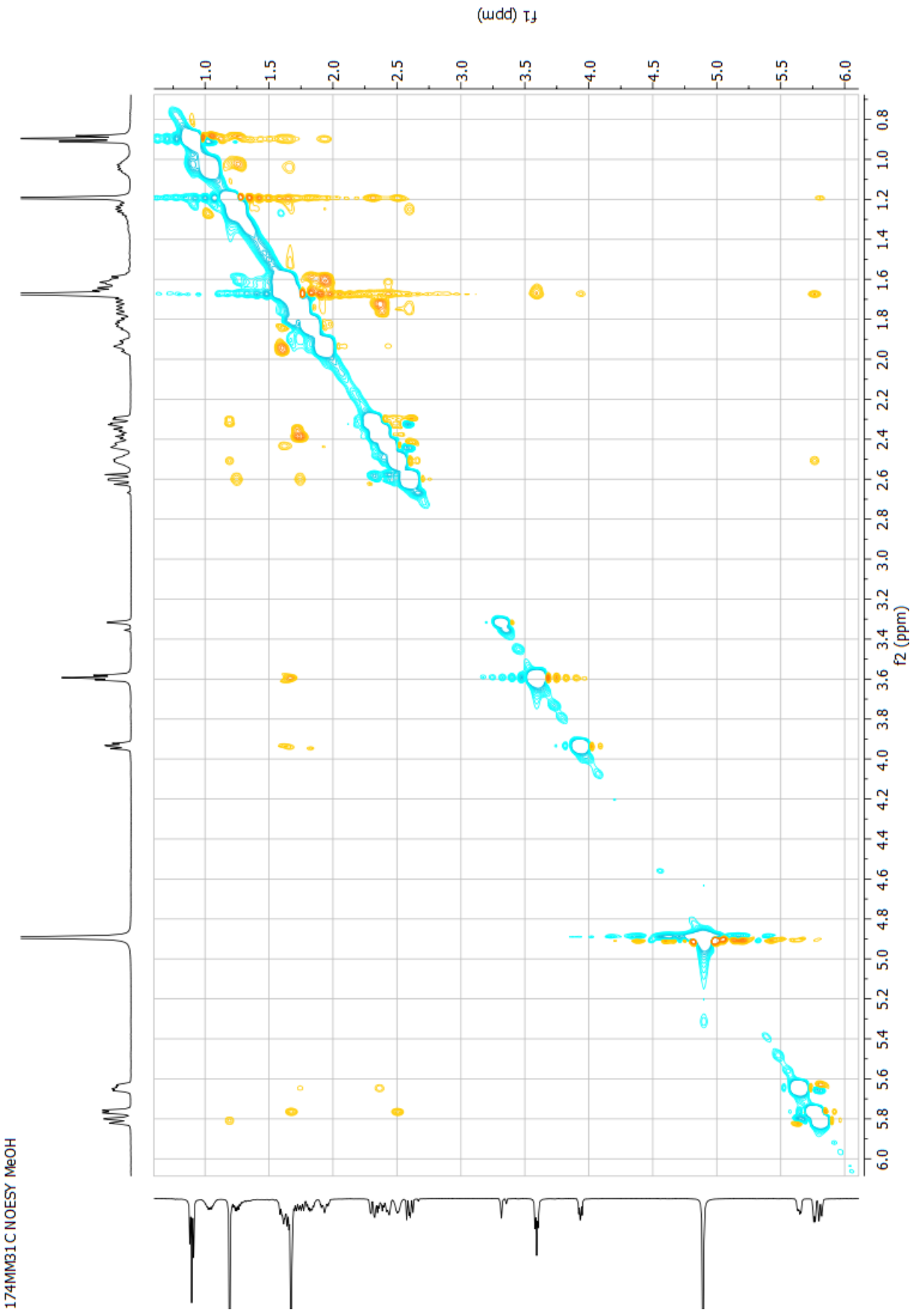

Appendix V. Data for 52C

Appendix V.36. LCMS chromatogram of 174MM52C

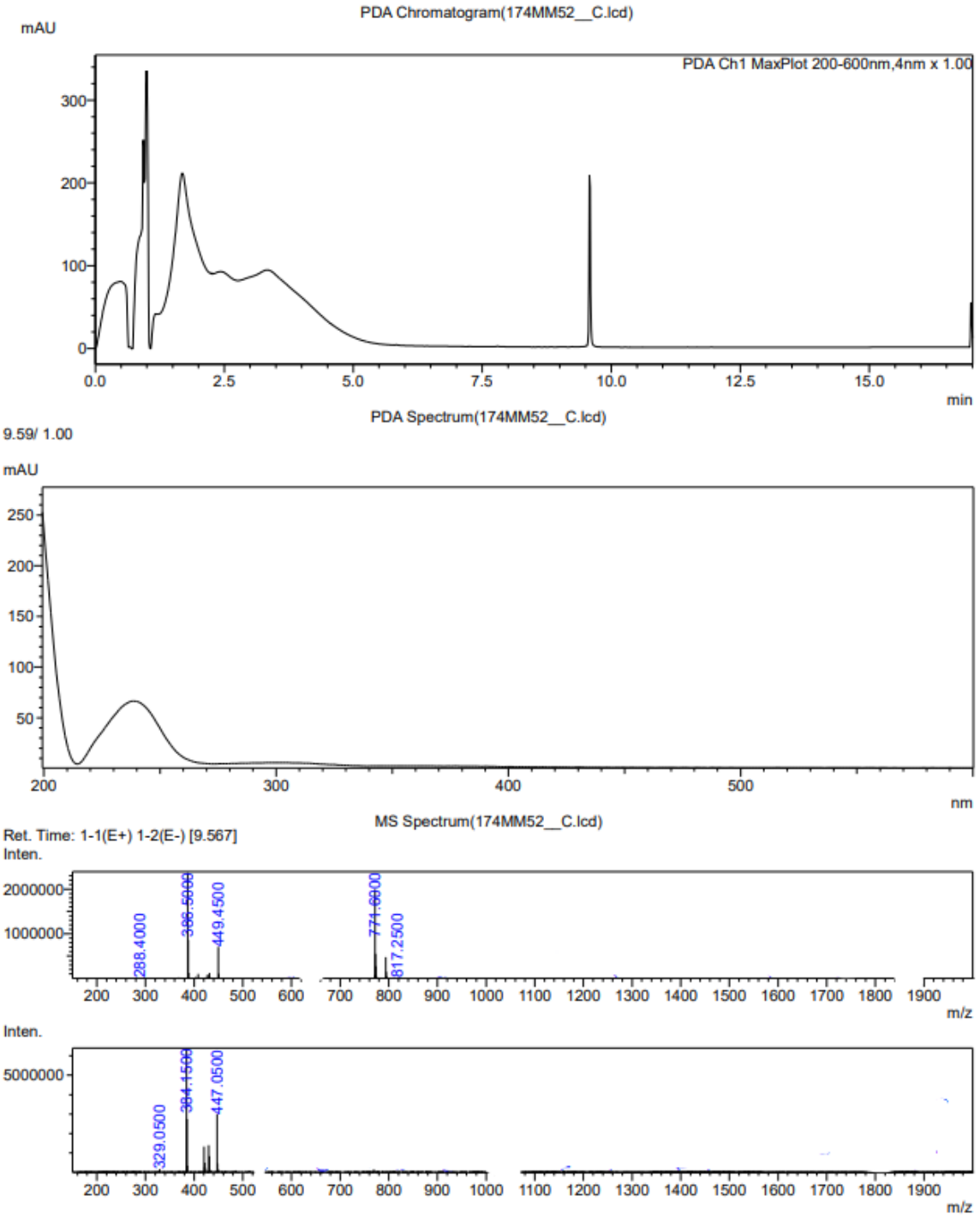

Appendix V.37. ^{1}H-NMR in MeOH of 174MM52C

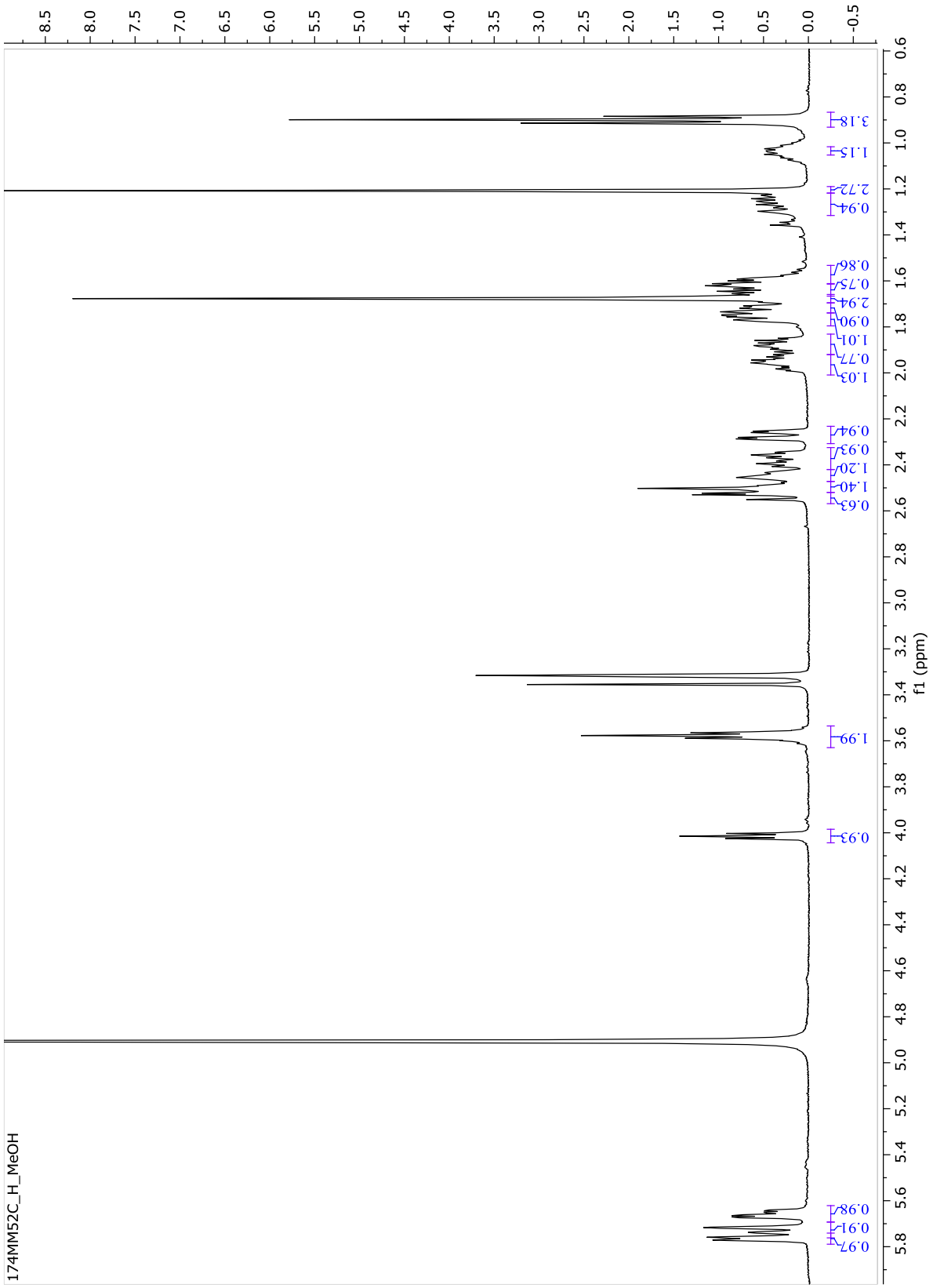

Appendix V.38. ^{13}C-NMR in MeOH of 174MM52C

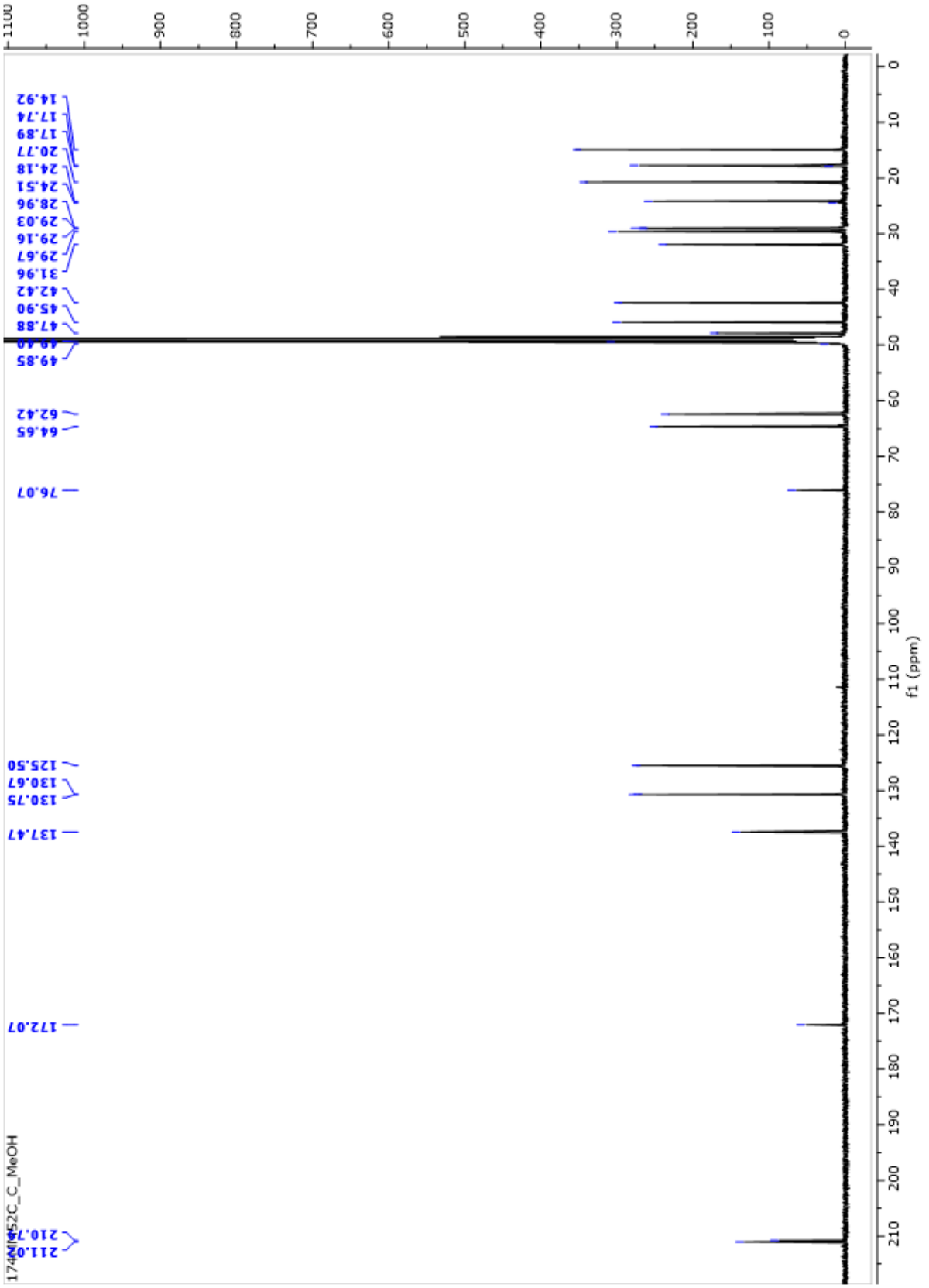

Appendix V.39. HSQCAD NMR in MeOH of 174MM52C

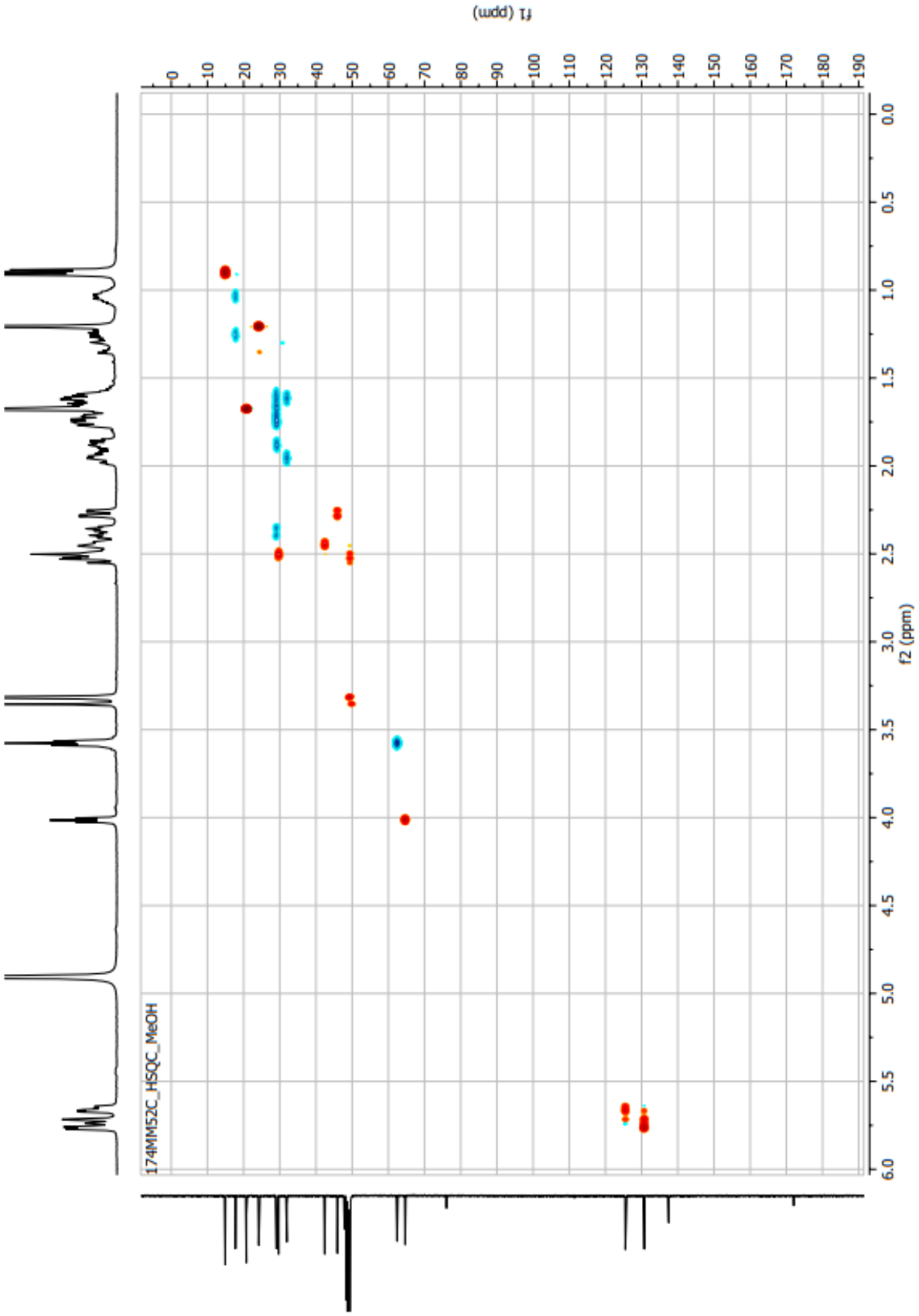

Appendix V.40. gHMBCAD NMR in MeOH of 174MM52C

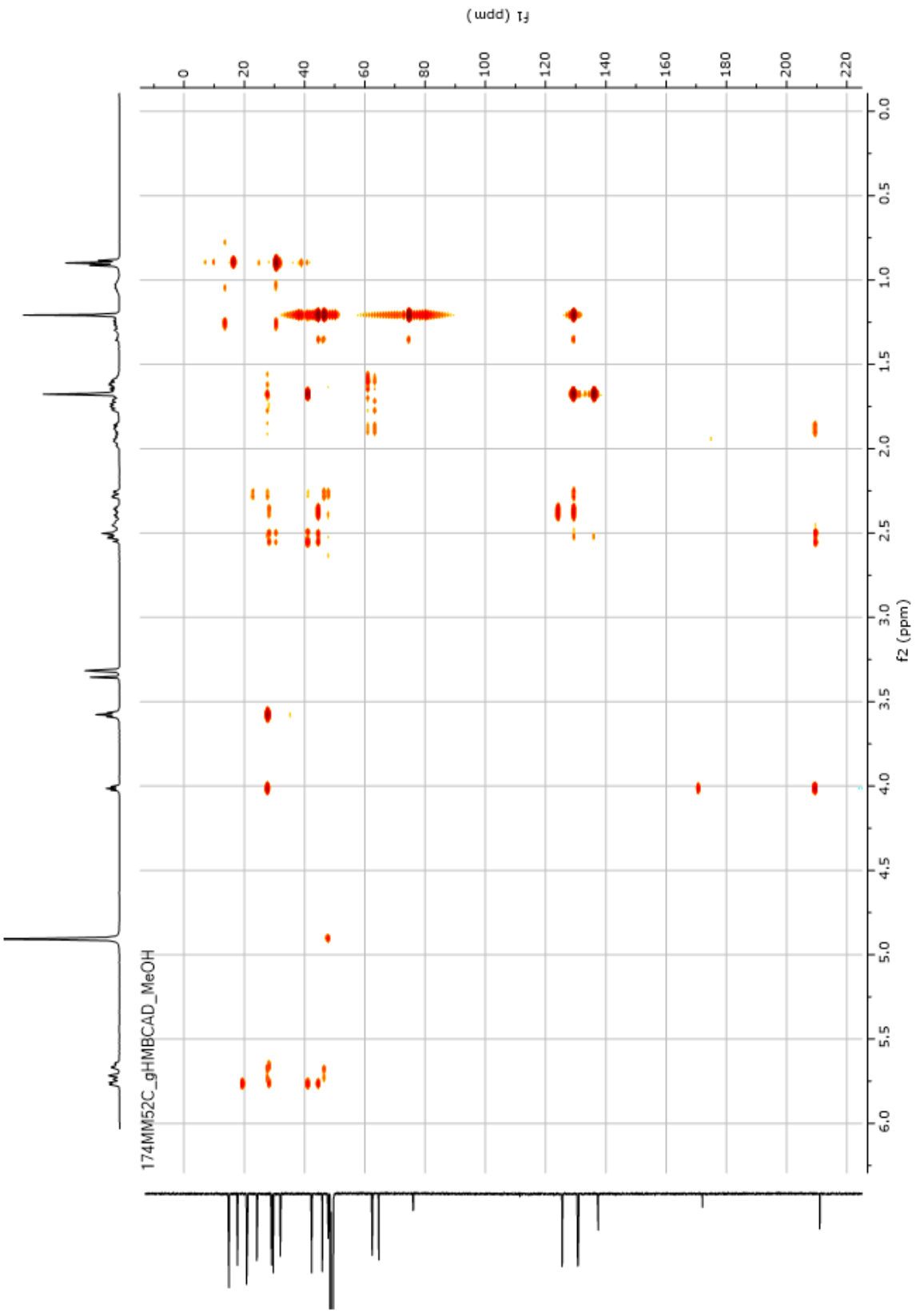

Appendix V.41. gCOSY NMR in MeOH of 174MM52C

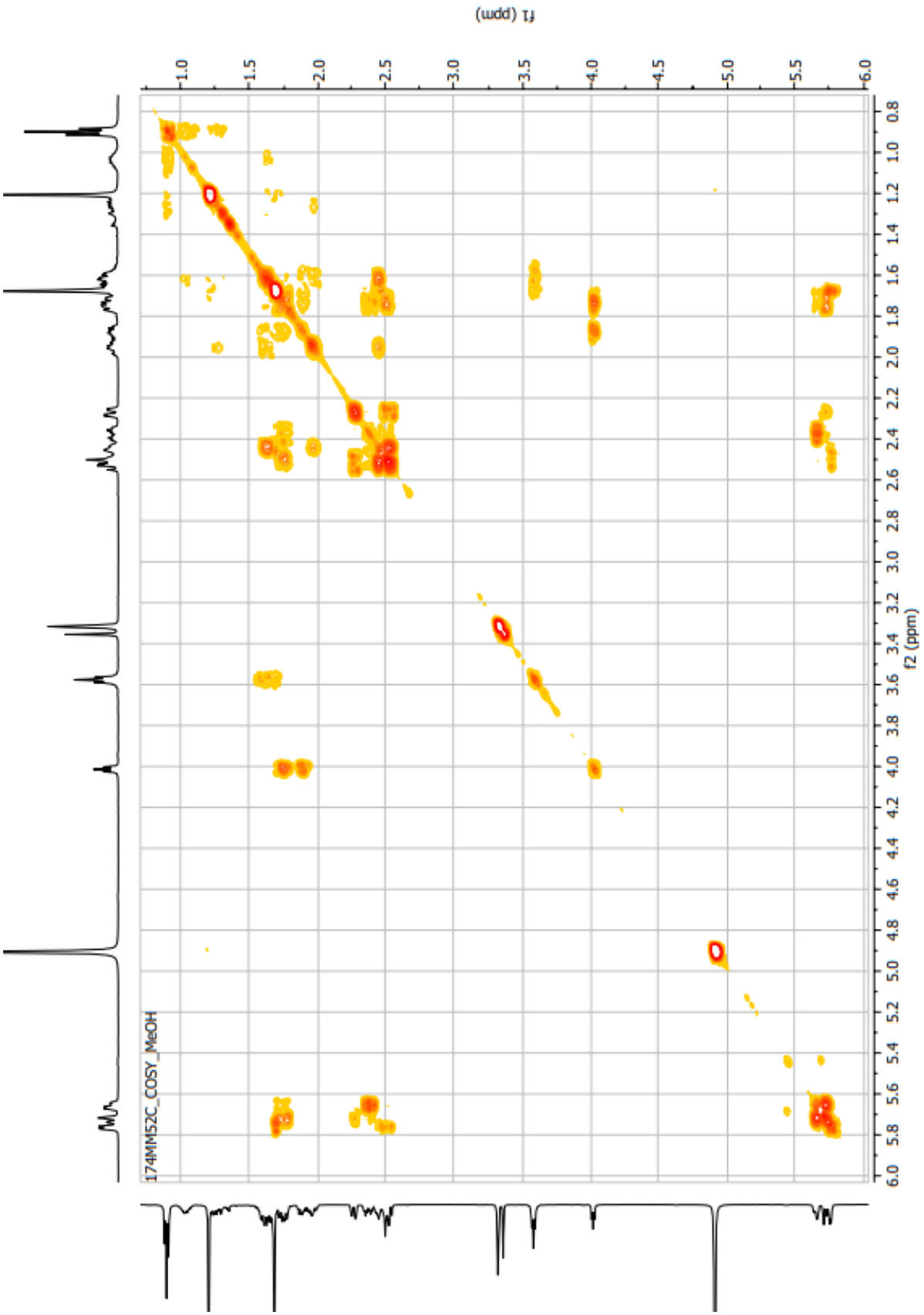

Appendix V.42. NOESY NMR in MeOH of 174MM52C

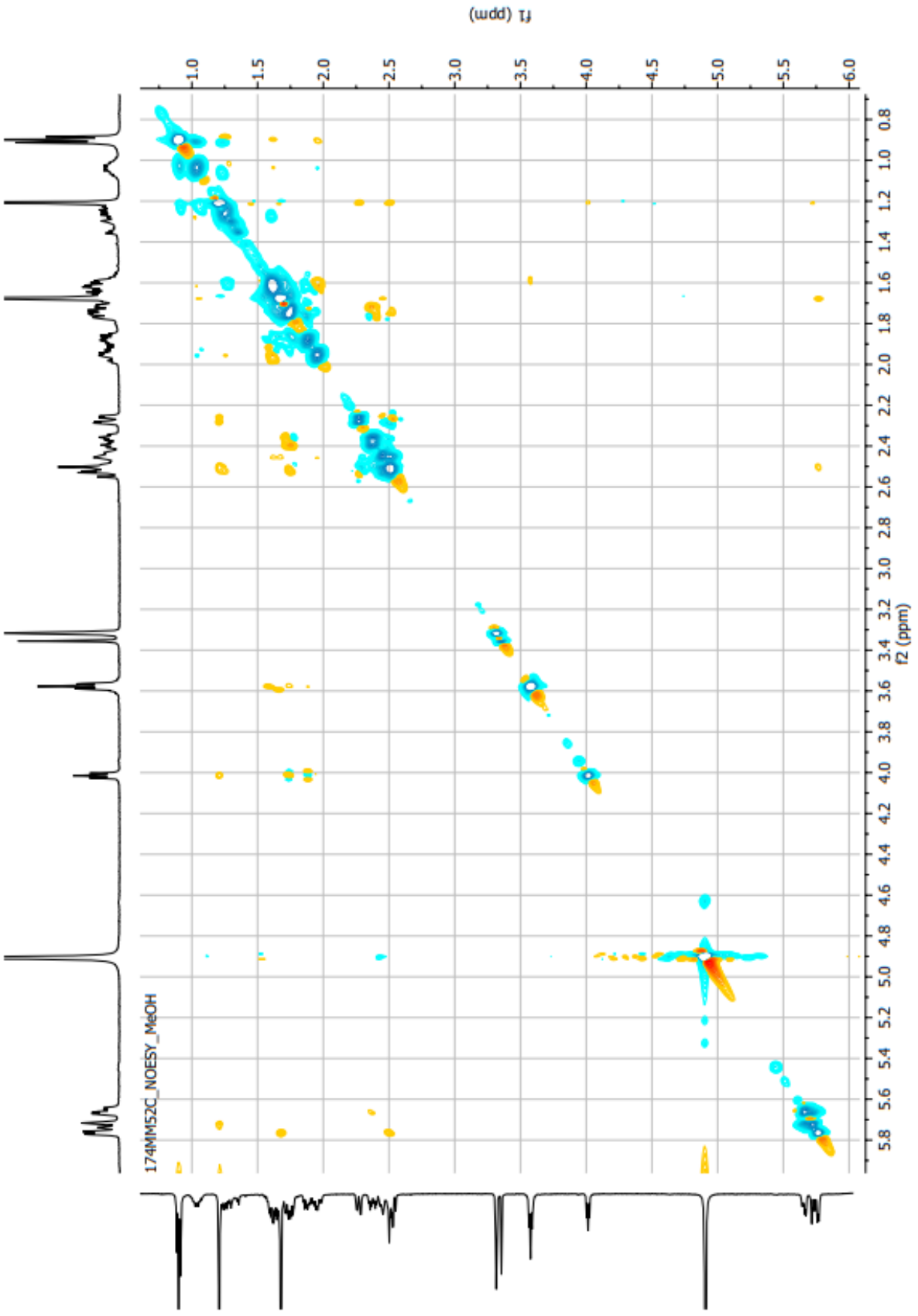

Appendix VI. 41D data

Appendix VI.43. ^{1}H NMR in MeOH of 174MM41D